COMPARISON OF THE INTERCARRIER INTERFERENCE CANCELLATION METHODS IN OFDM SYSTEMS

A THESIS SUBMITTED TO
THE GRADUATE SCHOOL OF NATURAL AND APPLIED SCIENCES
OF
MIDDLE EAST TECHNICAL UNIVERSITY

BY

BURKAY ETİLER

IN PARTIAL FULFILLMENT OF THE REQUIREMENTS
FOR
THE DEGREE OF MASTER OF SCIENCE
IN
ELECTRICAL AND ELECTRONICS ENGINEERING

AUGUST 2007

Approval of the thesis:

COMPARISON OF THE INTERCARRIER INTERFERENCE CANCELLATION METHODS IN OFDM SYSTEMS

submitted by **BURKAY ETİLER** in partial fullfillment of the requirements for the degree of **Master of Science in Electrical and Electronics Engineering Department, Middle East Technical University** by,

Prof. Dr. Canan Özgen _____
Dean, Graduate School of **Natural and Applied Sciences**

Prof. Dr. İsmet Erkmen _____
Head of the Department, **Electrical and Electronics Engineering**

Assoc.Prof.Dr.T. Engin Tuncer _____
Supervisor, **Electrical and Electronics Engineering Dept., METU**

Examining Committee Members

Assoc.Prof.Dr.Gözde Bozdağı Akar _____
Electrical and Electronics Engineering Dept., METU

Assoc.Prof.Dr.T. Engin Tuncer _____
Electrical and Electronics Engineering Dept., METU

Assist.Prof. Dr. Ali Özgür Yılmaz _____
Electrical and Electronics Engineering Dept., METU

Assist.Prof. Dr. Çağatay Candan _____
Electrical and Electronics Engineering Dept., METU

Mete Gök _____
System Engineer, MILSOFT

Date : 29.08.07

I hereby declare that all information in this document has been obtained and presented in accordance with academic rules and ethical conduct. I also declare that, as required by these rules and conduct, I have fully cited and referenced all material and results that are not original to this work.

Name, Last name : Burkay Etiler
Signature :

ABSTRACT

COMPARISON OF THE INTERCARRIER INTERFERENCE CANCELLATION METHODS IN OFDM SYSTEMS

Etiler, Burkay

M.S., Department of Electrical and Electronics Engineering

Supervisor : Assoc. Prof. Dr. T.Engin Tuncer

August 2007, 86 pages

In OFDM systems carrier frequency offset is observed due to Doppler shift and transmitter-receiver frequency mismatches. This offset induces ICI (Intercarrier Interference). In this thesis, repeated data methods and pilot-aided carrier frequency offset(CFO) estimation methods and windowing techniques are used to mitigate the frequency offset problem and a performance comparison is made between these ICI cancellation techniques.

Repeated data methods use only half of the bandwidth for information transmission to eliminate the ICI at the receiver. We have implemented repeated data methods including Self cancellation scheme and Symmetric Symbol Repetition (SSR) schemes to overcome ICI problem. We have also implemented Adjacent Conjugate Symbol Repetiton (ACSR) and Symmetric Conjugate Symbol Repetiton (SCSR) methods to mitigate both phase rotations and ICI.

CFO estimation and correction methods generally use pilot sequences. We implemented the “Conventional Pilots” and “Clustered Pilots” pilot-aided CFO

estimation techniques for ICI cancellation. Furthermore, we also implemented a new scheme by using the odd symmetry between pilot symbols.

Nyquist windowing techniques apply windowing at the receiver side. We have implemented second order polynomial class of Nyquist windows and Nyquist window with Franks pulse used to mitigate ICI.

These ICI cancellation methods are compared in AWGN and multipath Rayleigh fading channel models in terms of BER and carrier to interference ratio. It is shown that repeated data methods shows better performances than pilot-aided CFO estimation methods with a cost of increased bandwidth usage especially in high SNR's.

Keywords: OFDM, Intercarrier Interference (ICI), Carrier Frequency Offset(CFO), Self Cancellation, ICI Cancellation, CFO Estimation, Windowing

ÖZ

OFDM SİSTEMLERİNDE TAŞIYICILAR ARASI GİRİŞİMİ YOKETME METOTLARININ KARŞILAŞTIRILMASI

Etiler, Burkay
Yüksek Lisans, Elektrik ve Elektronik Mühendisligi Bölümü
Tez Yöneticisi: Doç. Dr. T. Engin Tuncer

Ağustos 2007, 86 sayfa

OFDM sistemlerinde Doppler kayması ve verici-alıcı arası frekans uyumsuzlukları sonucu taşıyıcı frekans kayması (TFK) gözlenmektedir. Bu kayma taşıyıcılar arası girişime (TAG) yol açmaktadır. Bu tezde frekans kayması problemini bastırmak için veri tekrarlama metotları ve yardımcı pilot yöntemleri kullanılmaktadır ve bu TAG yok etme metotları arasında performans karşılaştırması yapılmaktadır.

Veri tekrarlama metotları, veri gönderimi için bant genişliğinin sadece yarısını kullanarak alıcıda TAG'ı bastırmak amaçlı kullanılabilmektedir. TAG problemini yok etmek için Kendi Yok Etme ve Simetrik Sembol Tekrarlama metotları uyguladık. Ayrıca hem TAG'ı hem de faz kaymalarını bastırmak için Komşu Konjuge Sembol Tekrarlama ve Simetrik Konjuge Sembol Tekrarlama metotlarını da uyguladık.

TFK kestirim ve düzeltme metotları genelde pilot verileri kullanmaktadır. TAG'ı yok etmek için Geleneksel Pilot ve Kümelenmiş Pilot TFK kestirim

tekniklerini uyguladık. Bundan başka, pilot semboller arası tek simetriyi kullanan yeni bir yöntemi de uyguladık.

Nyquist pencereleme teknikleri alıcı tarafında pencereleme uygulamaktadırlar. TAG'ı bastırmak için ikinci dereceden çokterimli Nyquist pencere sınıfını ve Franks vurumu kullanan Nyquist penceresini kullandık.

Bu TAG yok etme metotlarını Toplanır Beyaz Gauss Gürültülü ve Çokyollu Rayleigh Sönümlenmeli kanal modellerinde bit hata oranı ve taşıyıcı girişim oranı cinsinden karşılaştırdık. Özellikle yüksek sinyal gürültü oranlarında veri tekrarlama metotlarının artırılmış bant genişliği bedeli ödeyerek yardımcı pilot kullanan TFK kestirim metotlarından daha iyi performans gösterdikleri gösterilmiştir.

Anahtar kelimeler: OFDM, taşıyıcı arası girişim, Rayleigh Sönümlenmesi, taşıyıcı frekans kayması, Kendi Yok Etme, Taşıyıcı frekans kayması kestirimi, Pencereleme

To My Family

ACKNOWLEDGEMENTS

I would like to thank Assoc. Prof. Dr. T. Engin Tuncer, for his help, professional advice and valuable supervision during the development of this thesis. This thesis would not be completed without his guidance and support.

I wish to thank to Tübitak-BAYG, for the scholarship they provided me for my thesis work.

I would like to thank my family for their continuous support in my life.

I would also like to thank Gökçe Han for her endless love and moral support.

TABLE OF CONTENTS

LIST OF FIGURES

LIST OF TABLES

LIST OF ABBREVIATIONS

ADSL	Asymmetric Digital Subscribers Line
AWGN	Additive White Gaussian Channel
BER	Bit Error Rate
BPSK	Binary Phase Shift Keying
CFO	Carrier Frequency Offset
CP	Cyclic Prefix
FFT	Fast Fourier Transform
GI	Guard Interval
HIPERLAN	High Performance Radio Local Area Network
ICI	Inter Carrier Interference
IEEE	Institute of Electrical and Electronics Engineers
IFFT	Inverse Fast Fourier Transform
ISI	Inter Symbol Interference
LS	Least Square
MCM	Multi Carrier Communication
MMSE	Minimum Mean Square Error
OFDM	Orthogonal Frequency Division Multiplexing
QPSK	Quaternary Phase Shift Keying
RMSE	Root Mean Square Error
SNR	Signal-to-Noise Ratio
ZF	Zero Forcing

CHAPTER 1

INTRODUCTION

Orthogonal frequency division multiplexing (OFDM) is a technique that transmits signals through multiple carriers. These subcarriers have different frequencies and they are orthogonal to each other. OFDM is an example of the multi-carrier modulation (MCM) techniques. In both wired and wireless communications, such as the asymmetric digital subscriber line (ADSL) and the IEEE 802.11 standard, OFDM techniques have been applied.

Original OFDM principles are proposed by Chang in 1966 [1], and successfully achieved a patent in January of 1970. Later on, Saltzberg observed that the crosstalk was the severe problem in this system. Although each subcarrier in the principal OFDM systems overlapped with the neighbourhood subcarriers, the orthogonality can still be preserved through the staggered QAM (SQAM) technique. However, when a large number of subcarriers are required, then problems appear. In some early OFDM applications, the number of subcarriers could only be chosen up to 34. In those applications, a guard time interval was added to the 34 symbols to eliminate intersymbol interference (ISI) [2].

When more subcarriers are required, the modulation, synchronization, and coherent demodulation would be complicated for the OFDM system which also increases additional complexity. Weinstein and Ebert [3] applied a modified OFDM system with the discrete Fourier Transform (DFT) to generate the orthogonal subcarriers waveforms in 1971. Their scheme reduced the implementation complexity significantly, by making use of the IDFT modules and the digital-to-analogue converters.

Modern OFDM systems with Cyclic prefix (CP) or cyclic extension was first introduced by Peled and Ruiz in 1980 [4]. In their scheme, conventional null guard interval is substituted by cyclic extension for fully loaded OFDM modulation and this guarantees the orthogonality among the subcarriers. This new scheme results an ICI reduction with a trade-off the transmission efficiency. Therefore, it has been adopted by the current IEEE standards.

In the same year, 1980, Hirosaki introduced an equalization algorithm to suppress both ISI and ICI [5]. In the meantime, Hirosaki also applied QAM modulation, pilot tone, and trellis coding techniques, which operated in voice-band spectrum.

The first one who introduced a pilot-based method to reduce the interference emanating from the multipath and co-channels was Cimini in 1985 [6]. In 1989, Kalet suggested a subcarrier-selective allocating scheme [7]. Kalet allocated more data through transmission of "good" subcarriers near the centre of the transmission frequency band so these subcarriers will suffer less channel distortion.

In the 1990s, OFDM systems are modified for high data rate communications. For example in the IEEE 802.11 standard, the carrier frequency can go up as high as 2.4 GHz or 5 GHz, moreover, the IEEE 802.16 standard proposes yet higher carrier frequencies ranging from 10 GHz to 60 Ghz.

Applications of OFDM

Since 1960s, the OFDM techniques had been applied for ANDEFT and KINEPLEX,. The implementation of OFDM became more convenient after the IFFT/FFT technique was introduced.

The OFDM applications can be divided into two categories wired and wireless technologies:

Wired OFDM applications are Asymmetric Digital Subscriber Line (ADSL) and high speed DSL.

Wireless OFDM applications may be seen in numerous standards such as IEEE 802.11, IEEE 802.16. At present, many people still work to modify the IEEE 802.16 standard, which may result in an even higher data rate up to 100Mbps. Another example for wireless OFDM applications can be HiperLAN.

Digital Video Broadcasting (DVB), which was widely used in Europe and Australia, also uses the OFDM structure. In the DVB standards, the data rate could go up as high as 15Mbps and the number of subcarriers can be more than 8,000.

The organization of the thesis as follows: In Chapter 2 mathematical model OFDM structure is given and performance of OFDM is illustrated under no ICI condition. Chapter 3 analyses the ICI problem, factors inducing ICI and solutions methods for the ICI are given. Chapter 4 details the ICI cancellation methods and mathematical expressions of the ICI cancellation process are given. In chapter 5 performance comparison of the ICI cancellation methods are done. Finally we will conclude our study in Chapter 6.

CHAPTER 2

OFDM SYSTEM OVERVIEW

Since the original OFDM model was proposed in the 1960s [1], the core structure of OFDM has hardly changed. The key idea of OFDM is that a single user would make use of all orthogonal subcarriers in divided frequency bands. Therefore, the data rate can be increased significantly. Since the bandwidth is divided into several narrower subchannels, each subchannel requires a longer symbol period. OFDM offers several advantages over existing wireless communication techniques. The advantages of OFDM are:

High Bandwidth Efficiency: Since adjacent subchannels overlap each other,but not interfere, high spectral efficiency can be obtained with OFDM.

Robustness to Time Dispersion: OFDM signals are typically much longer than the delay spread of the channel. By using of a cyclic extension to the OFDM signal, intersymbol interference (ISI) due to time dispersion can be completely avoided.

Robustness to Frequency Selective Fading: Time-dispersive channels produce deep fades at some frequencies due to destructive interference, while other frequencies may experience power gains due to constructive interference. Channel coding may be used to exploit the increased carrier-to-noise ratio on the enhanced subcarriers to recover lost data from faded subcarriers.

Robustness to Timing Offsets: OFDM systems are less sensitive to timing offsets than CDMA systems, if the receiver's FFT window is still fully contained within the OFDM frame. Timing offsets manifest themselves as phase rotations in the data symbols. For coherent digital modulation techniques, equalizers will treat

these phase rotations the same as phase offsets from channel distortion. In differential modulation techniques such as DQPSK, this phase rotation has no effect on the decision variables.

There exist a few trade-offs to consider when designing OFDM systems, with two of the most notable trade-offs are:

Increased Sensitivity to Carrier Frequency Offsets: Carrier frequency offsets may exist due to Doppler shifts and differences in the oscillator frequencies at the transmitter and the receiver. The resulting offset causes a net shift of the signal spectrum which may compromise the subcarrier orthogonality. The result is an increase in the noise level due to ICI, which degrades system performance.

High Peak/Average Power Ratio in Waveform: An OFDM signal is the composite of independent sinusoids with random phase shifts, which shares many characteristics with band-limited white noise. The signal has a high peak-to-average power ratio, which requires the use of expensive, highly linear power amplifiers.

2.1 OFDM Model

The OFDM model is depicted in Figure 1.

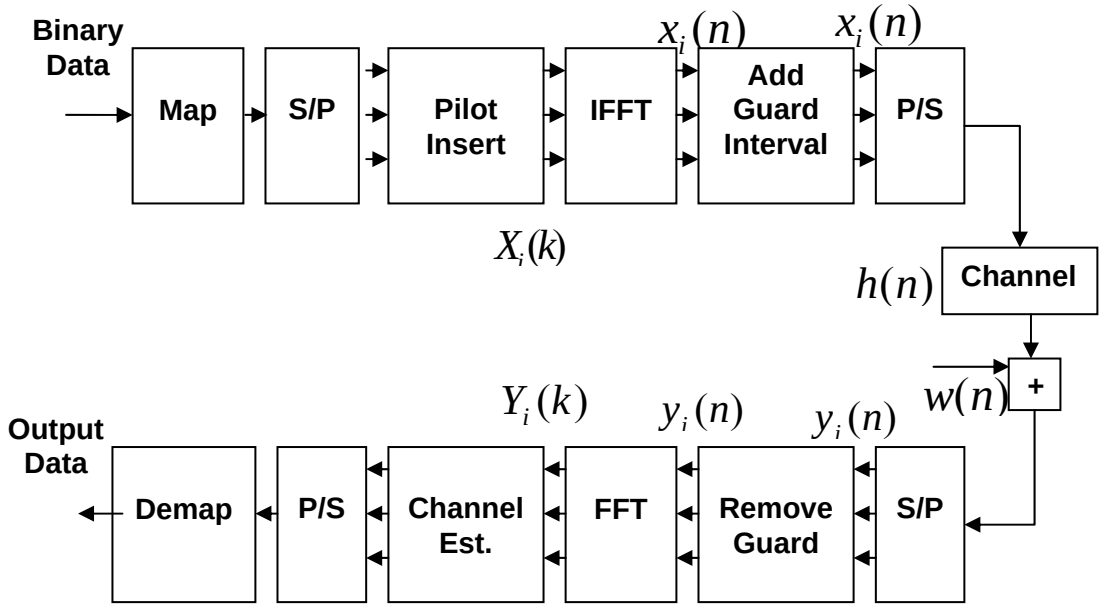

Figure 1 - OFDM Model

2.1.1 IFFT and orthogonality

After the parallel symbol streams are generated, pilot symbols are inserted (for channel estimation) and IFFT block takes the IFFT of the parallel modulated symbols. IFFT operation can be expressed as [8]:

$$x_i(n) = \frac{1}{N}\sum_{k=0}^{N-1} X_i(k) e^{\frac{j2\pi nk}{N}} \tag{1}$$

where $X_i(k)$'s are encoded parallel modulated data in the i^{th} OFDM symbol.

The orthogonality of discrete-time Fourier bases can be described as follows [9]:

$$\sum_{k=0}^{N-1} \cos\left(\frac{2\pi kn}{N}\right) \cos\left(\frac{2\pi km}{N}\right) = \delta(n-m) \tag{2}$$

This equation proves that the output sequences of the IFFT are orthogonal to each other.

2.1.2 Guard Interval and Cyclic Prefix

In multipath fading channel models, many time-delayed replicas of the transmitted waveform might be found at the receiver [10]. That is, the output data after the channel is affected by not only the current input but also the previous inputs named as Inter-Symbol-Interference (ISI). This problem is severe in OFDM systems where a block processing of data is performed at the receiver. The main purpose of guard interval (GI) in Figure 1 is to eliminate this inter symbol interference (ISI). There exists more than one option for GI, such as:

Zero padding (ZP) is a guard interval type that no waveform is transmitted in the GI duration. Main disadvantage of ZP is that the zero-padded waveform can destroy the orthogonality of subcarriers and results in intercarrier interference (ICI). On the other hand, when ZP is used for guard, the system gains resistance against channel nulls, and this is an advantage for Zero-Padded OFDM systems. Note that when channel frequency response has deep fades or nulls, the sample on the corresponding subcarrier will be lost.

The cyclic prefix (CP) is the most common guard interval (GI) and in this study cyclic prefix is used for guard interval purpose. In the CP scheme, the GI is a copy of the partial waveform. As shown in Figure 2, an end-portion of waveform is copied and inserted prior to the beginning of waveform. The advantage of CP is that the help of FFT can preserve the orthogonality of subcarriers. Therefore, when CP is applied instead of zero-padding GI, both ICI and ISI are eliminated.

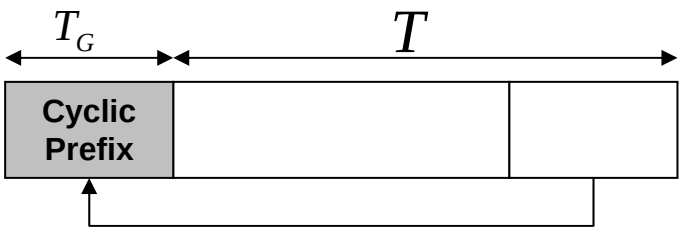

Figure 2 - Generate Cyclic Prefix

The time duration of CP, denoted as T_G in the Figure 2 , is often chosen according to the following:

$$T_G = \frac{T}{2^k} \tag{3}$$

where k is an integer. For example, k is chosen 2 in the IEEE 802.11a standard, and k=1,2…..6 in Europe DVB standards. In our simulations k is chosen to be 2 , note that k shall depend on the maximum delay time of the channel.

When the guard interval is employed, the portions of waveforms received in the GI duration will be totally discarded, as shown in the bottom half of Figure 3. Thus, the ISI could be completely eliminated accordingly.

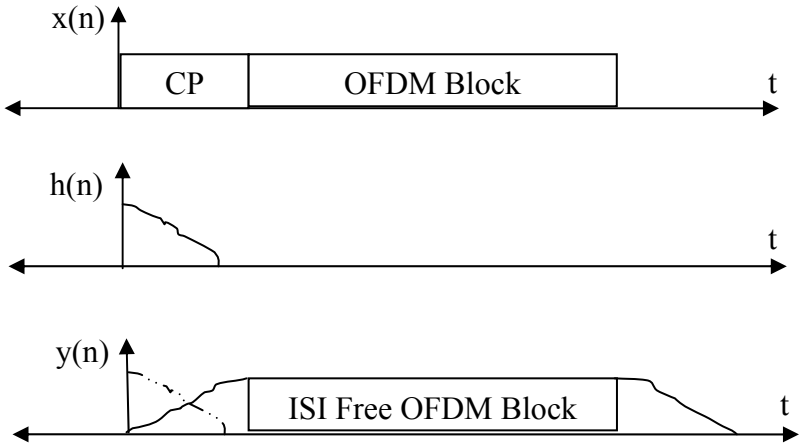

Figure 3 - Elimination of ISI

The main rule for guard interval is; GI duration must be larger than the maximum channel delay time. Otherwise, it could not entirely remove the ISI.

2.1.3 Channel

After adding Guard Interval, $x_i(n)$ parallel data is converted to serial data and then passes through a channel and added white Gaussian noise. After this channel effect, the obtained data will be:

$$y(n) = h(n) * x(n) + w(n) \tag{4}$$

where $w(n)$ is additive white Gaussian noise and * is the convolution operation.

2.1.4 Receiver

On the receiver side, guard interval is extracted from y(n) and the FFT of y(n) is taken :

$$Y_i(k) = \sum_{n=0}^{N-1} y_i(n)\, e^{\frac{-j2\pi nk}{N}} \tag{5}$$

Finally the received parallel data Y(k) is converted to serial and then decoded at the receiver.

2.1.5 Channel Estimation

Following FFT block, the pilot signals are extracted and the estimated channel frequency response $\hat{H}(k)$ for the data sub-channels is obtained in channel estimation block with the Least Squares (LS) channel estimation technique that is defined as:

$$\hat{H}(m) = \frac{Y(m)}{X(m)} \tag{6}$$

where *Y(m)* is the received data at the m^{th} pilot position, X(m) is the transmitted data at the m^{th} pilot position and $\hat{H}(m)$ is the estimated channel frequency response.

After channel estimation, Zero forcing (ZF) equalizer is used and the data is obtained by:

$$\hat{X}(k) = \frac{Y(k)}{\hat{H}(m)} \tag{7}$$

2.2 Performance of OFDM

In this part, the performance of the OFDM system is considered using the simulation results. The simulations are performed under AWGN and Multipath Rayleigh fading frequency selective channels (Rural Area Model according to COST 207 model) [11]. The selected system parameters are in the below Table 1.

Table 1 - OFDM simulation Parameters

PARAMETERS	VALUES
Number of subcarriers	256
Number of Pilots	16
Length of Cyclic Prefix	64
Number of OFDM symbols	4
Carrier frequency	2 GHz
Sampling Time	0.2 μs
Subcarrier Spacing	7,8125 MHz
Constellation	BPSK, QPSK
Channel Type	Rural Area model (COST 207)
Number of Trials	10000

We will make comparisons in terms of the Bit Error Rate (BER) in the detected output under changing SNR conditions, considering the AWGN and Multipath Rayleigh Fading Channel types.

2.2.1 AWGN Channel

The AWGN channel is the simplest channel model used in most communication systems. The thermal noise in the receivers can be characterized as an additive white Gaussian process. In our OFDM simulation within the AWGN channel, OFDM model in the Figure 1 will be used by taking $h(n) = \delta(n)$. Note that when considering OFDM simulation in AWGN channel , "Pilot Insert" and "Channel Estimation" blocks are not used in the OFDM model, since $h(n) = \delta(n)$ and there is no need for channel impulse response estimation.

Bit Error Rate performance of OFDM under AWGN Channel with different BPSK, QPSK and 16 QAM modulation schemes are shown below in figure 4.

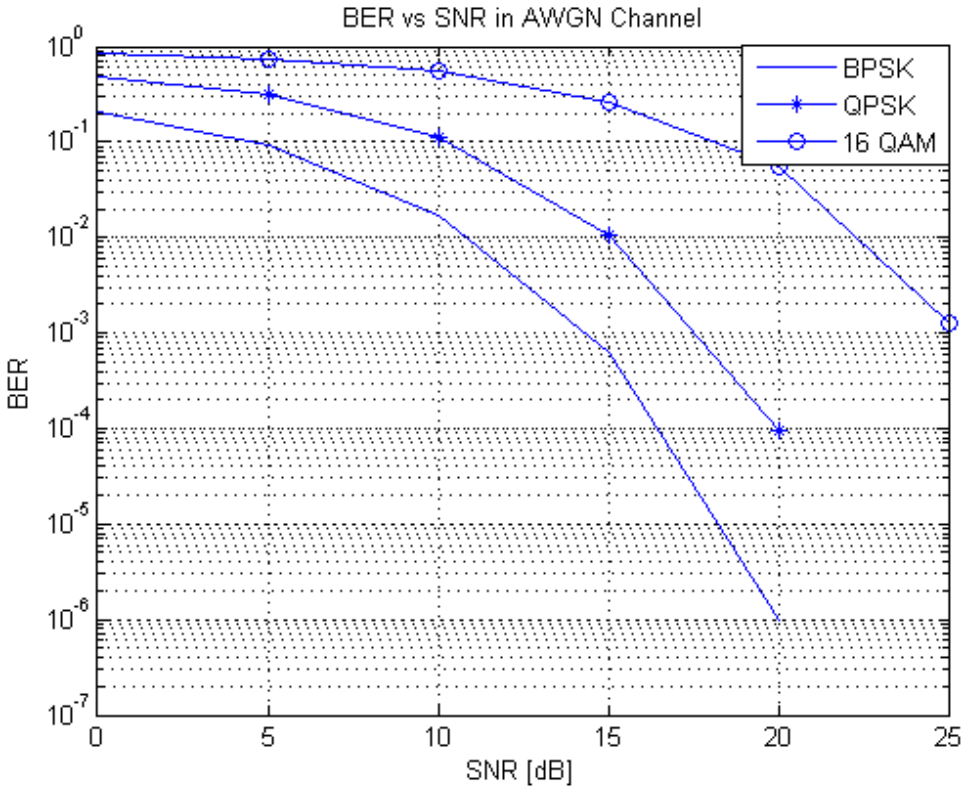

Figure 4 - BER performance of OFDM with different modulation schemes

It is evident that OFDM with BPSK has the best performance and OFDM with 16 QAM has the worst performance in terms of BER.

2.2.2 Multipath Rayleigh Fading Channel

In radio channels, the received signal is the sum of a number of signals arriving through different propagation paths. Each signal path is affected by a random amplitude attenuation and a phase shift that tend to change over time.

The mobile radio channel is based on the propagation of radio waves in a complex transmission environment. For mobile radio applications, the channel is time varying because the motion between the transmitter and receiver results in propagation path because the motion between the transmitter and receiver results in propagation path changes. The channel impulse response can be represented as:

$$h(t) = \sum_{m=0}^{M-1} a_m(t)\delta(t-\eta_m) \tag{8}$$

where M is the total number of paths, $a_m(t)$'s are independent complex Gaussian variables with unit variance and η_m's are delays of the each path in μs [12]. The low-pass equivalent of the fading channel model may be depicted as in Figure 5.

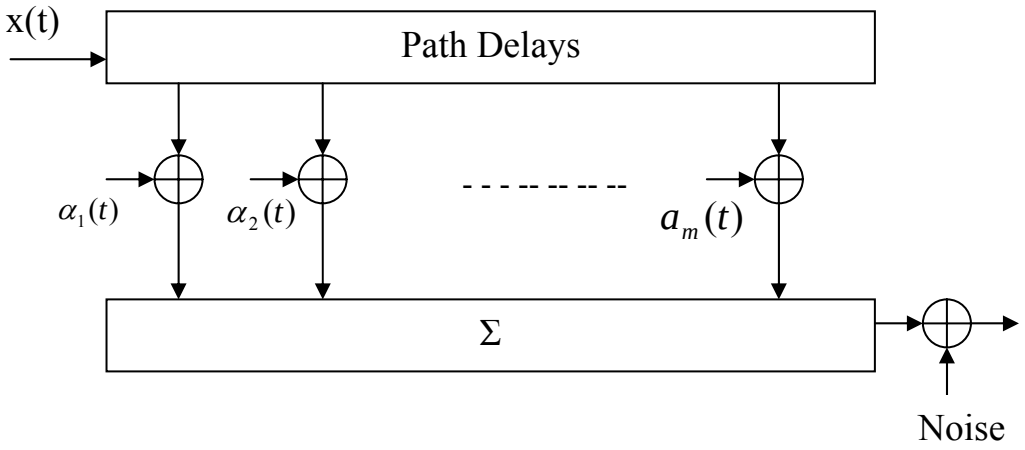

Figure 5 - Multipath Fading Channel Model

In this study, the Rural Area (RA) model according to COST 207 is used in the simulations. The COST 207 model was presented as an outdoor wireless channel

model in Europe [11], where power gain, time delay and Doppler spreading categories were specified for four typical environments. The four typical environments were rural area (RA), typical urban area (TU), bad urban area (BU), and hilly terrain (HT). The parameters of the 4 tap Rural Area channel model are given in the Table 2.

Table 2 - Parameters of the COST207 Rural Area (RA) model

Tap Number	1	2	3	4
Delay (μs)	0	0.2	0.4	0.6
Power (dB)	0	-2	-10	-20
Doppler Category	RICE	CLASS	CLASS	CLASS

In Table 2, Power (dB) shows the normalize path gain (dB) of each path. RICE means Ricean distribution, while Class means classical (Jake) Doppler spectrum.

Doppler spectrum determines the time variations of the channel. The most commonly used, and in a certain sense, the worst-case Doppler spectrum is the classical Doppler spectrum which is also called Jakes spectrum.

In this spectrum type, all the angle between vehicle velocity vector and radio wave are assumed to be uniformly distributed [13]. The classical Doppler spectrum can be defined as:

$$S(f) = \frac{1}{\left[1 - (\frac{f}{f_D})^2\right]^{1/2}} \quad \text{for} \quad f \in (-f_D, f_D) \tag{9}$$

where f_D is maximum Doppler shift, and

$$f_D = \frac{v.f_c}{c} \tag{10}$$

where v is the velocity of the mobile and f_c is the carrier frequency.

In multipath fading model, channel estimation and equalization is used in order to estimate channel impulse response and equalize the received data. In this study, Least Squares (LS) channel estimation and Zero forcing (ZF) equalizer is used by employing pilots. Bit Error Rate performance of OFDM under Multipath Rayleigh Fading Channel (with f_D=50 Hz) with BPSK modulation scheme is shown below in figure 6.

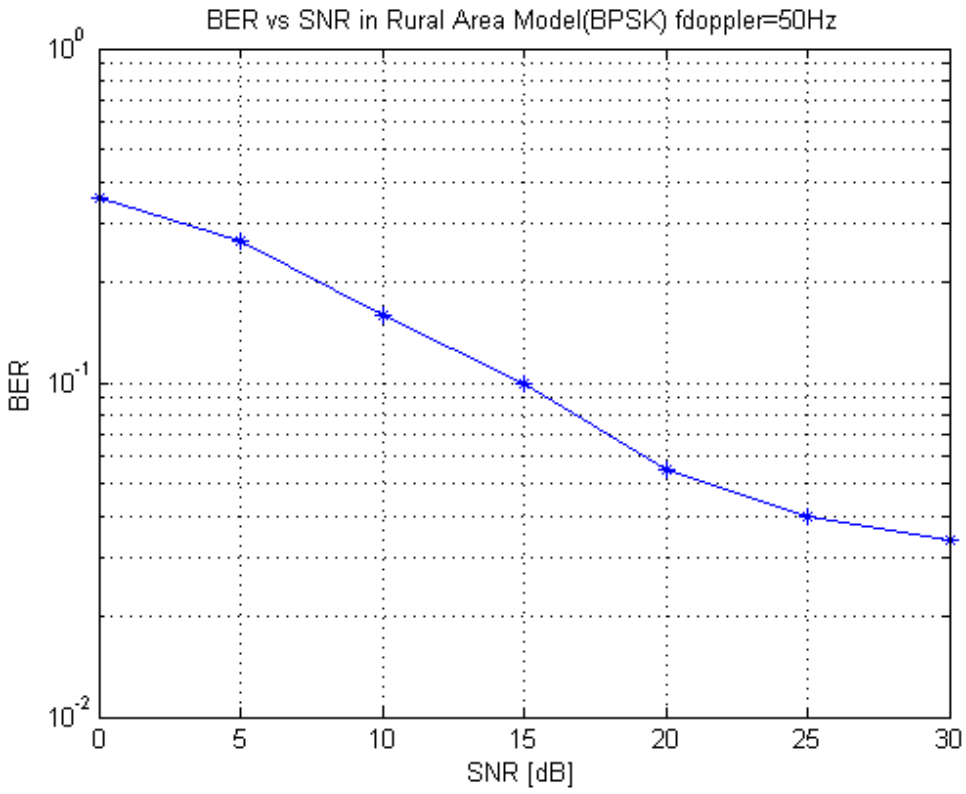

Figure 6 - BER performance of OFDM in Multipath Rayleigh Fading channel

CHAPTER 3

ICI PROBLEM and CANCELLATION

3.1 Factors Inducing ICI

Inter-carrier interference (ICI) is a special problem in the OFDM system. In this section, the factors inducing ICI will be investigated.

There are two factors that cause the ICI, namely frequency offset and time variations. However, mainly we will interest in frequency offset effects since time variations can be modelled as frequency offsets.

Time Variations: In previous literature [14], certain time variations of channels can be modelled as a white Gaussian random noise when subcarrier number is large enough. In general, time variations can be modelled as frequency offsets, such as Doppler shift. Effect of time variations to ICI is out of scope of this study.

Frequency Offset: The main disadvantage of OFDM, is its susceptibility to small differences in frequency at the transmitter and receiver, namely the frequency offset. This frequency offset can be caused by Doppler shifts due to relative motion between the transmitter and receiver, or by differences between the frequencies of the local oscillators at the transmitter and receiver namely the synchronization errors.

In addition, multipath fading has an effect on ICI too. Actually, the multipath fading does not cause ICI, but it will make the ICI problem worse. In a multipath

fading medium, ICI is more complicated to calculate, because there are many time-delayed versions of received signals with different gains and different phase offsets.

In this thesis, our main concern is the normalized carrier frequency offset (CFO) which can be expressed as

$$\varepsilon = \frac{\Delta f}{f_{sub}} = \Delta f T_s \tag{11}$$

where ε is the normalized CFO, f_{sub} denotes the subchannel spacing, T_s is the subcarrier symbol period and Δf is carrier frequency offset (CFO). Δf can be expressed by:

$$\Delta f = f_D + f_{sync} \tag{12}$$

where f_D is Doppler shift and f_{sync} is the synchronization error between transmitter and receiver. These effects are explained in the following part in detail:

3.1.1 Doppler Effect

Doppler effect occurs when there exists a relative motion between receiver and transmitter. In general, the Doppler frequency shift is expressed in terms of the relative velocity, the angle between the velocity direction and transmitter, and the carrier frequency, as shown in Figure 7.

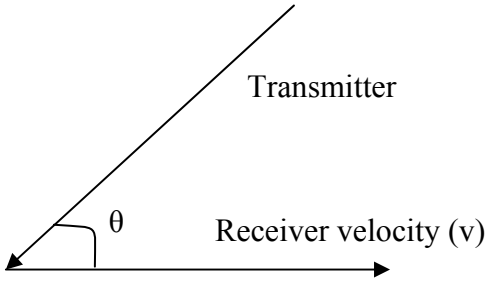

Figure 7 – Angle of the Doppler Effect

The value of Doppler shift can be given as:

$$f_D = \frac{v.f_c}{c}\cos(\theta) \tag{13}$$

where θ is the angle between the receiver velocity vector and transmitter, v is the receiver velocity, c is the speed of light and, f_c is the carrier frequency. θ is generally modelled as a uniformly distributed random variable between 0 and 2π.

3.1.2 Synchronization Errors

In general, most of the wireless receivers cannot make perfect frequency synchronization. Practical oscillators for synchronization are usually unstable and this effect introduces frequency offset. Although this small offset is negligible in some communication systems, it is a severe problem in the OFDM systems. In most situations, the oscillator frequency offset varies from 20 ppm (Parts Per Million) to 100 ppm. Hence, the frequency offset could not be ignored.

3.2 Analysis of ICI

In an AWGN channel, the frequency offset is modelled as a time varying multiplicative factor introduced in the channel [15], as shown in Figure 8.

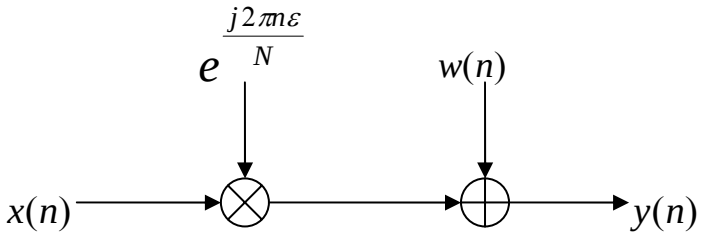

Figure 8 - Frequency Offset Model

The received signal is given as:

$$y(n) = x(n)\, e^{\frac{j2\pi n\varepsilon}{N}} + w(n) \tag{14}$$

where ε is the normalized frequency offset and *w(n)* is the AWGN introduced in the channel. Since in AWGN channel $h(n) = \delta(n)$, h(n) is not considered in this formulation.

To understand the effect of ε on the received symbol stream, we will analyze the received symbol Y(k) on the k^{th} sub-carrier [16], [17] . Obtaining (15) from (5) is detailed in Appendix A. Received symbol on the k^{th} sub-carrier is expressed as:

$$Y_i(k) = X_i(k)\, S(0) + \sum_{l=0, l\neq k}^{N-1} X_i(l)\, S(l-k) + n_k \qquad \text{k=0,1,…..N-1} \tag{15}$$

where, $X_i(k)$ is the transmitted symbol for the k^{th} subcarrier in the i^{th} block, N is the total number of subcarriers , n_k is the FFT of w(n). The sequence $S(l-k)$ is defined as the ICI coefficient between l^{th} and k^{th} subcarriers. These ICI components are the interfering signals and they are transmitted on sub-carriers other than the k^{th} sub-carrier. The ICI coefficients are given by [18] :

$$S(l-k) = \exp(\, j\pi(l+\varepsilon-k)(1-\frac{1}{N}))\frac{\sin(\pi(l+\varepsilon-k))}{N\sin(\pi(l+\varepsilon-k)/N)} \tag{16}$$

In equation (15), $X_i(k)S(0)$ represents the desired signal and if there is no frequency error, this term takes its maximum value.

$\sum_{l=0, l\neq k}^{N-1} X_i(l)S(l-k)$ term defines the ICI components in the received data. An analysis of $|S(l-k)|$ is shown in Figure 9 when *l*=0 and N=32. In this figure, the frequency offset values are taken ε =0.2 and ε =0.4. The figure shows that as ε

becomes larger, the desired part $|S(0)|$ decreases and the undesired part $|S(l-k)|$ increases.

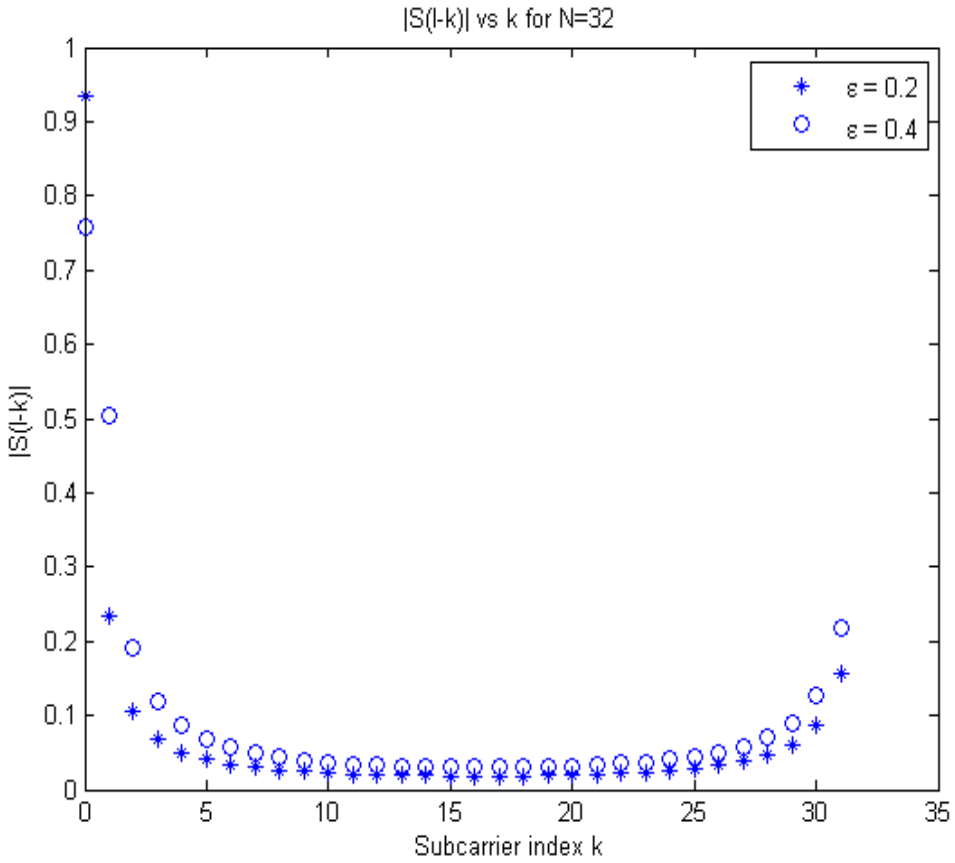

Figure 9 - ICI component $|S(l-k)|$ versus k for N=32

Due to the frequency offset, the signal energy in the k^{th} subcarrier is reduced and this energy is transferred to the other subcarriers. This energy gain by the other subcarriers is the ICI energy.

In the figure, it can easily be seen that the adjacent carrier of the k^{th} carrier steals more energy than the other subcarriers; that means adjacent carrier has the maximum contribution to the ICI [17], [18]. This fact is used in the ICI self-cancellation technique that will be explained in the next chapter.

3.3 Carrier to Interference Ratio (CIR)

The carrier-to-interference ratio (CIR) is the ratio of the signal power to the power in the interference components. CIR serves as a good indication of signal quality. While deriving CIR expression, the additive noise is omitted and it is assumed that the transmitted data have zero mean and statistically independent.

To obtain the CIR expression, desired signal power level, and ICI power shall be defined first. The system ICI power level can be evaluated by using the CIR [19]. The desired received signal power on the k^{th} subcarrier can be defined as:

$$E\left\{\left|C(k)\right|^2\right\} = E\left\{\left|X(k)S(0)\right|^2\right\} \tag{17}$$

The ICI power on the k^{th} subcarrier can be defined as:

$$E\left\{\left|I(k)\right|^2\right\} = E\left\{\left|\sum_{l=0,l\neq k}^{N-1} X(l)S(l-k)\right|^2\right\} \tag{18}$$

CIR is the ratio of the signal power to the power in the interference components. Therefore, the CIR expression for subcarrier k, where 0 < k < N-1 can be obtained as:

$$CIR = \frac{\left|S(k)\right|^2}{\sum_{l=0,l\neq k}^{N-1}\left|S(l-k)\right|^2} = \frac{\left|S(0)\right|^2}{\sum_{l=1}^{N-1}\left|S(l)\right|^2} \tag{19}$$

Figure 10 shows average CIR (in dB) as a function of ε when N=64.

It is evident from (19) that the average CIR is a function of N and ε, but the analysis shows that the CIR, for a given ε, results in a maximum change of 0.068 dB when N>8. Consequently, we can say that the average CIR only depends on the normalized frequency offset ε approximately.

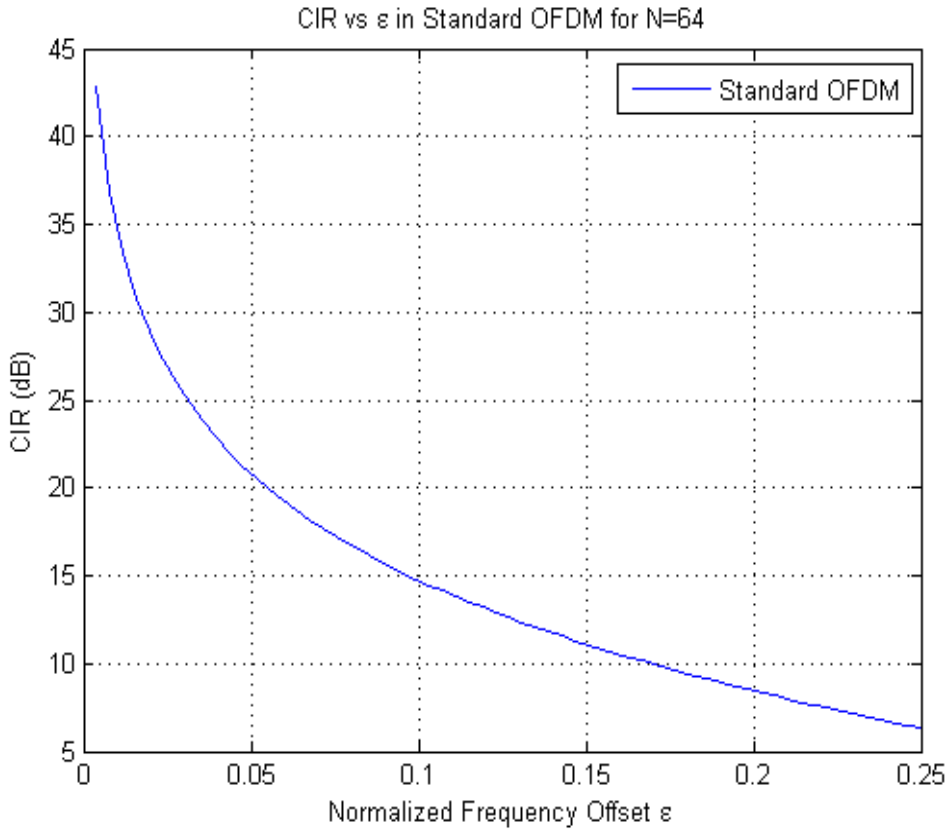

Figure 10 - CIR versus ε for a Standard OFDM system

In the figure, it can be seen that carrier to interference ratio for an OFDM system is inversely proportional to ε because when ε increases, $|S(l-k)|$ increases and $|S(0)|$ decreases as shown previously in Figure 9.

3.4 Solutions for ICI

There are different solutions for the ICI problem. These solutions can be grouped mainly in three groups:

- Windowing techniques
- CFO estimation and Correction techniques
  - Data-Aided methods
  - Blind methods
- Repeated Data Methods

3.4.1 Windowing Techniques

In this technique, OFDM structure is modified to create a windowing effect to the signal. The windowing techniques in OFDM can be categorized into two groups. One group applies windowing in the transmit side, which only applies in the systems without cyclic prefix [20]. Another group, Nyquist windowing techniques, apply windowing in front of FFT at the receiver side [21]. Note that, Nyquist windows reduce the side lobe and this provides the carrier orthogonality.

We will detail two different types of receiver windowing functions in the next chapter; second order polynomial class of Nyquist windows [22] and Nyquist window with Franks pulse used [23].

3.4.2 CFO Estimation and Correction Techniques

These techniques use pilot sequences, virtual carriers, and blind signal processing techniques. In these methods, the CFO is estimated first and then CFO correction is done.

In CFO correction process, received data $y_i(n)$ is multiplied with $e^{\frac{-j2\pi\hat{\varepsilon}n}{N}}$ in order to compensate the frequency offset effect that is defined in (14). Then FFT of the product is taken and corrected data can be expressed by:

$$\hat{x}_i(n) = FFT\left\{ y_i(n) e^{\frac{-j2\pi\hat{\varepsilon}n}{N}} \right\} \tag{20}$$

We can separate these methods into two groups; data-aided methods and blind methods. Data-aided methods use pilot sequences or virtual carriers to estimate CFO. [24]-[29]. Maximum Likelihood method for CFO estimation is used by repeating the transmitted data [19], which was proved equivalent to MUSIC-based algorithms.

Blind methods generally use some part of the transmitted data or guard interval [30]-[34]. J. Van de Beek and M. Sandell used blind ML estimation of time and frequency offset method [30]. Liu and Tureli proposed MUSIC-based and ESPRIT-based algorithms to estimate CFO [33]. It shows that the data-aided methods yield much better performance than that of blind methods at the cost of bandwidth efficiency.

We will detail the conventional pilot-aided and clustered-pilot aided CFO estimation methods in the next chapter.

3.4.3 Repeated Data Methods

The repeated data methods for ICI cancellation are first examined by Zhao with ICI self cancellation scheme [18]. Compared with other schemes, only half the bandwidth is used for information transmission in the repeated data methods. In other words, only half of the full data rate can be achieved and this is the disadvantage of these methods. The redundant information in the repeated data methods can be applied to eliminate the ICI at the receiver and this elimination brings an important advantage since these methods show really better performance than other schemes. The principles of ICI self-cancellation and its derivatives will be studied in the next chapter.

CHAPTER 4

ICI CANCELLATION IN OFDM SYSTEMS

4.1 Repeated Data Methods for ICI Cancellation

In this part, repeated data methods will be mentioned. In these methods, only half the bandwidth is used for information transmission. At first Self Cancellation scheme and Symmetric Symbol Repetition (SSR) scheme will be analyzed. Since, these methods are affected by phase rotation especially in higher modulation schemes such as 16 QAM, Adjacent Conjugate Symbol Repetition and Symmetric Conjugate Symbol Repetition schemes are implemented afterwards to mitigate this effect.

4.1.1 Self Cancellation Scheme

The ICI self-cancellation scheme is a very simple way for suppressing ICI in OFDM. The main idea is to modulate one data symbol onto a group of subcarriers with predefined weighting coefficients. By doing so, the ICI signals generated within a group can be "self-cancelled".

Remember that in (15), $X_i(k)S(0)$ represents the desired signal and $\sum_{l=0,l\neq k}^{N-1} X_i(l)S(l-k)$ term defines the ICI components in the received data. To have a better understanding of ICI component, $|S(l-k)|$, $\mathrm{Re}(S(l-k))$ and $\mathrm{Im}(S(l-k))$ are shown below with ε=0.4 and N=16.

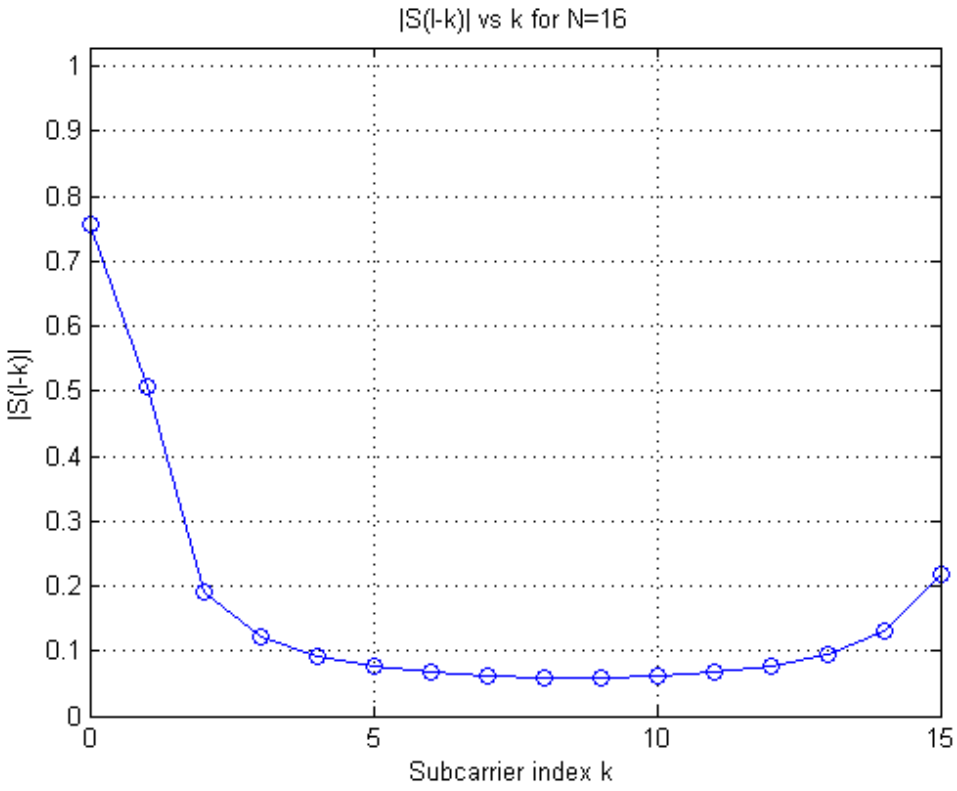

Figure 11 - $\left|S(l-k)\right|$ versus k for N=16(ε=0.4)

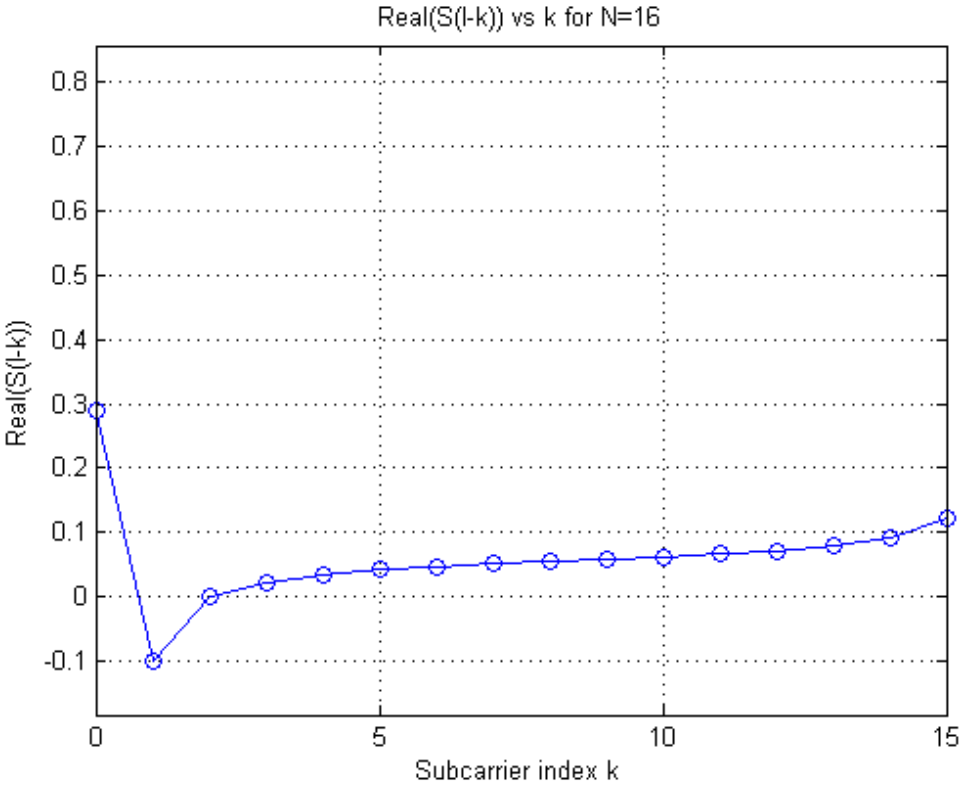

Figure 12 - Real(S(l-k)) versus k for N=16 (ε=0.4)

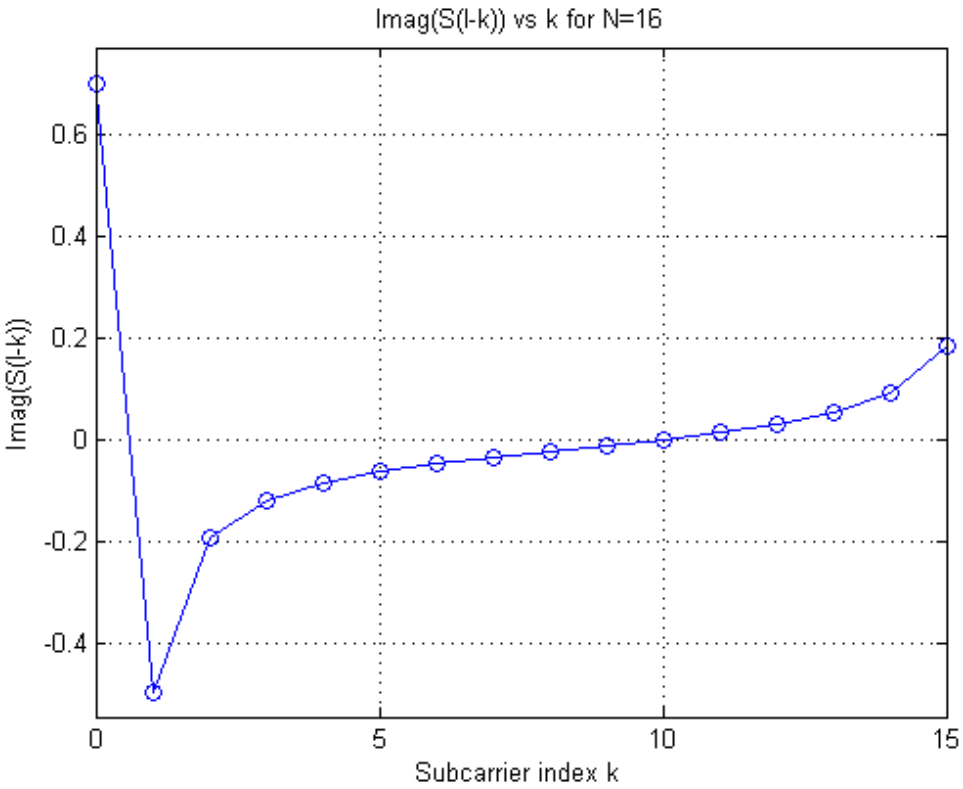

Figure 13 - Imag(S(l-k)) versus k for N=16(ε=0.4)

Modulation

In the above figures real, imaginary and magnitude parts of the ICI component *S(l-k)* changes with respect to the subcarrier index. But nearly for all *(l-k)* values, the difference between *S(l-k)* and *S(l-k+1)* is very small. This fact gives Zhao the Self Cancellation idea [17], [18]. Her point of view is:

"If a complex data pair (X, -X) is modulated onto two adjacent subcarriers (l, l+1), then the ICI signals generated by the subcarrier l will be cancelled out significantly by the ICI generated by $(l+1)^{st}$ *subcarrier"* [18].

We want to analyse the new received data on subcarrier k. First let us assume that data pairs (X,-X) are modulated onto adjacent subcarriers, such as:

$$X(1) = -X(0), X(3) = -X(2), \ldots\ldots\ldots\ldots, X(N-1) = -X(N-2) \qquad (21)$$

then the modulated data on subcarrier k is:

$$Y'(k) = \sum_{\substack{l=0 \\ l=even}}^{N-2} X(l)\left[S(l-k) - S(l+1-k)\right] + n_k \tag{22}$$

It is clear that, the new ICI coefficient is:

$$S'(l-k) = S(l-k) - S(l+1-k) \tag{23}$$

The figure below is a comparison between $S(l-k)$ and $S'(l-k)$ on a logarithmic scale.

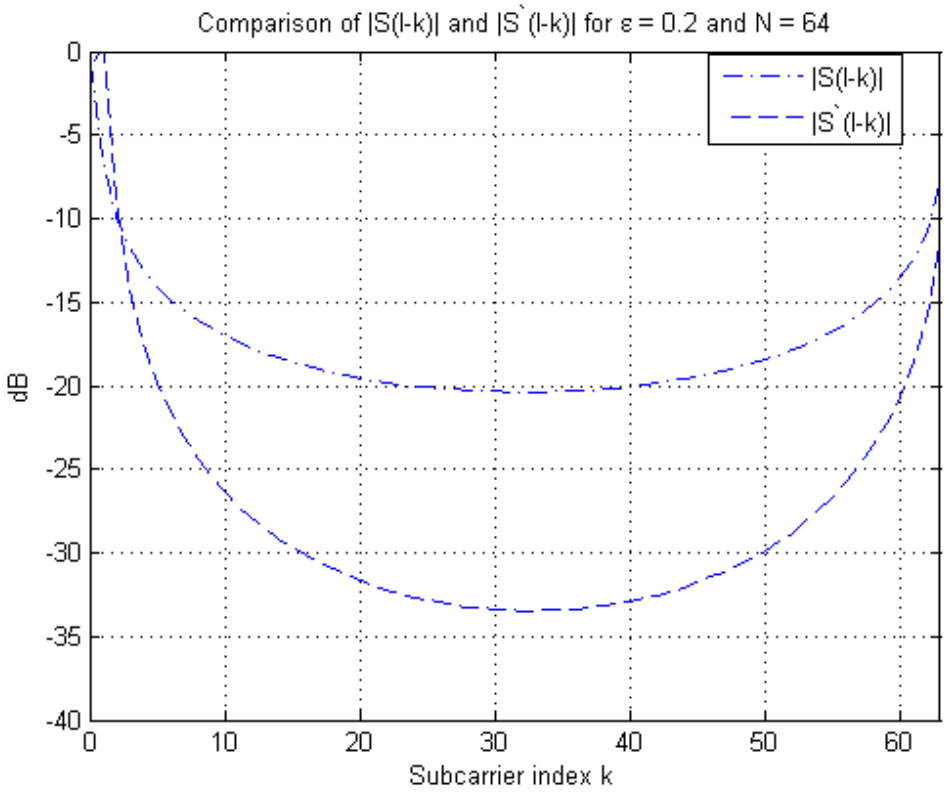

Figure 14 - Comparison of $S(l-k)$ and $S'(l-k)$ for N=64 and ε=0.2

From the figure, it can be seen that, for most of the values $|S'(l-k)| << |S(l-k)|$ which means that ICI decreases when a complex data pair *(X,-X)* is modulated in adjacent subcarriers. This result depends on two facts:

- In the summation (22) l takes only even values while in (15) l takes all values. This reduces the total number of the interference signals in (22) that is half of the interference signals in (15).
- The ICI signals in (22) are much smaller than those in (15)

Therefore, both the number of ICI signals and the amplitudes of the ICI coefficients have been reduced and this is called by Zhao as "ICI Cancelling Modulation" [18].

Demodulation

At the "ICI cancelling modulation" phase, half of the bandwidth is used for redundant symbols, and this signal redundancy makes it possible to improve the system performance at the receiver side. This is key idea in so-called "ICI cancelling demodulation" [18], which will be analyzed in this section. The demodulation works in such a way that each signal at the $(k+1)^{st}$ subcarrier is multiplied by "-1" and then added with the one at the k^{th} subcarrier. Here note that k denotes even number. So the new data sequence is used for making symbol decision.

First, we shall express the received (modulated) data on the $(k+1)^{st}$ subcarrier by just taking "k+1" instead of "k" in (22):

$$Y'(k+1) = \sum_{\substack{l=0 \\ l=even}}^{N-2} X(l)\left[S(l-k-1) - S(l-k)\right] + n_{k+1} \tag{24}$$

and the new obtained (demodulated) data for the k^{th} subcarrier is [18]:

$$\begin{aligned} Y''(k) &= Y'(k) - Y'(k+1) \\ &= \sum_{l=0, l=even}^{N-2} X(l)\left[-S(l-k-1) + 2S(l-k) - S(l-k+1)\right] + n_k + n_{k+1} \end{aligned} \tag{25}$$

Therefore, the corresponding ICI coefficient then becomes [18]

$$S''(l-k) = -S(l+1-k) + 2S(l-k) - S(l-k+1) \tag{26}$$

For standard OFDM the ICI component is $S(l-k)$, for ICI cancelling modulation we have found $S'(l-k)$ and for combined ICI cancelling modulation and demodulation we have found $S''(l-k)$. The figure below shows the amplitude comparison (on logarithmic scale) of these three coefficients for N=64 and ε=0.2:

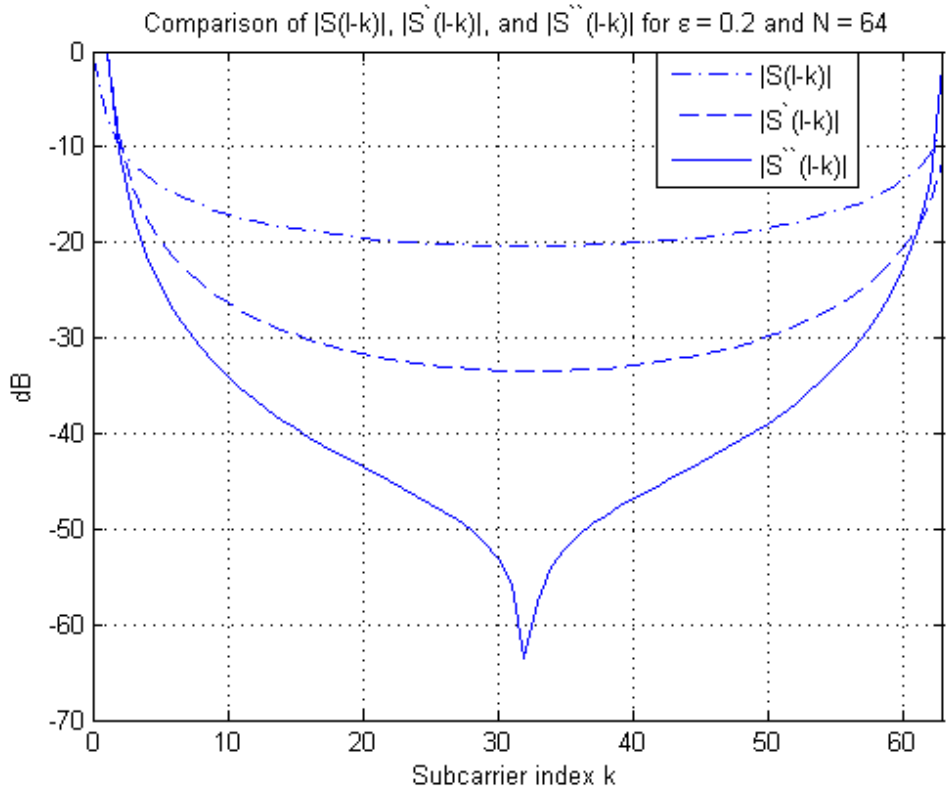

Figure 15 - A comp. between $|S(l-k)|, |S'(l-k)| and |S''(l-k)|$ for N=64, ε=0.2

It is evident that, for the majority of (*l-k)* values $|S(l-k)| >> |S'(l-k)| >> |S''(l-k)|$. Thus, the ICI signals become smaller if ICI cancelling modulation is applied. Moreover, the ICI cancelling demodulation can further reduce the residual ICI in the received signals. This combined ICI cancelling modulation and demodulation method is called the "ICI self-cancellation scheme" [17], [18].

Carrier to Interference Ratio

ICI self cancellation method also improves the CIR. The signal level increases by a factor of two, due to coherent addition, whereas the noise level is proportional to $\sqrt{2}$ because of noncoherent addition of the noise on different subcarriers. Using ICI coefficient given by (19), the theoretical average CIR of the ICI self-cancellation scheme can be derived as [18]:

$$CIR = \frac{\left|-S(-1)+2S(0)-S(1)\right|^2}{\sum_{l=2,l=even}^{N-1}\left|-S(l-1)+2S(l)-S(l+1)\right|^2} \tag{27}$$

Figure 16 shows theoretical average CIR comparison between ICI self cancellation scheme (27) and Standard OFDM (19). It is clear that, ICI self cancellation scheme gives more than 15-dB CIR improvement in the range $0<\varepsilon<0.25$.

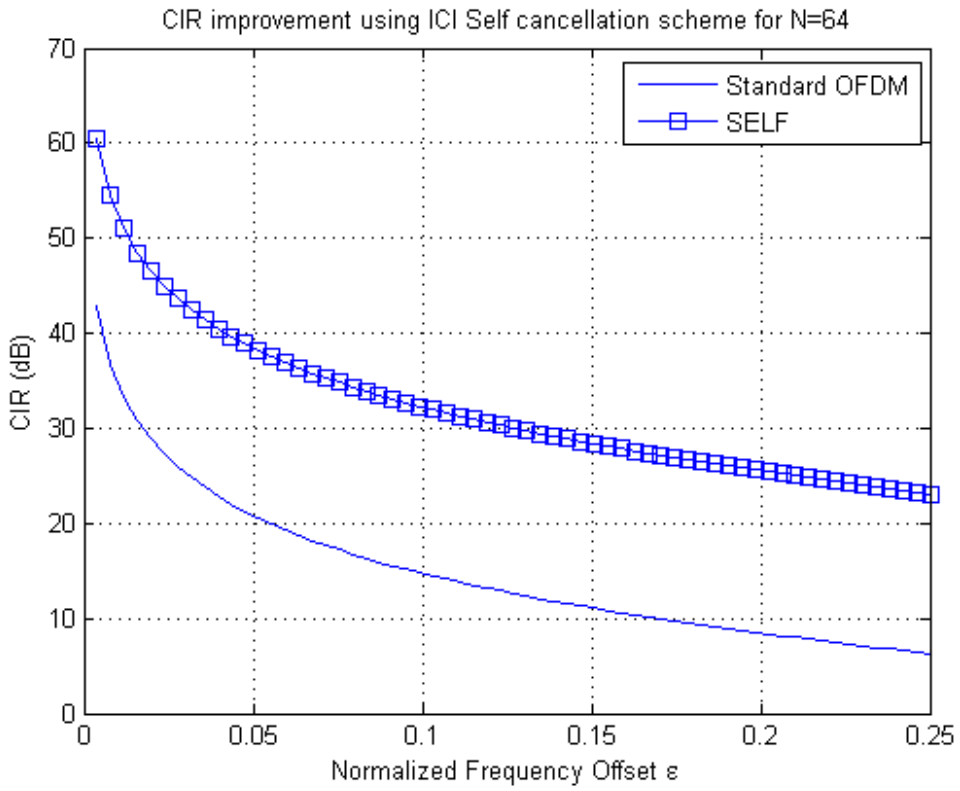

Figure 16 - CIR improvement using Self Cancellation scheme for N=64

4.1.2 Symmetric Symbol Repetition (SSR) Scheme

In Self Cancellation scheme, a complex data pair (X, -X) is modulated onto two adjacent subcarriers *(l, l+1)*, then the ICI signals generated by the subcarrier *l* will be cancelled out significantly by the ICI generated by *(l+1)* subcarrier. Sathananthan modified this scheme by using the odd symmetry in $S(l-k), \mathrm{Re}(S(l-k))$ and $\mathrm{Im}(S(l-k))$ [35].

He showed that ICI coefficients are approximately symmetric, such as $S(k) \cong S(N-1-k)$ for $k \neq 0$. Therefore, modulating complex data pairs (X,-X) onto k^{th} and $(N-1-k)^{th}$ subcarriers have a similar effect to decrease ICI. This is the key idea used in SSR scheme to reduce the ICI effects [35], [36]. This approach also offers frequency diversity because of the frequency separation between the same data symbols.

Modulation

In this scheme, same modulated symbols with opposite polarity are transmitted on subcarrier *k* and *(N - k - 1)*. Therefore, the data block becomes:

$$\left\{X(0), X(1), X(2), \ldots\ldots\ldots X\left(\frac{N}{2}-1\right), -X\left(\frac{N}{2}-1\right), \ldots\ldots\ldots\ldots -X(2), -X(1), -X(0)\right\} \qquad (28)$$

Thus, this cancellation technique halves the data throughput like self cancellation scheme.

Demodulation

The receiver combines the received samples $Y'(k)$ and $Y'(N-k-1)$ and the decision variable becomes [35], [36]:

$$Y''(k) = Y'(k) - Y'(N-k-1)$$

$$Y''(k) = \left[\begin{array}{l} (2S(0) - S(N-1) - S(1-N))X(k) \\ + \sum_{l=0}^{N/2-1} (S(l-k) - S(k-l) - S(N-k-1-l) - S(l+k+1-N))X(l) \end{array} \right] + n_k + n_{k+1} \quad (29)$$

Carrier to Interference Ratio

The average CIR of SSR scheme can be expressed as [35], [36]:

$$CIR_m = \frac{\left| -S(N-1) + 2S(0) - S(1-N) \right|^2}{\sum_{l=1}^{N/2-1} \left| S(l) + S(-l) - S(N-1-l) - S(l+1-N) \right|^2} \quad (30)$$

Figure 17 shows the CIR improvement of SSR scheme to the standard OFDM.

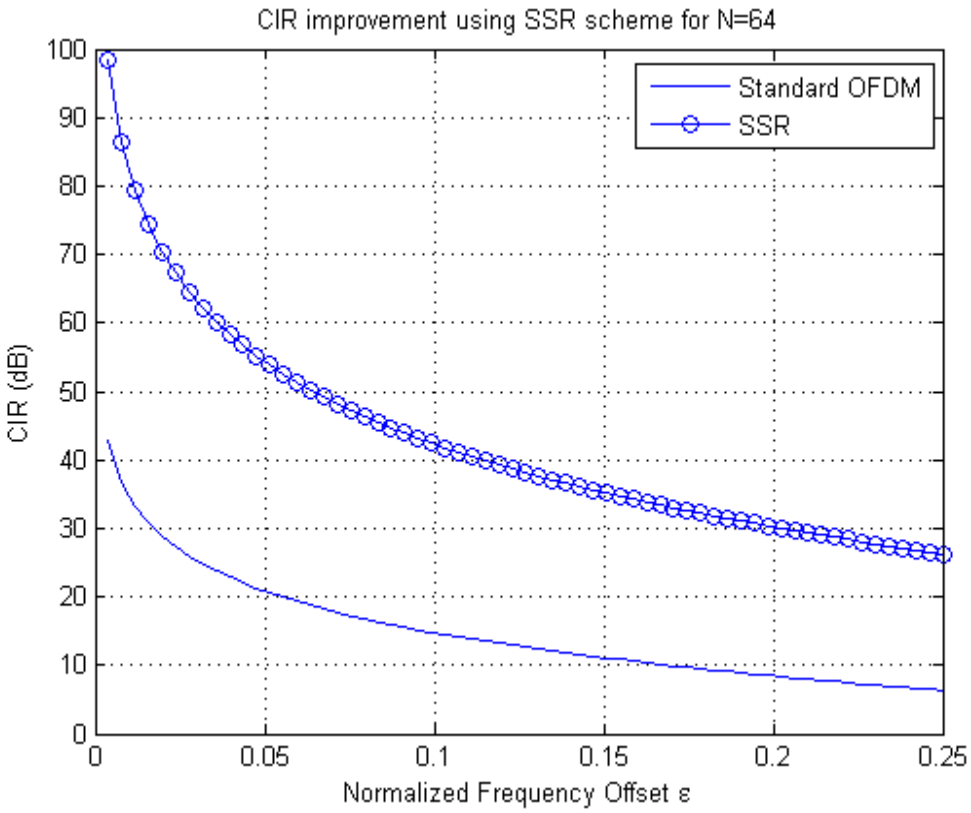

Figure 17 - CIR improvement using SSR scheme for N=64

Previously mentioned Self Cancellation and SSR methods are not effective in removing the constant phase error caused by frequency offset. In these schemes, the simple mapping of modulated symbols at the transmitter and the linear combining of received samples at the receiver preserve the constant phase rotation of each symbols. To analyse the phase rotation on the ICI component, (for N>>1) we can approximately write (16) as:

$$S(l-k) \cong \frac{\sin \pi\varepsilon}{N \sin \frac{\pi}{\varepsilon}(k+\varepsilon)} e^{j\pi\varepsilon} \tag{31}$$

Above equation (31) shows that, CFO leads to both ICI coefficient and phase rotation of desired signals. This phase rotation is constant and equal to "πε" on each subcarrier. This phase rotation degrades the error performance if coherent detection is used at the receiver. Particularly, these effects are significant with higher order modulation schemes such as 16-QAM.

To mitigate this effect, two ICI cancellation schemes named as "Adjacent Conjugate Symbol Repetition (ACSR)" and "Symmetric Conjugate Symbol Repetition (SCSR)" are proposed by Santhananthan [35]. These schemes are capable of removing the phase rotation as well as ICI.

4.1.3 Adjacent Conjugate Symbol Repetition (ACSR) Scheme

Modulation

Like the Self cancellation scheme mentioned in 4.1.1, a complex data pair is modulated on to k^{th} and $(k+1)^{st}$ (adjacent) subcarriers in ACSR. However, in ACSR complex data pair (X,X*) is used instead of (X,-X) to mitigate the phase rotation effect, where "*" denotes the complex conjugate. Therefore, the data block will be:

$$\left\{X(0), X^*(0), X(1), X^*(1), \ldots\ldots X(\frac{N}{2}-1), X^*(\frac{N}{2}-1)\right\} \tag{32}$$

Demodulation

The receiver combines the received samples $Y'(k)$ and $Y'(k+1)$ and the decision variable is expressed as [35]:

$$\begin{aligned} Y''(k) &= Y'(k) + \text{Y'*(k+1)} \\ Y''(k) &= \{S(0) + S^*(0)\}X(k) + \sum_{l=0,2..l\neq k}^{N-1}\{S(l-k) + S^*(k-l)\}X(l) \\ &+ \sum_{l=0,\text{l=even}}^{N-1}\{S(l+1-k) + S^*(l-1-k)\}X^*(l) + n_k - n^*_{k+1} \end{aligned} \tag{33}$$

ACSR removes the phase rotation but note that its ICI terms are enhanced because a self-interference (SI), in addition to intercarrier interference (ICI), is introduced due to the nature of this mapping. However, the gain from suppressing the phase rotation is significant compared to its increased ICI and mitigates this self interference effect.

Carrier to Interference Ratio

Its average CIR can be expressed as [35]:

$$CIR_{ACSR} = \frac{\left|S(0) + S^*(0)\right|^2}{\sum_{l=2,l=even}^{N-1}\left|S(l) - S^*(l)\right|^2 + \sum_{l=0,l=even}^{N-1}\left|S(l+1) - S^*(l-1)\right|^2} \tag{34}$$

Note that, this unresolved phase error is not realized in the average CIR, which is usually used to evaluate the performance. Figure 18 shows the CIR improvement using ACSR scheme.

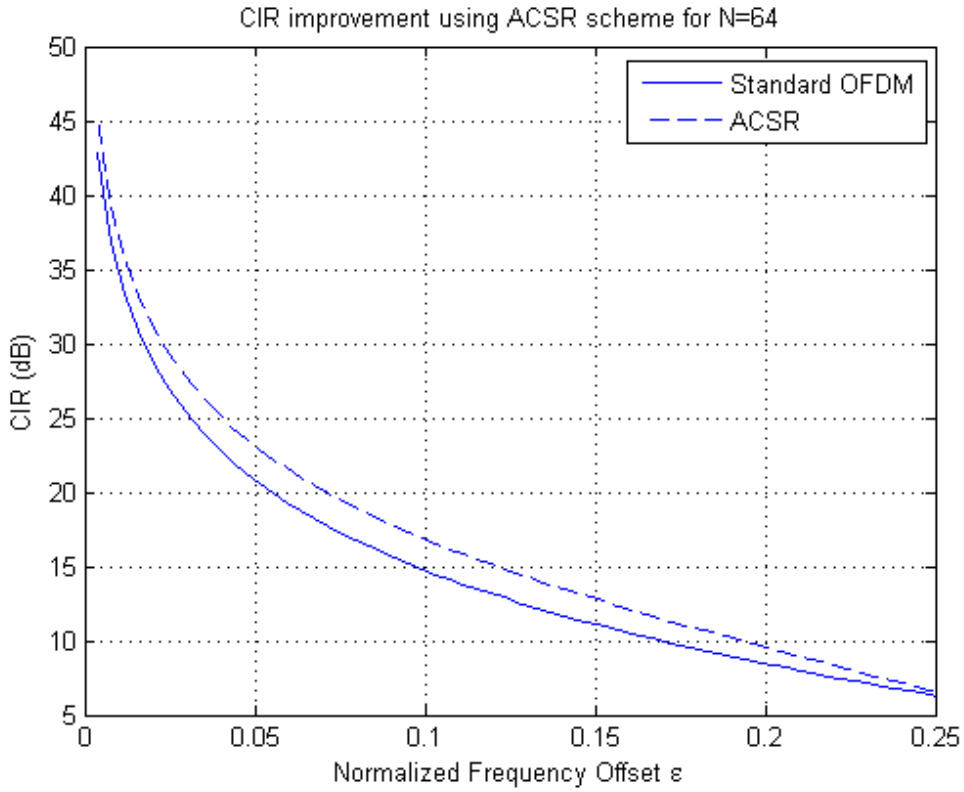

Figure 18 - CIR improvement using ACSR scheme for N=64

4.1.4 Symmetric Conjugate Symbol Repetition (SCSR) Scheme

Like the Symmetric Symbol Repetition (SSR) scheme mentioned in 4.1.2, SCSR scheme also uses the odd symmetry of $|S(l-k)|$. The complex data pair is modulated on to k^{th} and $(N-1-k)^{th}$ subcarriers but note that complex data pair (X,X*) is used instead of (X,-X) to mitigate the phase rotation effect.

Modulation

In SCSR, the data pair (X,X*) is mapped on k^{th} and $(N-1-k)^{th}$ subcarriers. Hence, the data block becomes:

$$\left\{X(0), X(1), X(2), \ldots\ldots\ldots X(\frac{N}{2}-1), X^*(\frac{N}{2}-1), \ldots\ldots\ldots\ldots X^*(2), X^*(1), X^*(0)\right\} \quad (35)$$

Demodulation

The receiver combines the received samples $Y'(k)$ and $Y'(N-1-k)$ and the decision variable becomes [35]:

$$Y''(k) = Y'(k) - Y'^*(N-k-1)$$
$$Y''(k) = \{S(0) + S^*(0)\}X(k) + \sum_{l=0, l\neq k}^{N/2-1}\{S(l-k) + S^*(k-l)\}X(l)$$
$$+ \sum_{l=0}^{N/2-1}\{S(N-1-l-k) + S^*(k+l+1-N)\}X^*(l) + n_k + n_{k+1} \quad (36)$$

Carrier to Interference Ratio

Its average CIR can be expressed as [35]:

$$CIR_{SCSR} = \frac{\left|S(0) + S^*(0)\right|^2}{\sum_{l=1}^{N/2-1}\left|S(l) + S^*(-l)\right|^2 + \sum_{l=1}^{N/2-1}\left|S(N-1-l) + S^*(l+1-N)\right|^2} \quad (37)$$

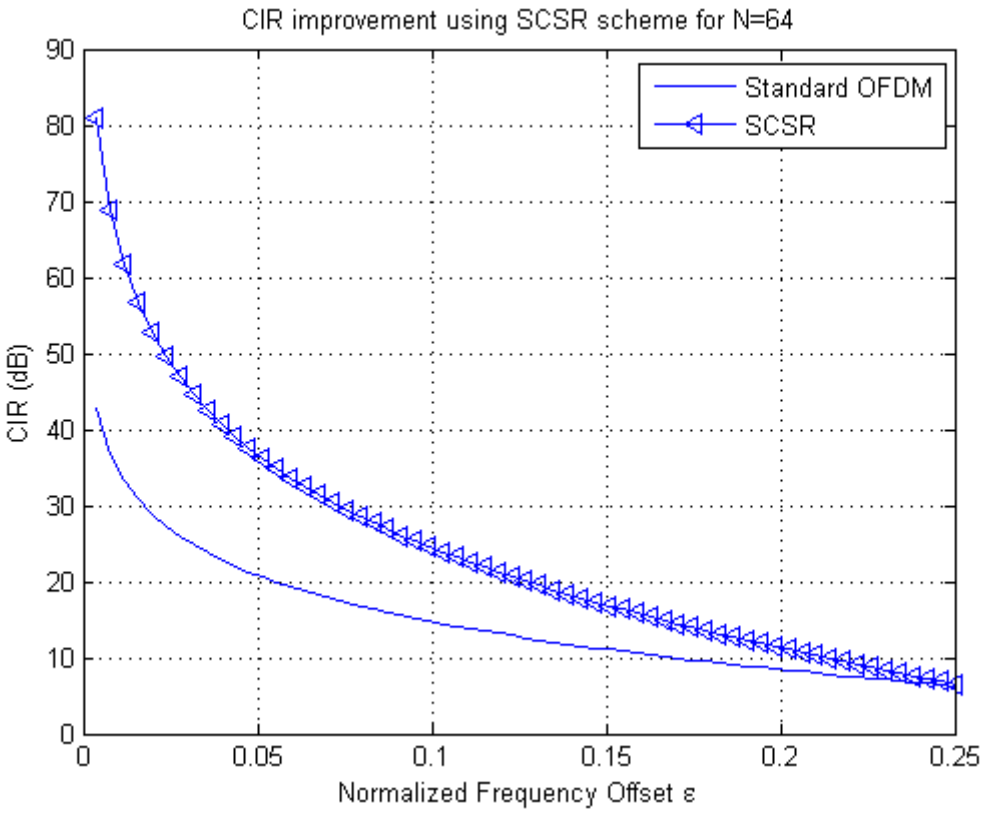

Figure 19 - CIR improvement using SCSR scheme for N=64

4.2 Pilot – Aided CFO Estimation Methods

In this section our main aim is to estimate a CFO by the help of pilots. The underlying principle of these algorithms is that the frequency estimation problem can be converted into a phase estimation problem by considering the phase shift between subsequent received subchannel samples. CFO data can be found from the phase rotation information and Zhang concerned this phase rotation between receiver and transmitter, and equation (38) is obtained as [37] :

$$y_i(n) = e^{(j(\theta_0+(i-1)\phi))} x_i(n) e^{\frac{j2\pi\varepsilon n}{N}} \tag{38}$$

where

$$\phi = 2\pi\varepsilon(1+\frac{G}{N}) \tag{39}$$

is the phase rotation induced by CFO , G is the guard interval length and N is the number of subcarriers. The normalized CFO (ε) can be expressed as:

$$\varepsilon = \frac{\Delta f}{f_{sub}} = \Delta f T \tag{40}$$

as it is mentioned in previous sections.

After taking FFT of the received data, $Y_i(k)$ can be expressed as:

$$Y_i(k) = e^{(j(\theta_0+(i-1)\phi))}\sum_{l=0}^{N-1} X_i(l)\, S\,(l-k) + n_k \tag{41}$$

Especially if we consider the received subcarrier at the m^{th} pilot position at the i^{th} OFDM symbol as $z_i(m)$ [37];

$$z_i(m) = e^{(j(\theta_0+(i-1)\phi))}\sum_{l=0}^{N-1} X_i(l)\, S\,(l-k) \tag{42}$$

Note that the coefficients have the following periodical property; $S(l-m) = S(N+l-m)$

4.2.1 Conventional Pilots – Aided CFO Estimation Scheme

The underlying principle of these algorithms is that the frequency estimation problem can be converted into a phase estimation problem by considering the phase shift between subsequent subchannel samples $z_i(m)$ and $z_{i+1}(m)$, where the subscripts *m* and *i* denote the index of pilot tones and the index of OFDM symbols, respectively.

From [37], we have;

$$z_i(m) = e^{(j(\theta_0+(i-1)\phi))}(S(0)X_i(m) + \sum_{l=0,l\neq m}^{N-1} S(l-m)X_i(l)) \tag{43}$$

and

$$z_{i+1}(m) = e^{(j(\theta_0+i\phi))}(S(0)X_{i+1}(m) + \sum_{l=0,l\neq m}^{N-1} S(l-m)X_{i+1}(l)) \tag{44}$$

It is assumed that, on each pilot tone, identical pilot symbols are transmitted for all OFDM blocks. Assuming the m^{th} subchannel is a pilot tone, all the pilot symbols on m^{th} subchannel should have [37] :

$$X_1(m) = X_2(m) = X_3(m)..... = X_B(m) \tag{45}$$

where B is the total number of OFDM blocks. Using the one pilot tone, an unbiased estimate of the phase can be obtained from a block of B OFDM symbols as [27]-[29]:

$$\hat{\phi}_m = \arctan\left[\frac{\mathrm{Im}\left\{\sum_{i=1}^{B-1} z_i{}^*(m)z_{i+1}(m)\right\}}{\mathrm{Re}\left\{\sum_{i=1}^{B-1} z_i{}^*(m)z_{i+1}(m)\right\}}\right] \tag{46}$$

Subsequently, the normalized CFO can be obtained as,

$$\hat{\varepsilon}_m = \frac{\hat{\phi}_m}{2\pi(1+\frac{G}{N})} \tag{47}$$

that is the normalized CFO estimate for m^{th} pilot tone.

Taking into account all the pilot tones, the averaged estimated CFO can be computed as [37]:

$$\bar{\varepsilon} = \frac{1}{P}\sum_{m\in S}\hat{\varepsilon}_m \tag{48}$$

where P denotes the total number of pilot tones and S represents the set of all pilot tone positions.

After $\bar{\varepsilon}$ is estimated, a CFO correction shall be done to correct the received signals, which suffer the ICI induced by CFO. CFO correction can be expressed as:

$$\hat{x}_i(n) = FFT\left\{ y_i(n) e^{\frac{-j2\pi\bar{\varepsilon}n}{N}} \right\} \tag{49}$$

Carrier to Interference Ratio

Average CIR of conventional pilots method can be expressed as [37]:

$$CIR_m = \frac{|S(0)|^2 |X_i(m)|^2}{\sum_{l=1}^{N-1}|S(l)|^2} \tag{50}$$

where CIR_m denotes the CIR of $z_i(m)$.

If the pilot symbols are designed as pseudo random binary sequence (PRBS), then the average CIR of the conventional pilots method can be expressed as:

$$CIR_m = \frac{|S(0)|^2}{\sum_{l=1}^{N-1}|S(l)|^2} \tag{51}$$

which is equal to the CIR of the standard OFDM system. Therefore, if PRBS pilot symbols are used, no CIR improvement can be obtained by this method.

However, when the pilot symbols are designed as $|E_P|$=2, for all pilots then CIR improvement can be expressed as:

$$CIR_m = \frac{4.|S(0)|^2}{\sum_{l=1}^{N-1}|S(l)|^2} \tag{52}$$

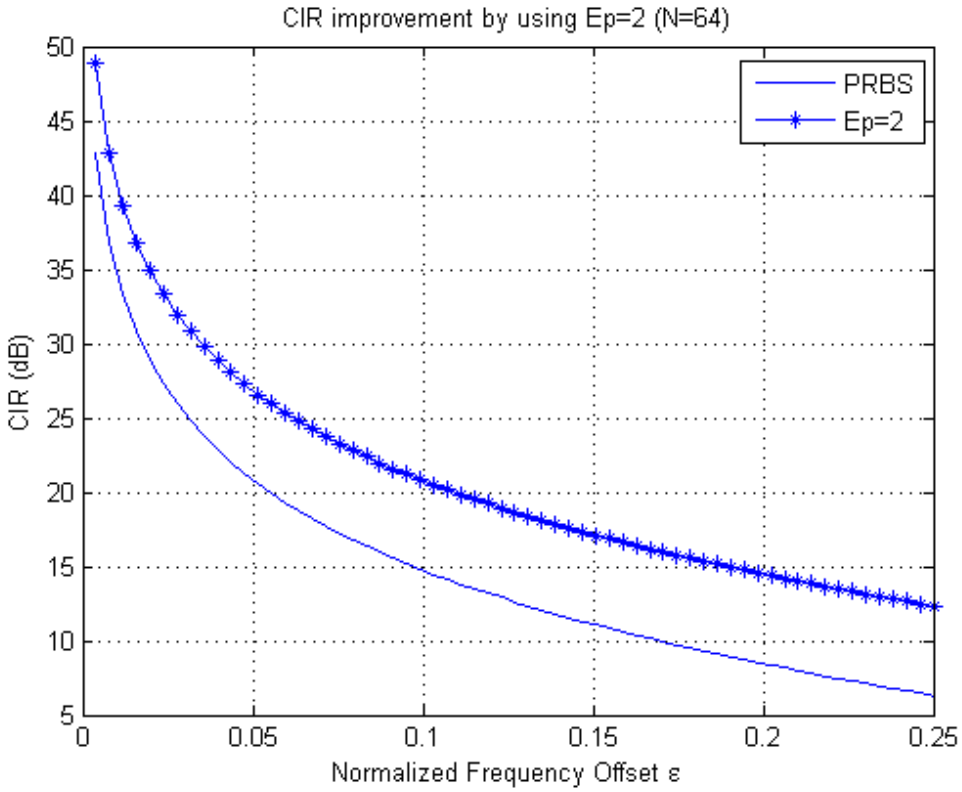

Figure 20 - CIR imp. of Conventional Pilots scheme when pilot power is changed

Figure 20 shows a comparison on CIR performances for conventional pilots scheme when pilot signal power (Ep) is changed. From the figure, it is evident that, when pilot power (Ep) increases, carrier to interference ratio increases for conventional pilots scheme.

4.2.2 Clustered Pilots – Aided CFO Estimation Scheme

More pilot symbols may give a better CFO estimate but at the expense of a lower bandwidth efficiency. Therefore, it is necessary to explore how to locate a limited number of pilot symbols. In other words, given a fixed number of pilots, it is desirable to consider an effective scheme of assigning their positions to give a better CFO estimate.

Unlike the conventional approach, in this chapter, the pilot tones in this study are organized into pairs/clusters [37]. In each pair/cluster, the adjacent pilot symbols to be transmitted are always set to be antipodal, that is, X is transmitted at the left pilot tone and $(-X)$ at the right pilot tone in each cluster , similar to the Self Cancellation scheme [18].

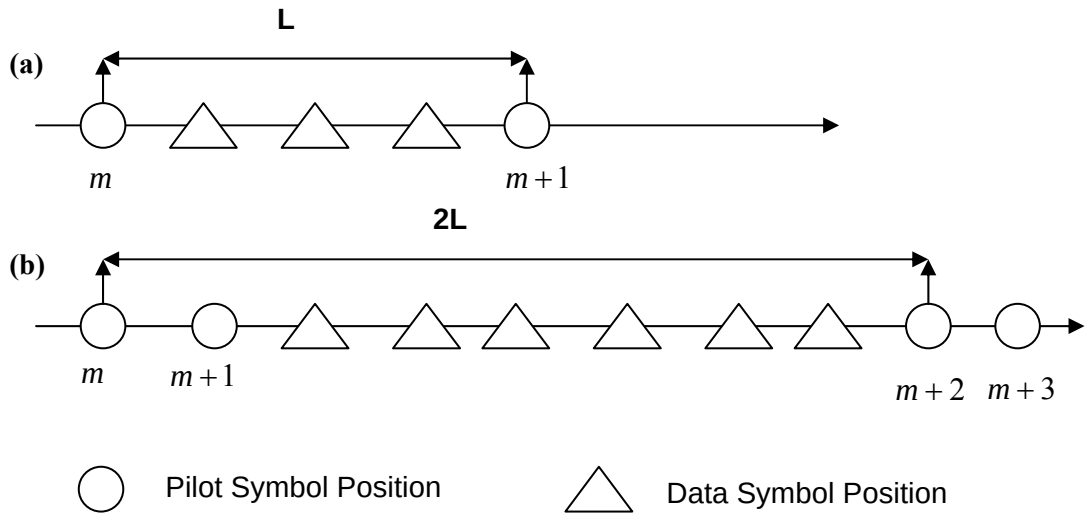

Figure 21 - Comparison of conventional pilot pattern and clustered pilot pattern
(a) conventional pilot pattern (b) clustered pilot pattern

From Figure 21, L denotes the pilot spacing and m denotes the pilot position. The pilot spacing of the equi-spaced (conventional) pilot pattern is L, so the pilot spacing of the clustered pilot pattern should be $2L$. Note that the number of pilot symbols in the clustered pilot pattern is the same as the conventional pilots scheme, but the pilot spacing (L) doubles.

Let S_l, S_r and S denote the sets of the left, right and all pilot positions in one OFDM symbol, respectively. In clustered pilots method, in one pilot cluster, it has $X_i(m) = -X_i(m+1)$ for $m \in S_l$ and $(m+1) \in S_r$ [37].

Modulation

The modulated data on the left pilot tone can be expressed as [37]:

$$z'_i(m) = e^{(j(\theta_0+(i-1)\phi))}\left[\begin{array}{l}\{S(0)-S(1)\}X_i(m) \\ +\sum_{l\in S_l, l\neq m}(S(l-m)-S(l-m-1))X_i(l)+\sum_{l\notin S}S(l-m)X_i(m)\end{array}\right] \quad (53)$$

and the modulated data at the right pilot tone can be written as :

$$z'_i(m) = e^{(j(\theta_0+(i-1)\phi))}\left[\begin{array}{l}\{S(-1)-S(0)\}X_i(m) \\ +\sum_{l\in S_l, l\neq m}(S(l-m-1)-S(l-m))X_i(l)+\sum_{l\notin S}S(l-m-1)X_i(m)\end{array}\right] \quad (54)$$

Demodulation

Next, the values for the clustered pilot tones are subtracted in pairs and the demodulated data at the receiver can be defined as [37]:

$$Z''_i(m) = z'_i(m) - z'_i(m+1) \quad (55)$$

therefore,

$$Z''_i(m) = e^{(j(\theta_0+(i-1)\phi))}\begin{bmatrix}(2S(0)-S(1)-S(-1))X_i(m)\\ +\sum_{l\in S_l, l\neq m}(2S(l-m)-S(l-m+1)-S(l-m-1))X_i(l)\\ +\sum_{l\in S}(S(l-m)-S(l-m-1))X_i(l)\end{bmatrix} \quad (56)$$

From the above equation (54), it can be seen that $Z''_i(m)$ depends on the first and second order difference of the weighting coefficients. In (15) the relationship of the weighting coefficients was illustrated in Figure 15 for the case of N = 64 and $\varepsilon = 0.2$. From figure 15 it is evident that

$$\left|2S(l)-S(l+1)-S(l)\right|^2 << \left|S(l)-S(l-1)\right|^2 \quad (57)$$

for any $l \in S_l$ and $l \neq 0$. Therefore, we can simplify (56) to:

$$Z''_i(m) = e^{(j(\theta_0+(i-1)\phi))}\begin{bmatrix}(2S(0)-S(1)-S(-1))X_i(m)\\ +\sum_{l\notin S}(S(l-m)-S(l-m-1))X_i(l)\end{bmatrix} \quad (58)$$

After replacing $z_i(m)$ with $Z''_i(m)$, the unbiased estimate of phase for clustered pilots method is defined as [37]:

$$\hat{\phi}_m = \arctan\left[\frac{\mathrm{Im}\left\{\sum_{i=1}^{B-1} Z''^*(m)Z''_{i+1}(m)\right\}}{\mathrm{Re}\left\{\sum_{i=1}^{B-1} Z''^*(m)Z''_{i+1}(m)\right\}}\right] \quad (59)$$

Subsequently, the normalized CFO can be obtained as,

$$\hat{\varepsilon}_m = \frac{\hat{\phi}_m}{2\pi(1+\frac{G}{N})} \quad (60)$$

where $\hat{\varepsilon}_m$ is the normalized CFO estimate for m^{th} pilot tone.

Taking into account all the pilot tones, the averaged estimated CFO for clustered pilots can be computed as [37]:

$$\bar{\varepsilon} = \frac{1}{P}\sum_{m\in S} \hat{\varepsilon}_m \tag{61}$$

After $\bar{\varepsilon}$ is estimated, a CFO correction shall be done to correct the received signals, which suffer the ICI induced by CFO. CFO correction can be expressed by (49).

Carrier to Interference Ratio

The signal power of $Z''_i(m)$, E_S, can be evaluated as [40]:

$$\mathrm{E}_S = \left|2S(0) - S(1) - S(-1)\right|^2 \tag{62}$$

and the ICI power of $Z''_i(m)$, E_I, is given by [40]:

$$\mathrm{E}_I = \sum_{l\notin S}\left|S(l) - S(l-1)\right|^2 \tag{63}$$

Hence, the average CIR of the clustered pilot tones can be denoted by [37]:

$$CIR_m = \frac{\left|2S(0) - S(1) - S(-1)\right|^2 \left|X_i(m)\right|^2}{\sum_{l\notin S}\left|S(l) - S(l-1)\right|^2} \tag{64}$$

Figure 22 shows the CIR improvement of Clustered Pilots scheme for N=64, if PRBS pilot signals are used. Figure 23 shows the CIR improvement of Clustered Pilots scheme for N=64 if pilot signal energy is chosen to be 2.

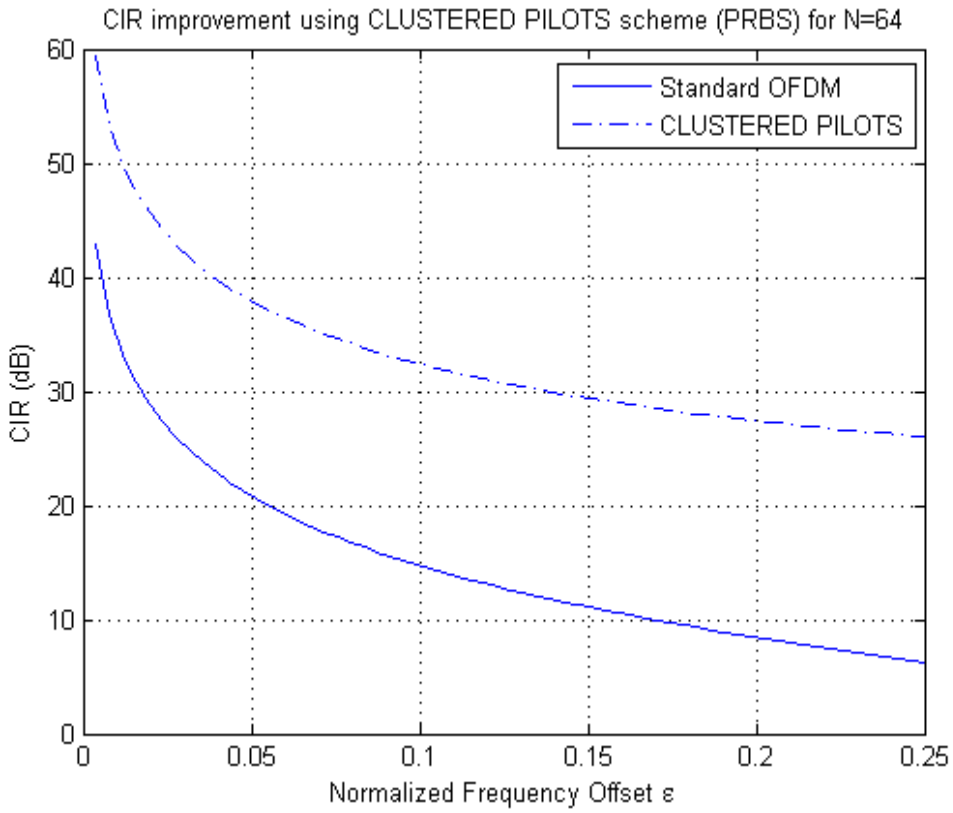

Figure 22 - CIR improvement using Clustered Pilots scheme (PRBS) for N=64

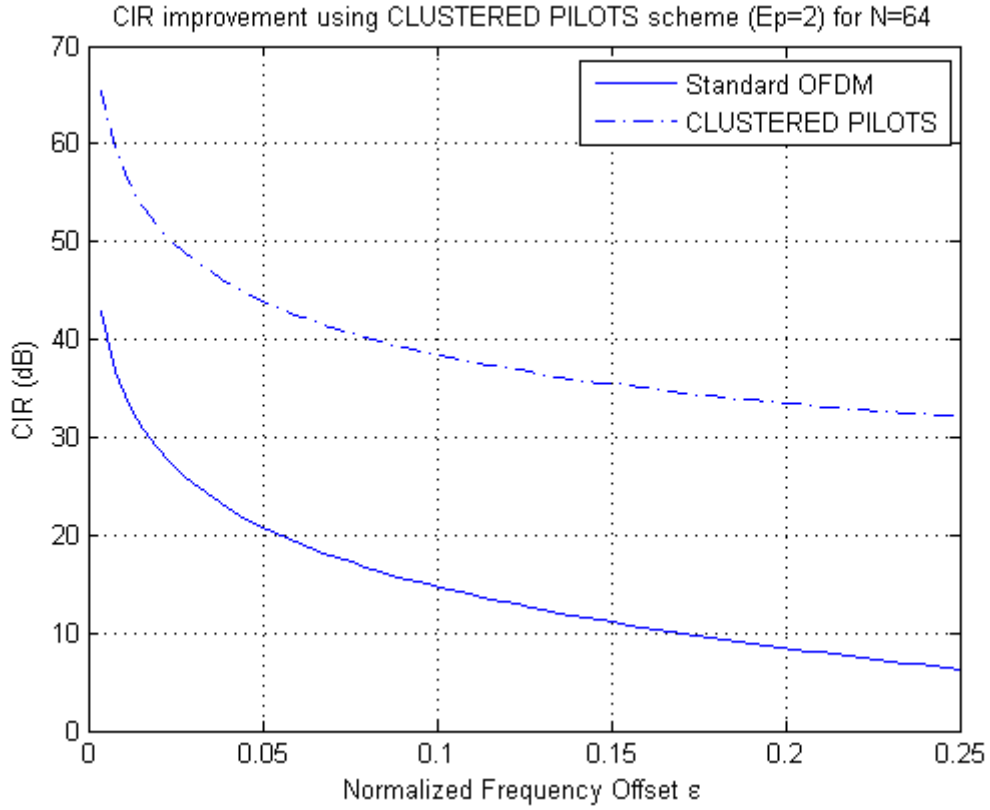

Figure 23 - CIR improvement of Clustered Pilots scheme for N=64

Comparing with conventional pilot scheme CIR (51), it can be seen that the CIR is significantly improved by the clustered pilot tones scheme.

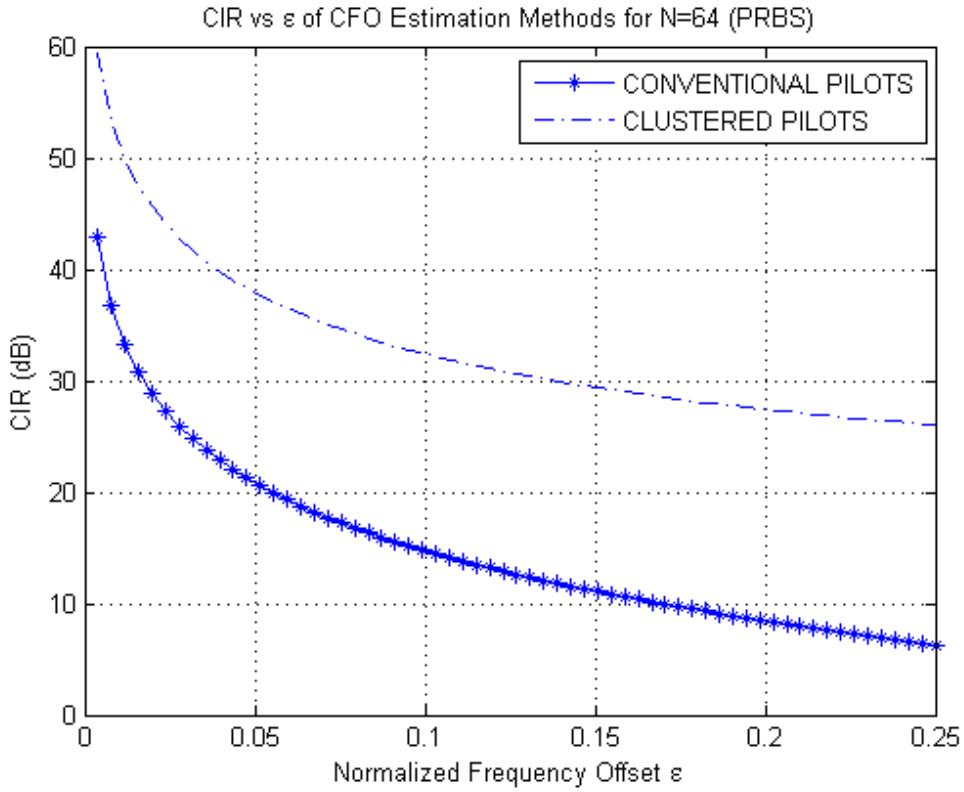

Figure 24 - CIR comparison of CFO Estimation methods for N=64

4.2.3 Another CFO estimation scheme– Symmetric Pilots

In part 4.2.2, in clustered pilots for CFO estimation scheme, a complex data pair (X, -X) is modulated onto two adjacent pilot subcarriers *m* and *m+1* and then the ICI signals generated by the subcarrier *m* will be cancelled out significantly by the ICI generated by *m+1* pilot subcarrier. As we discussed in section 4.1.2 , Sathananthan modified this scheme by using the odd symmetry in $S(l-k), \mathrm{Re}(S(l-k))$ and $\mathrm{Im}(S(l-k))$ [36].

He showed that ICI coefficients are approximately symmetric, such as $S(k) \cong S(N-1-k)$ for $k \neq 0$. Therefore, modulating complex data pairs (X,-X) onto k^{th} and $(N-1-k)^{th}$ subcarriers also have a similar effect to decrease ICI.

In this study a newly CFO estimation scheme named as “Symmetric Pilots” is compared with “conventional” and “clustered” pilot schemes to obtain a better CFO estimate. In this scheme, complex data pairs (X,-X) is modulated onto m^{th} and $(P-1-m)^{th}$ pilot subcarriers to use odd symmetry of the pilot symbols. Note that P denotes the total number of pilots in an OFDM block

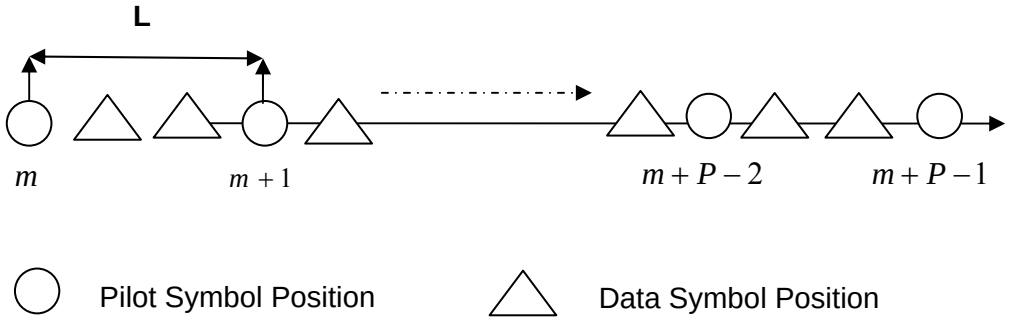

Figure 25 - Symmetric Pilots pattern

Modulation

In symmetric pilots method, complex data pairs (X,-X) is modulated onto m^{th} and $(P-1-m)^{th}$ pilot subcarriers such as $X_i(m) = -X_i(m+P-1)$, $X_i(m+1) = -X_i(m+P-2)$ and so on. Therefore, the modulated pilots sequence will be for one OFDM block is:

$$\left\{X(0), X(1), X(2), \ldots\ldots\ldots X\ (\frac{P}{2}-1), -X(\frac{P}{2}-1), \ldots\ldots\ldots\ldots -X\ (2), -X(1), -X(0)\right\} \quad (65)$$

Demodulation

Then, the values for the symmetric pilot tones are subtracted and the demodulated data on the m^{th} pilot carrier can be defined as:

$$Z''_i(m) = z'_i(m) - z'_i(P-1-m) \tag{66}$$

therefore;

$$Z''_i(m) = e^{(j(\theta_0+(i-1)\phi))}\left[\begin{array}{l}(2S(0)-S(P-1)-S(1-P))X_i(m)\\ +\sum_{l=0}^{P/2-1}(S(l-m)-S(m-l)-S(P-m-1-l)-S(l+m+1-P))X_i(l)\end{array}\right] \tag{67}$$

The unbiased estimate of phase for symmetric pilots method can be defined as in (59) and the averaged estimated CFO can be computed by using (60) and (61).

Carrier to Interference Ratio

The average CIR of symmetric pilots method can be defined as:

$$CIR_m = \frac{\left|-S(P-1)+2S(0)-S(1-P)\right|^2\left|X_i(m)\right|^2}{\sum_{l\in P}^{P/2-1}\left|S(l)+S(-l)-S(P-1-l)-S(l+1-P)\right|^2} \tag{68}$$

4.3 Windowing Techniques

A time limited window, which reduces the side lobe and conserves the orthogonality is called Nyquist Window. The usually used Nyquist windows in the literature are rectangular window, raised cosine window [21], and the "better than" Nyquist window [20].

In the next section, firstly we will consider two different pulses those are used for Nyquist windowing; second order continuous window (SOCW) pulse [22] and the Franks pulse for ICI reduction in OFDM systems [23]. Assume no noise is considered on the channel, the received OFDM signal after down conversion is:

$$y(t) = e^{j(2\pi\Delta ft+\vartheta)}\sum_{n=0}^{N-1}X(n)e^{j2\pi ft} \quad \text{for } -T<t<T \tag{69}$$

where T is the OFDM symbol duration and Δf is the frequency offset.

SOCW method uses the *y(t)* and its "negative time" signal for producing the decision variable. The frequency offset creates a constant phase in *y(T+t)*, so *y(T+t)* cannot be used directly for the "negative time" signal. To remove this constant, a two-sided signal $\tilde{y}(t)$ is constructed:

$$\tilde{y}(t) = \begin{cases} y(t) & 0 \le t \le T \\ cy(T+t) & -T \le t \le 0 \end{cases} \tag{70}$$

where the c is the compensating constant and $c = e^{-j2\pi\Delta fT}$ in noise free condition or for large N. So the decision variable of the m^{th} sub channel correlation demodulator is given as:

$$\tilde{X}(m) = \int_{-T(1+\alpha)/2}^{T(1+\alpha)/2} \tilde{y}(t) w_r(t) e^{-j2\pi f_m t} dt \tag{71}$$

Above expression can be simplified as:

$$\tilde{X}(m) = X(m) e^{j\theta} W_r(-\Delta f) + e^{j\theta} \sum_{n=0, n\neq m}^{N-1} X(n) W_r\left(\frac{m-n}{T} - \Delta f\right) \tag{72}$$

where $w_r(t)$ is the receiver window function, $W_r(f)$ is the Fourier transform of $w_r(t)$ and α is the roll-off factor. Note that, $w_r(t)$ is assumed to be time-limited and of unit energy. When $w_r(t)$ satisfies the Nyquist criterion, it can generally be expressed as :

$$w_r(t)=\begin{cases}\dfrac{1}{T}, & 0\le|t|\le\dfrac{T(1-\alpha)}{2}\\ \dfrac{1}{T}\left[1-x(-|t|\dfrac{2}{\alpha T}+\dfrac{1}{\alpha})\right], & \dfrac{T(1-\alpha)}{2}\le|t|\le\dfrac{T}{2}\\ \dfrac{1}{T}x(|t|\dfrac{2}{\alpha T}-\dfrac{1}{\alpha}), & \dfrac{T}{2}\le|t|\le\dfrac{T(1+\alpha)}{2}\\ 0, & |t|\ge\dfrac{T(1+\alpha)}{2}\end{cases} \tag{73}$$

where x(t) is the normalized elementary function, and it is a continuous function of t for $t\in[0,1]$. In (72), the first term $X(m)e^{j\theta}W_r(-\Delta f)$ is the desired signal and the second term $e^{j\theta}\sum_{n=0,n\neq m}^{N-1}X(n)W_r(\frac{m-n}{T}-\Delta f)$ is the ICI component. Therefore we can express the Carrier to Interference Ratio (CIR) (over all sub carriers) of Nyquist windowing techniques as [22]:

$$CIR_{Nyquist}=\frac{\left|W_r(-\Delta f)\right|^2}{\frac{1}{N}\sum_{m=0}^{N-1}\sum_{n=0,n\neq m}^{N-1}\left|W_r(\frac{m-n}{T}-\Delta f)\right|^2} \tag{74}$$

Equation (74) shows that the CIR depends on the desired symbol location, the total number of sub carriers and the windowing function $w_r(t)$.

To compare the windowing techniques to the other ICI cancellation techniques in terms of BER, an analysis of error probability for the OFDM receiver is given here. Assume that the sub carrier modulation is QPSK, the average bit energy-to-noise ratio is given as [7]:

$$\bar{\gamma}_b=\frac{\left|W_r(-\Delta f)\right|^2}{\frac{1}{N}\sum_{m=0}^{N-1}\sum_{n=0,n\neq m}^{N-1}\left|W_r(\frac{m-n}{T}-\Delta f)\right|^2+{\sigma_\mu}^2} \tag{75}$$

where $\sigma_\mu^{\,2}$ is the average power of the noise term. The bir error rate can be written as [38]:

$$P_b = \frac{1}{2}\left(1 - \sqrt{\frac{\bar{\gamma}_b}{1+\bar{\gamma}_b}}\right) \tag{76}$$

4.3.1 Second Order Continuity Window (SCOW)

Song and Leung proposed a class of window functions with x(t) is defined by a second order polynomial of t [22]:

$$x(t) = a_0 + a_1 t + a_2 t^2 \tag{77}$$

Note that $w_{SCOW}(t)$ can be obtained by substituting (77) into (73). If the Fourier transform of $w_{SCOW}(t)$ is taken:

$$W_{SCOW}(f) = \frac{\sin(\pi f T)}{\pi f T}\left[\begin{array}{l} -2(a_1+2a_2)\dfrac{\sin(\pi\alpha f T)}{\pi\alpha f T} + 2a_2\left(\dfrac{\sin(\pi\frac{\alpha}{2}fT)}{\pi\frac{\alpha}{2}fT}\right)^2 + \\ 2(a_0+a_1+a_2)\cos(\alpha\pi f T) + 1 - 2a_0 \end{array}\right] \tag{78}$$

Note that, the discontinuity in the time domain will give rise to slow attenuation in the frequency domain and large sensitivity to frequency offset that leads ICI. In order to maintain the continuity of $w_r(t)$ at $t = \pm T(1-\alpha)/2$, t=$\pm T/2$ and $t = \pm T(1+\alpha)/2$ Song and Leung set $x(0) = 0.5$ and $x(1) = 0$ that leads to $a_0 = 0.5$ and $a_2 = -0.5 - a_1$. In this case the $W_{SCOW}(f)$ is simplified to [22]:

$$W_{SCOW}(f)=\frac{\sin(\pi fT)}{\pi fT}\left[2(1+a_1)\frac{\sin(\pi\alpha fT)}{\pi\alpha fT}-(1+2a_1)\left(\frac{\sin(\pi\frac{\alpha}{2}fT)}{\pi\frac{\alpha}{2}fT}\right)^2\right] \tag{79}$$

This window function is referred as second order continuity window (SOCW). Note that, the performance of SOCW is affected from roll-off factor(α) and a_1.

4.3.2 Franks Pulse for Nyquist Windowing

Franks proposed a pulse for Nyquist windowing that is expressed by [21]:

$$w_{FRANKS}(t)=\begin{cases}1, & 0\le|t|\le\dfrac{T(1-\alpha)}{2}\\ 1-\dfrac{|t|}{T}, & \dfrac{T(1-\alpha)}{2}\le|t|\le\dfrac{T(1+\alpha)}{2}\\ 0, & otherwise\end{cases} \tag{80}$$

Note that, $w_{SCOW}(t)=w_{FRANKS}(t)$ when $\alpha=1$ and $a_1=-0.5$. Taking the Fourier transform of $w_{FRANKS}(t)$:

$$W_{FRANKS}(f)=\left[\frac{\sin(\pi fT)}{\pi fT}\right]^2 \tag{81}$$

CHAPTER 5

PERFORMANCE COMPARISON OF ICI CANCELLATION TECHNIQUES

5.1 Performance Comparison of Repeated Data Methods

In 4.1.3 and 4.1.4, two new ICI cancellation schemes are analyzed to remove the phase error due to frequency offset error since Self and SSR ICI cancellation schemes are ineffective in removing the phase error while removing ICI. In this part, repeated data methods' performance will be compared in terms of BER versus SNR, and BER versus ε. Also a CIR comparison between these methods will we examined.

Figure 26 and 27 show a comparison between repeated data methods with modulation scheme used QPSK , ε=0.03 and ε=0.1 in AWGN Channel.

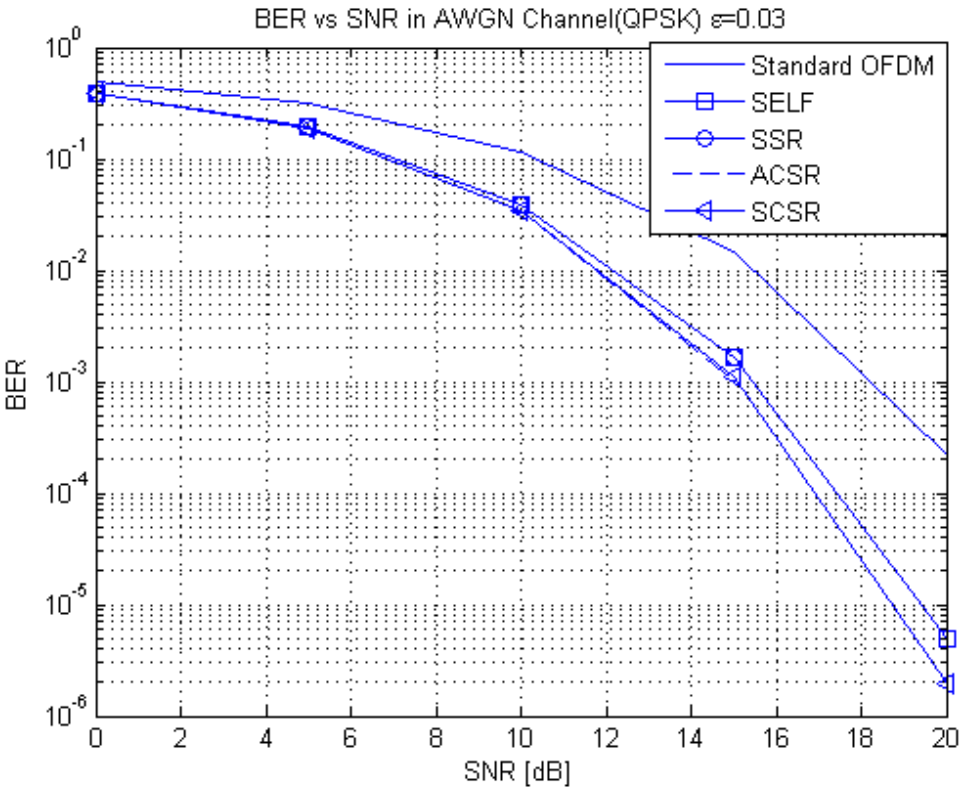

Figure 26 –BER of Repeated Data Methods in AWGN with QPSK (ε=0.03)

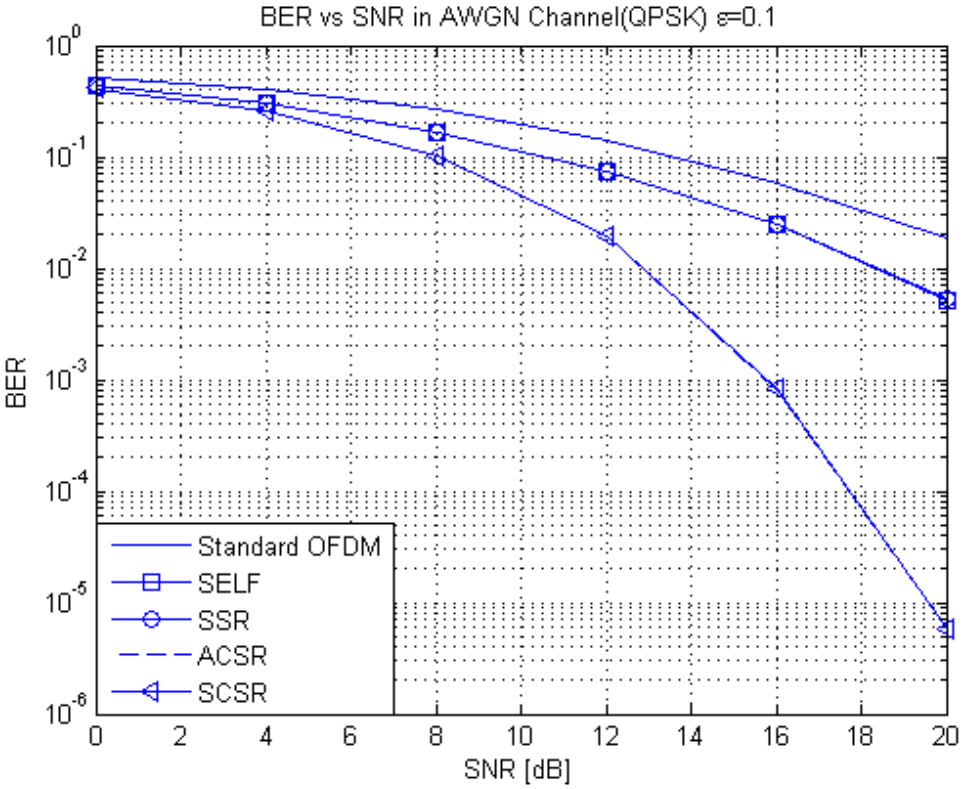

Figure 27 - BER of Repeated Data Methods in AWGN with QPSK (ε=0.1)

From the figure 26 it can be seen that, with QPSK used, all repated data methods have nearly the same performance. Note that the phase error is not a significant issue with modulation schemes such as BPSK and QPSK with very small ε. But in figure 27, when ε=0.1, performance advantage of ACSR and SCSR methods can be seen clearly especially in high SNR's.

Figure 28 shows a comparison between repeated data methods with modulation scheme used 16 QAM and ε=0.03:

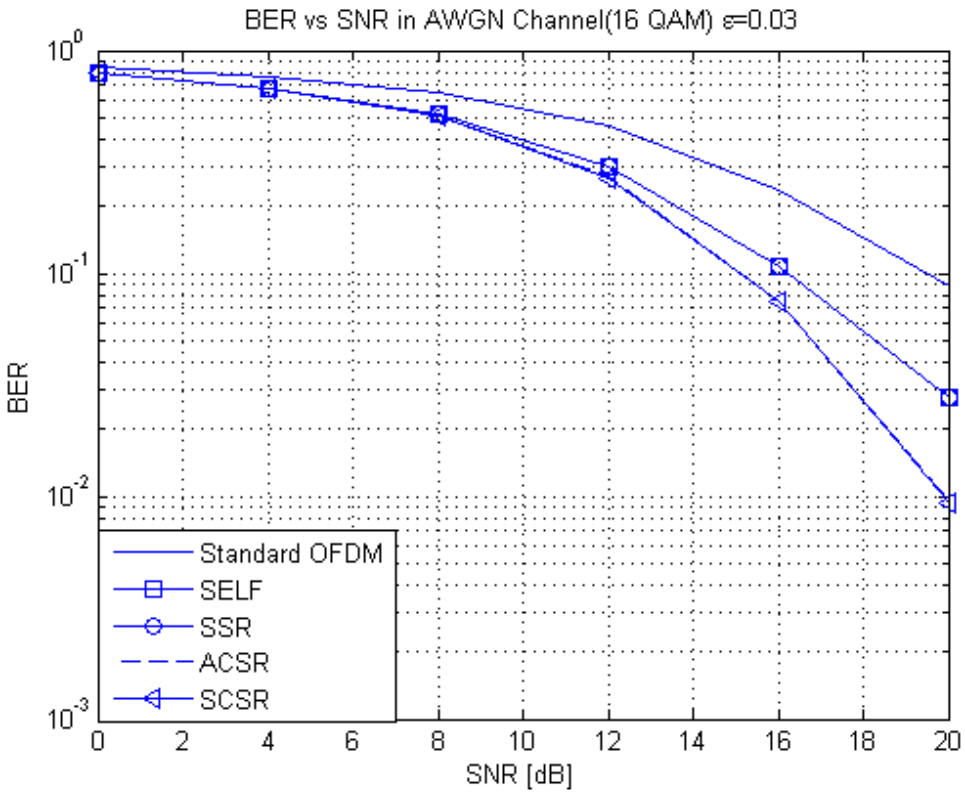

Figure 28 –BER of repeated data methods in AWGN with 16 QAM (ε=0.03)

Figure 28 shows that, with higher modulation schemes such as 16 QAM, SCSR and ACSR methods show great performance against Self and SSR cancellation methods especially in high SNR.

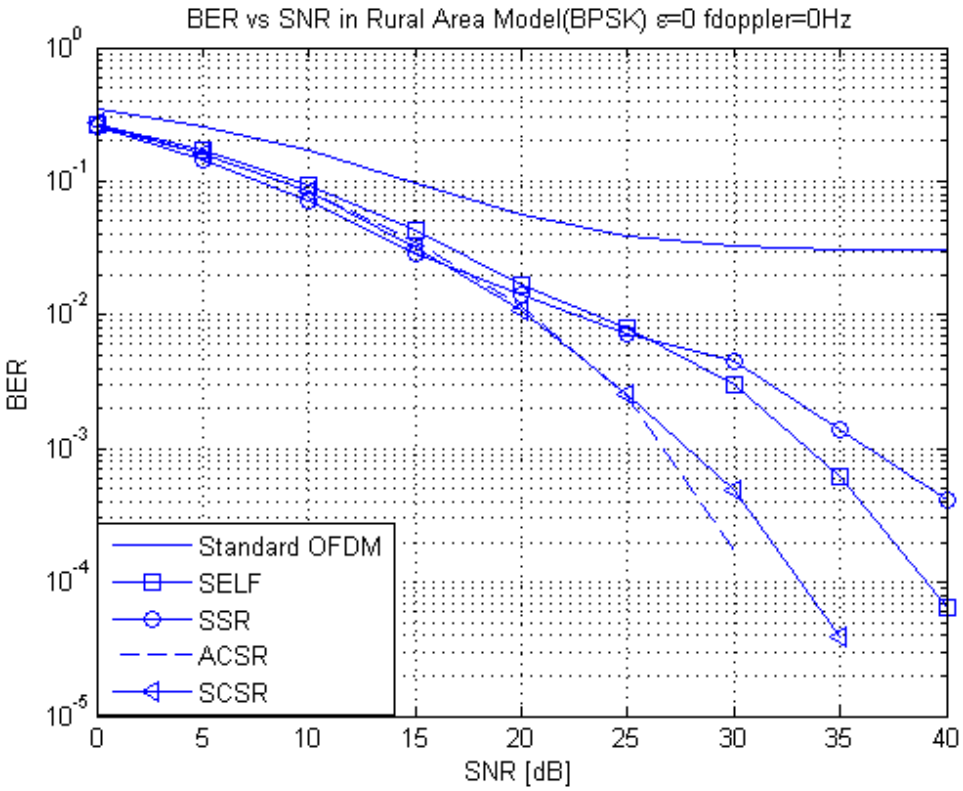

Figure 29 - BER comp. in Rural Area model with f_D=0 Hz (ε=0)

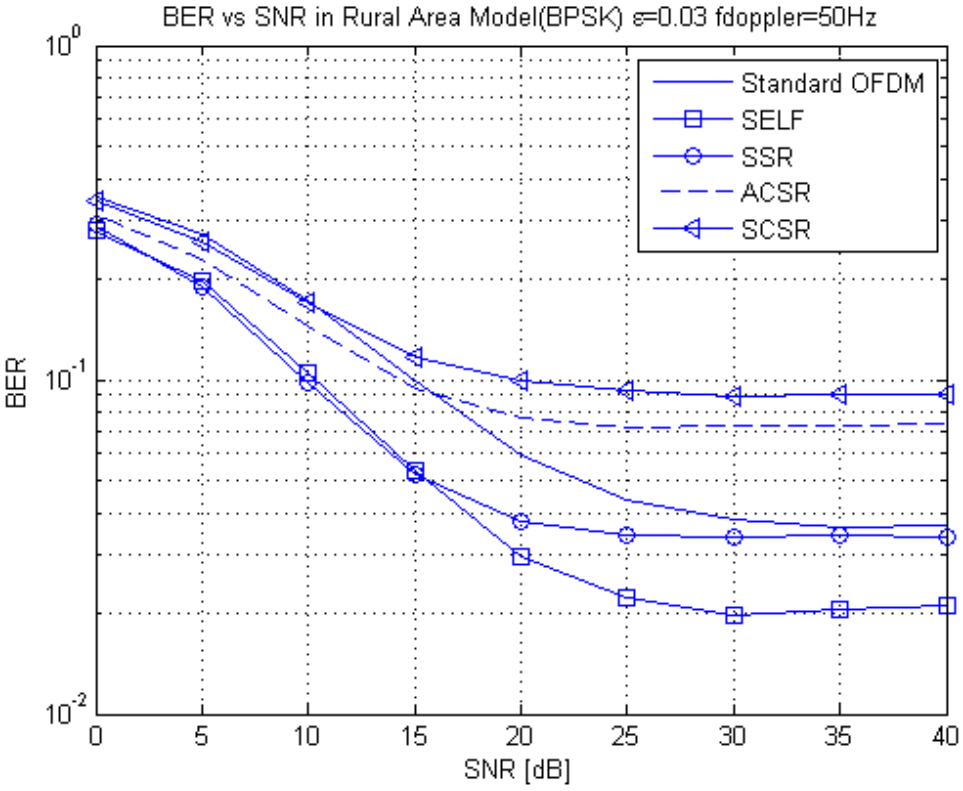

Figure 30 - BER comparison in Rural Area model with f_D =50 Hz (ε=0.03)

In a multipath Rayleigh fading channel (Rural Area Model), bit error performances decreased when compared to AWGN channel performances. Below the figures, fdoppler (f_D) denotes max Doppler shift of the Doppler spread. Figure 29 and 30 show the performance comparison of repeated data methods in Rural Area model. Note that, when $f_D = 0\,\text{Hz}$ all repeated data methods show nearly the same performance, however when $f_D = 50\,\text{Hz}$ Self cancellation and SSR techniques perform better.

Figure 31 shows performance comparison of repeated data methods in terms of CIR . Note that unresolved phase error is not realized in the average CIR, which is usually used to evaluate the performance.

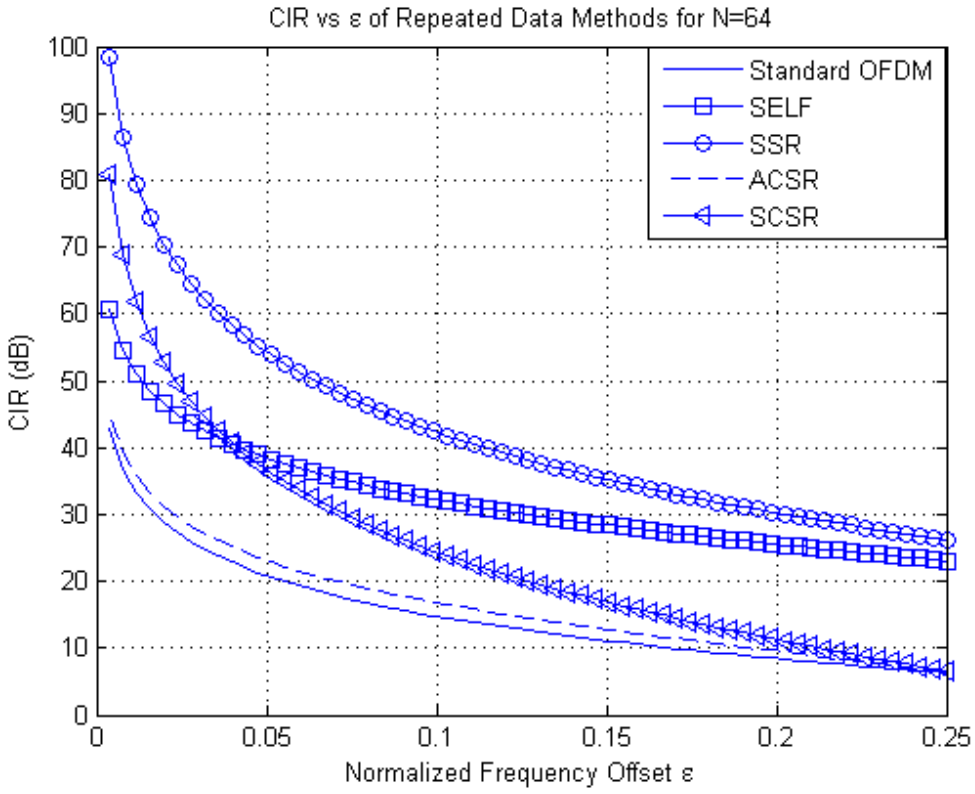

Figure 31 - CIR vs ε of Repeated Data Methods for N=64

It is evident that, SSR method has the best average CIR value among the other repeated data methods and all these cancellation schemes achieve CIR gain over standard OFDM. The average CIR gain reduces with increasing ε and SSR and Self

cancellation schemes perform better than others, since unresolved phase error is not realized in the average CIR.

5.2 Performance Comparison of Pilot–Aided Methods

In this part, a performance comparison will be studied between Conventional Pilots, Clustered Pilots and the newly tried "Symmetric Pilots". The comparison will be in terms of ; BER vs SNR and BER vs ε in AWGN Channel. Also BER vs SNR in multipath fading medium is investigated. Then, CIR comparisons of CFO estimation methods will we analyzed. Finally, optimal number of pilots is searched under a constant budget of data power.

Figure 32 and 33 show a comparison between repeated data methods with modulation scheme used QPSK , ε=0.03 and ε=0.1 in AWGN Channel:

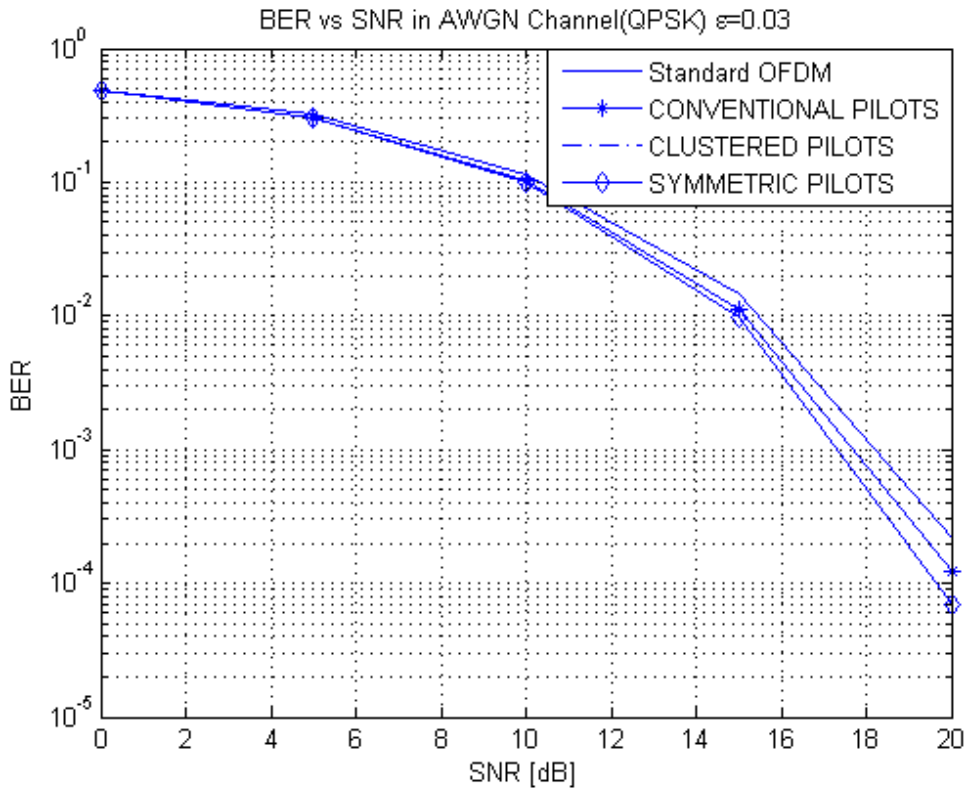

Figure 32 –BER performance of CFO est. methods in AWGN QPSK(ε=0.03)

From figures 32 and 33, it can be seen that, Clustered pilots and Symmetric has the same best performance among Conventional pilots scheme when QPSK used, however this performance difference increases when ε=0.1 is used.

If 16 QAM modulation technique is used in the simulation, then BER will be as in figure 34. Note that when 16 QAM modulation scheme is used, bit error rate of clustered pilots and Symmetric pilots method have a 2 dB gain over conventional pilots method at SNR=20 dB in figure 34.

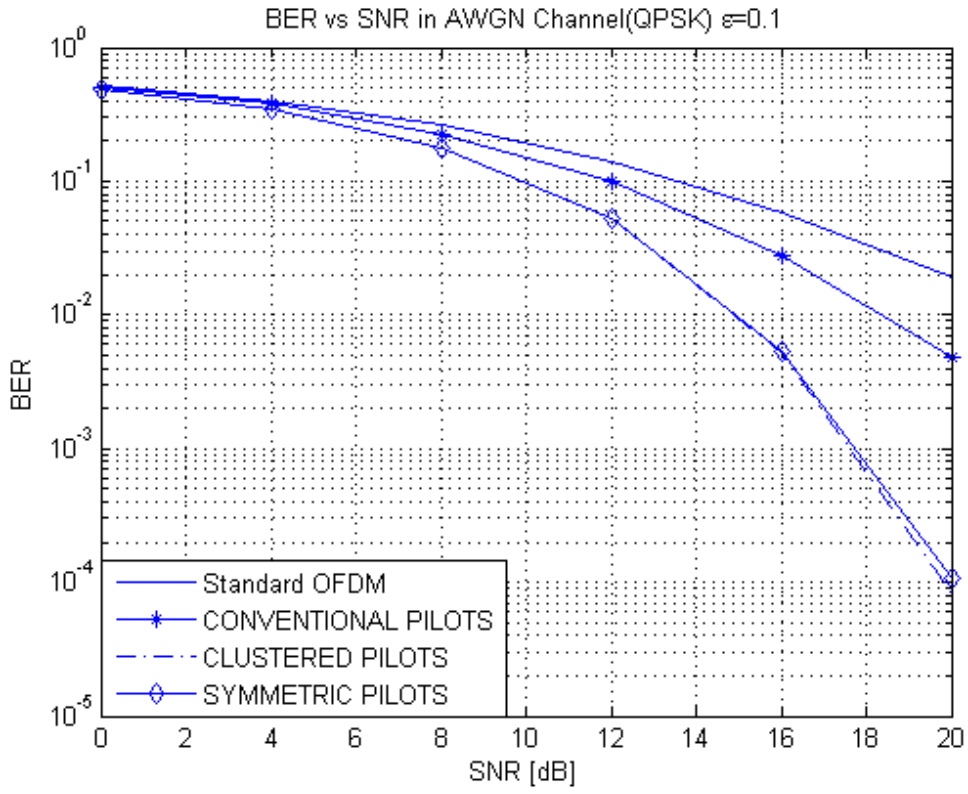

Figure 33 - BER performance of CFO est. methods in AWGN QPSK(ε=0.1)

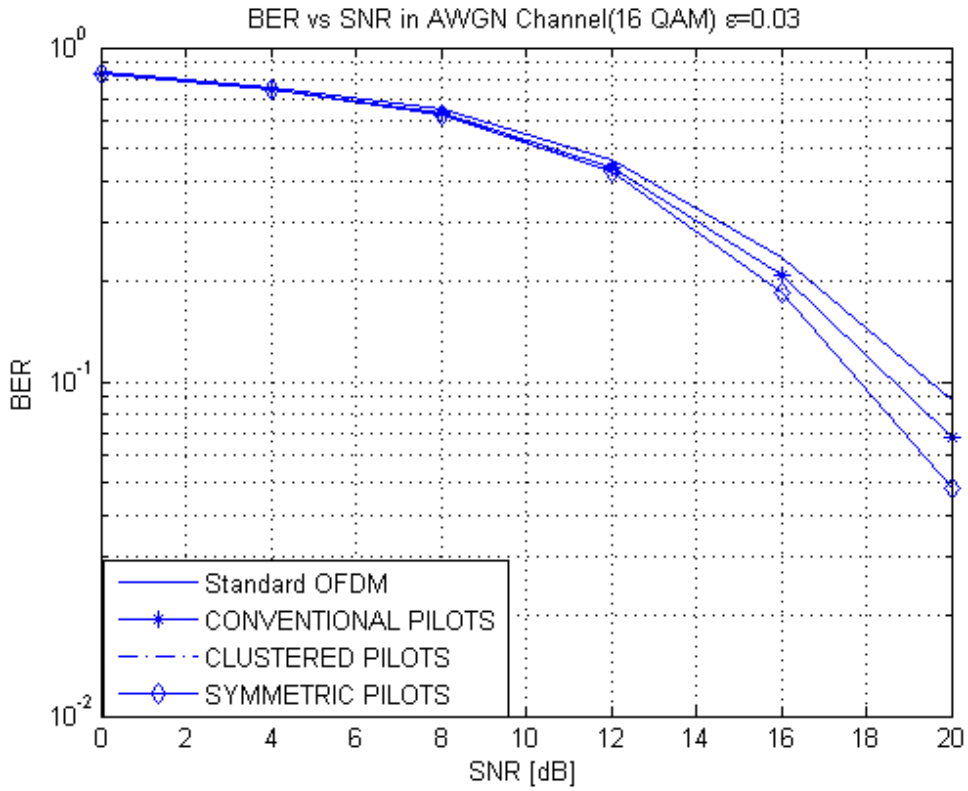

Figure 34 – BER comparison in AWGN with 16 QAM (ε=0.03)

In figure 35, bit error rates of pilot-aided methods in terms of normalized frequency offset is concerned when QPSK data is used. Note that SNR is constant and is equal to 15 dB. Figure 35 improves that when ε increases, bit error rates also increase. It is seen in figure 35 that, clustered and symmetric pilots schemes have lower increasing trend of BER than conventional pilots method while ε is increasing.

Figure 36 shows Root Mean Square of $\bar{\varepsilon}$ estimation error in terms of ε when QPSK data is used and SNR=10dB. This figure is important, since it shows that which pilot based CFO estimation works better and obtains a better estimate. It is evident that clustered and symmetric pilots methods obtain better estimates, but note that clustered pilots method has a slightly better performance than symmetric pilots method.

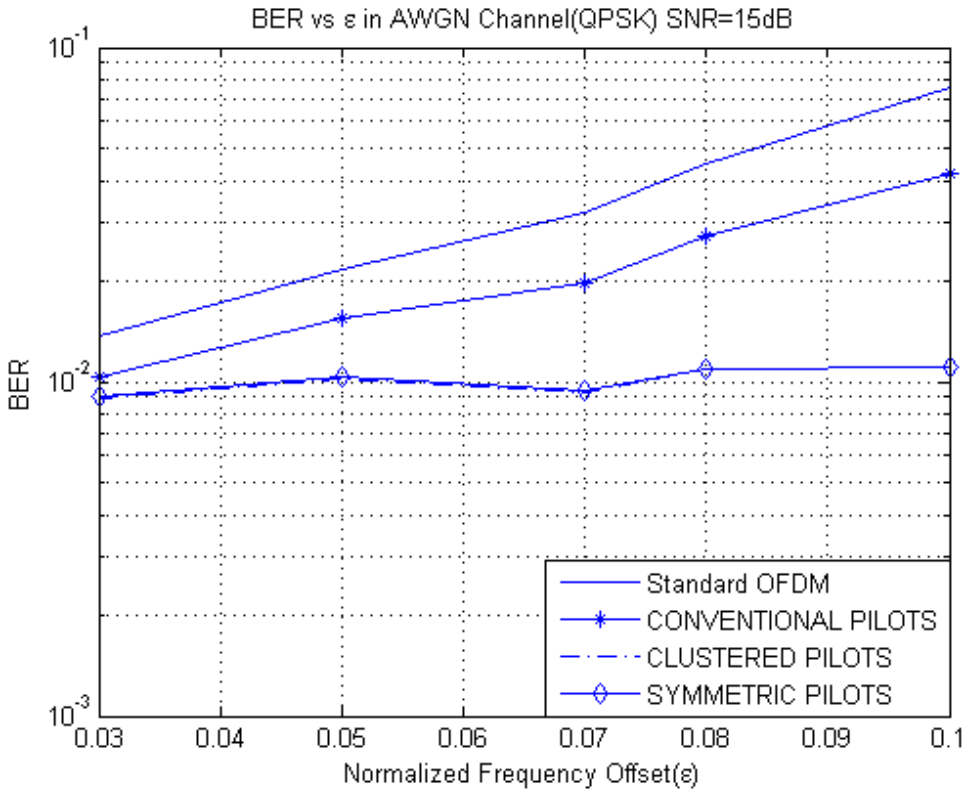

Figure 35 –BER vs ε in AWGN Channel with QPSK (SNR=15dB)

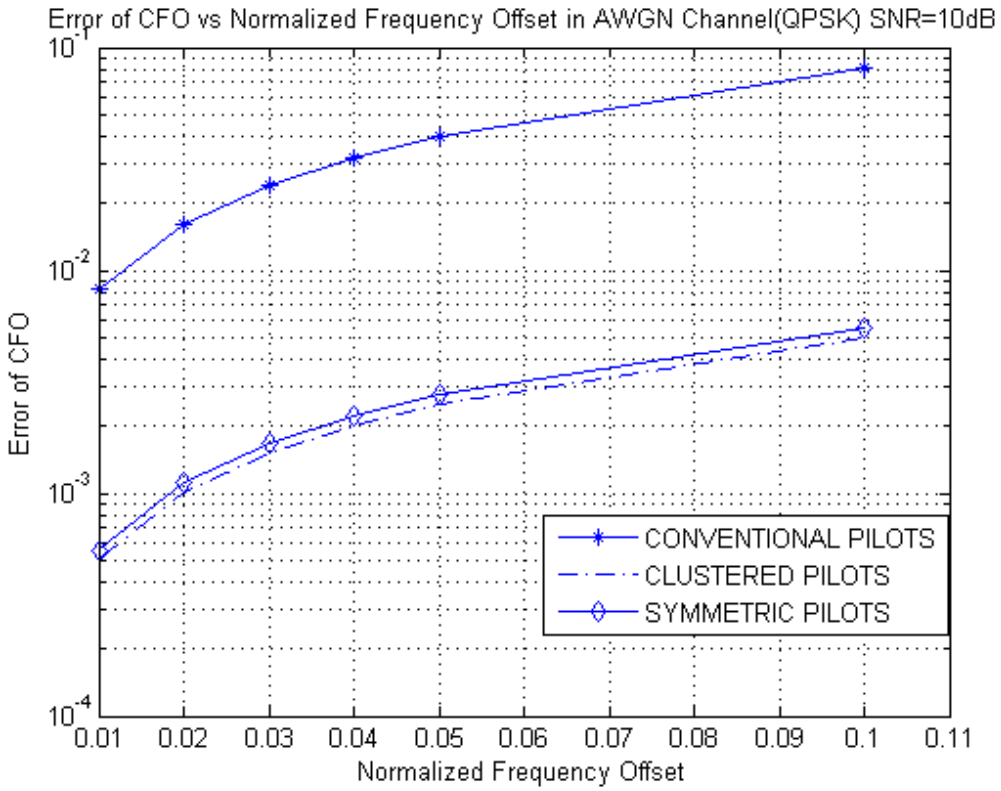

Figure 36 – RMSE of CFO estimate in AWGN Channel with QPSK (SNR=10dB)

Pilot-aided CFO estimation methods are also compared in multipath fading. It can be seen from figure 37 and 38 that ; when f_D increases, performance of pilot-aided methods decrease.

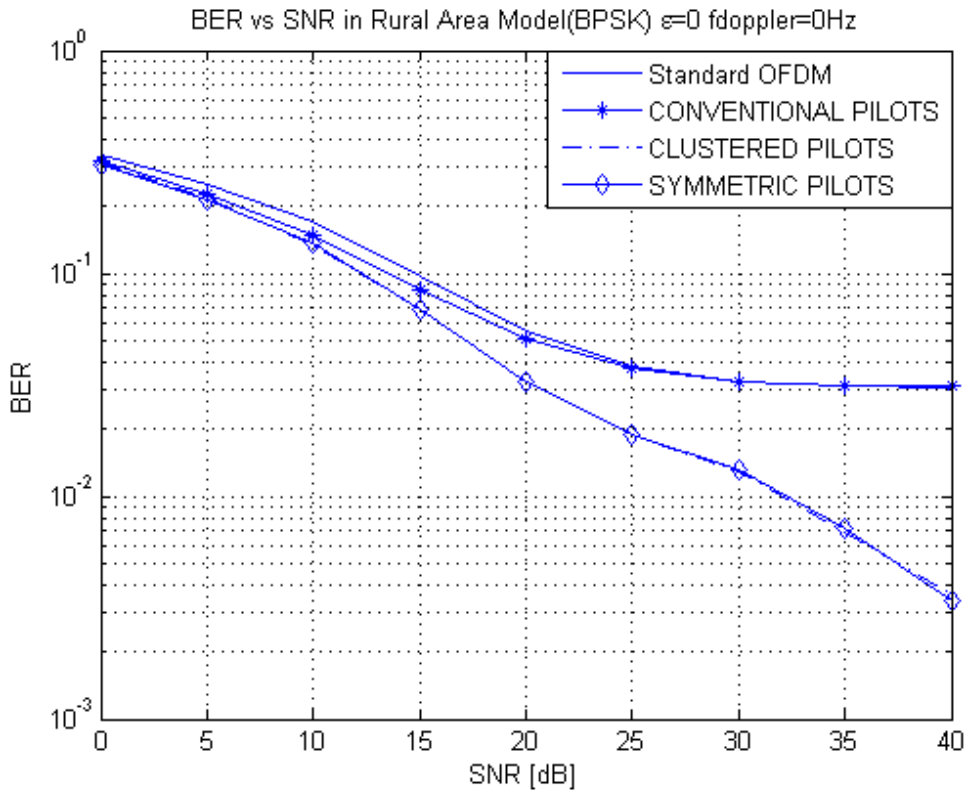

Figure 37 – BER in Rural Area model with BPSK (ε=0)(f_D =0Hz)

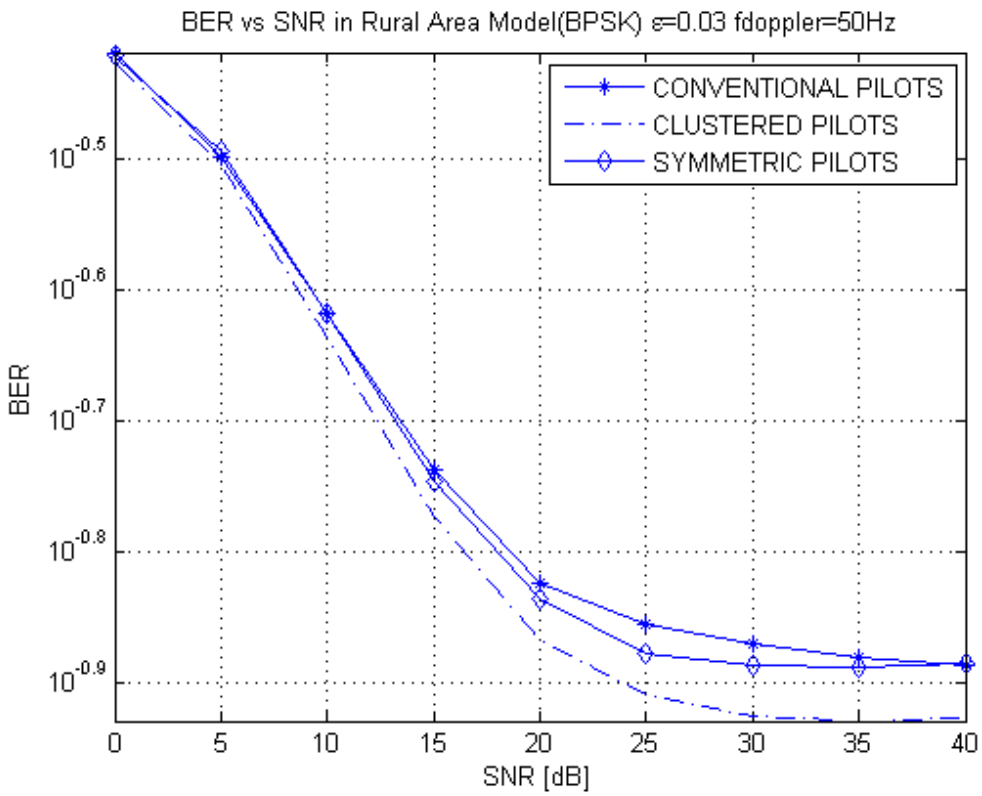

Figure 38 – BER in Rural Area model with BPSK (ε=0.03)(f_D =50Hz)

Pilot power to data power ratio

In the pilot-aided methods, pilot number is an important issue to be considered, since more pilot number usage decreases bandwidth efficiency. Therefore, in this section we analysed the bit error rate versus pilot number with assuming that total transmitted power is constant.

Suppose that the total transmitting power is NE, we have

$$NE = N_P E_P + N_D E_D \tag{82}$$

where E, E_P and E_D represent the average power of all transmit symbols, pilot symbols and data symbols, respectively.

The total number of pilot symbols equals N_P , where $N_P = \left\lceil \frac{N}{L} \right\rceil + 1$ and the total number of data symbols is $N_D = N - N_P$ where N is total number of subcarriers and L is the pilot spacing.

In figure 39, 40 and 41, total power E is fixed, and BER vs N_P graphs are plotted as N_P increasing. From the figures, it can easily be seen that, more pilot number gives better BER results. But there is a trade-off here, since more pilot number decreases band efficiency. Figure 39, 40 and 41 shows the BER vs N_P graphs with BPSK data, QPSK data and 16 QAM data respectively,: total power is fixed to 1024 and ε is chosen to be 0.03. Note that as SNR decreases BER increases in the figures.

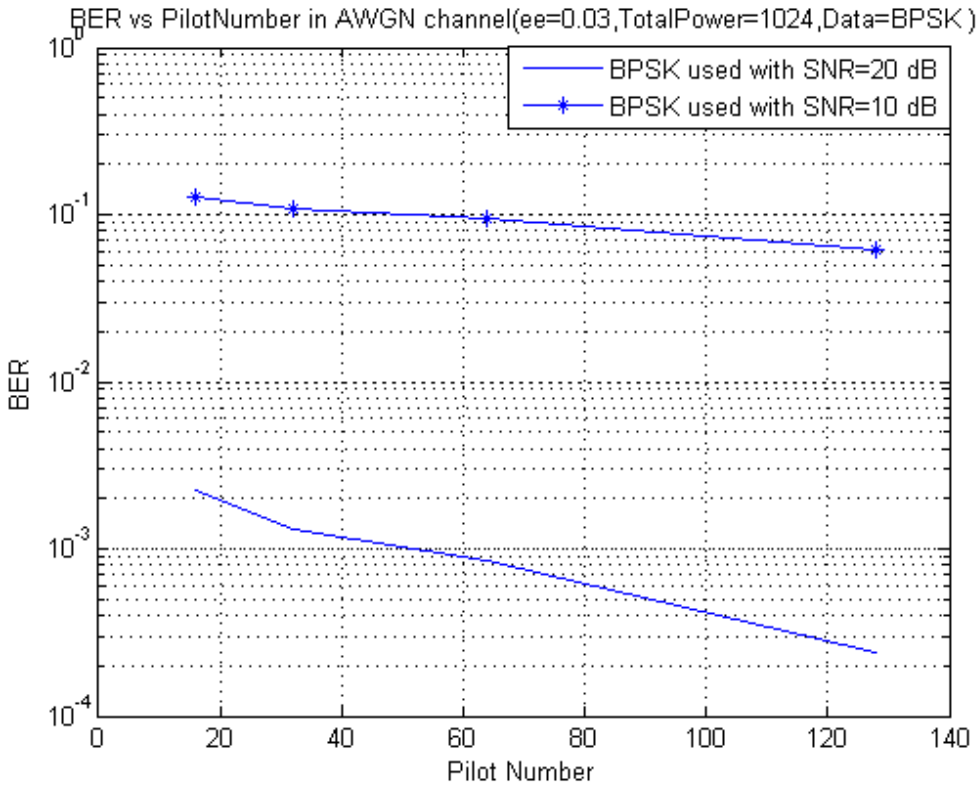

Figure 39 - BER vs PilotNumber with BPSK (Total Power=1024,ε=0.03)

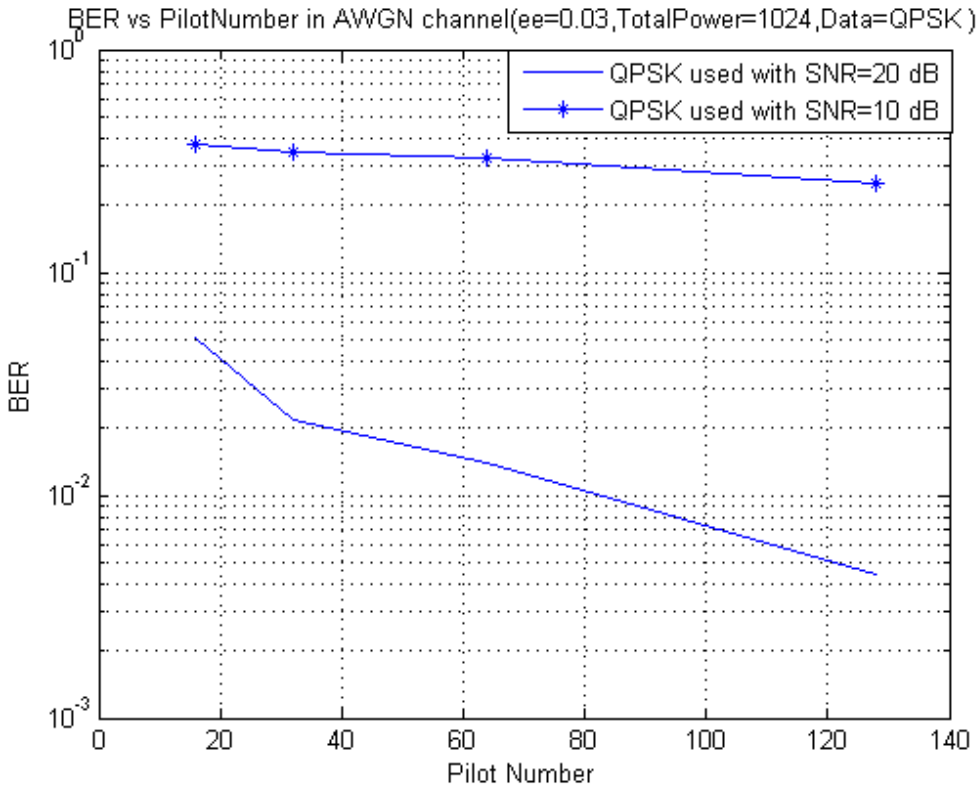

Figure 40 - BER vs PilotNumber with QPSK (Total Power=1024,ε=0.03)

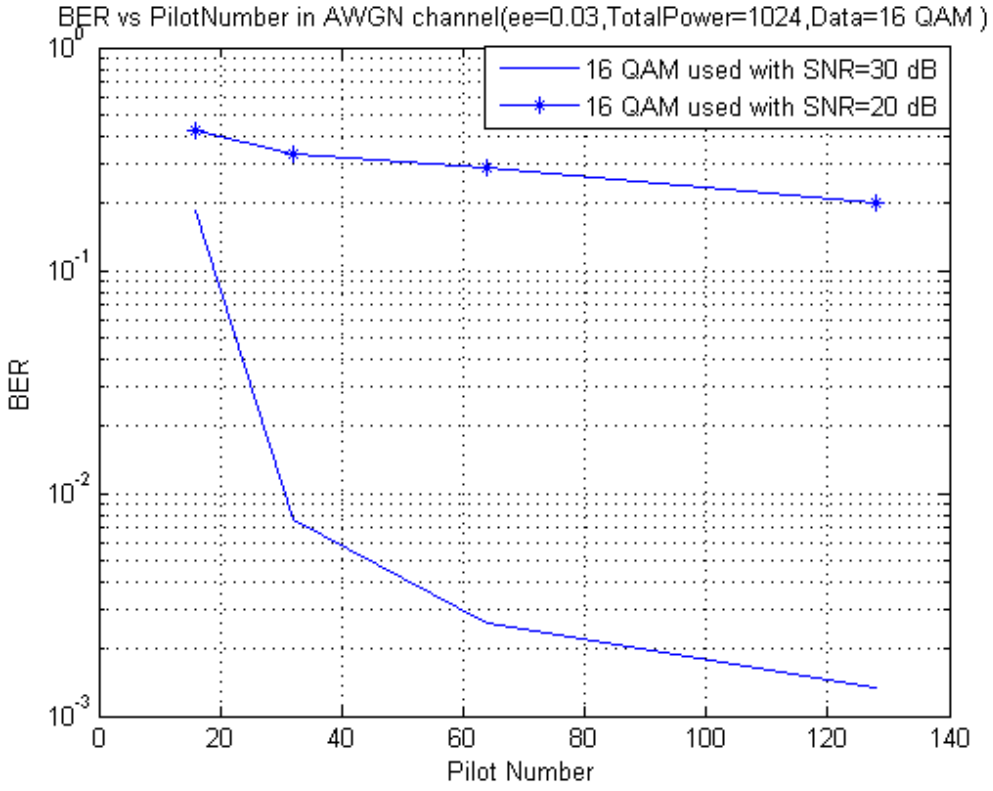

Figure 41 - BER vs PilotNumber with 16 QAM (Total Power=1024,ε=0.03)

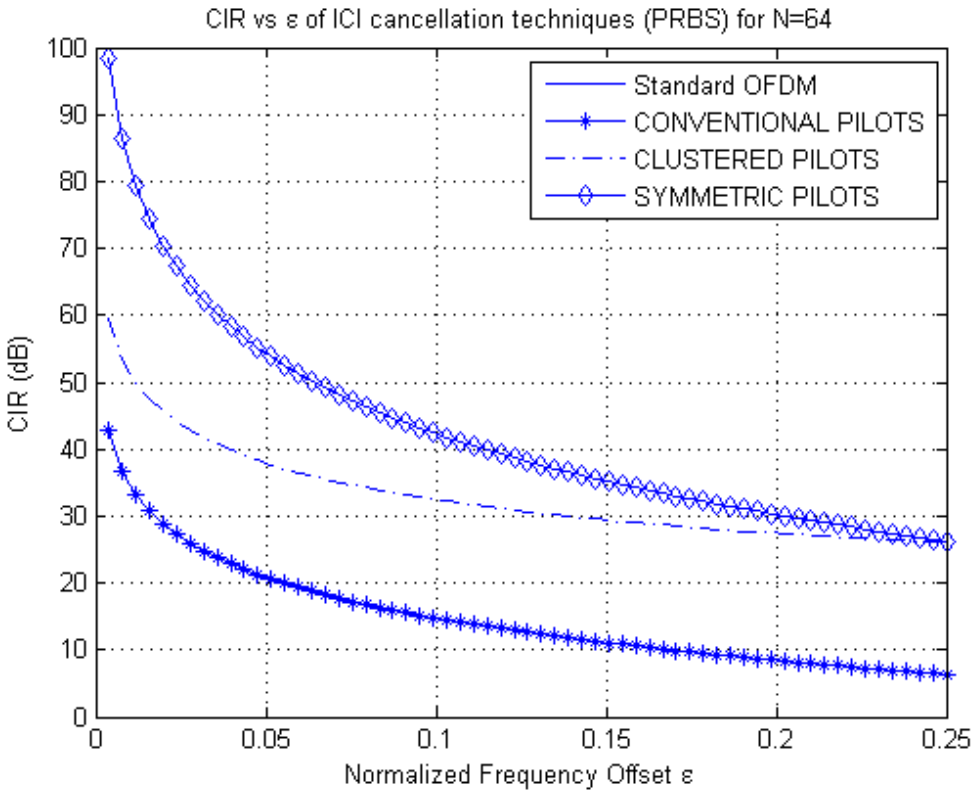

Figure 42 - CIR of CFO Estimation techniques when PRBS is used

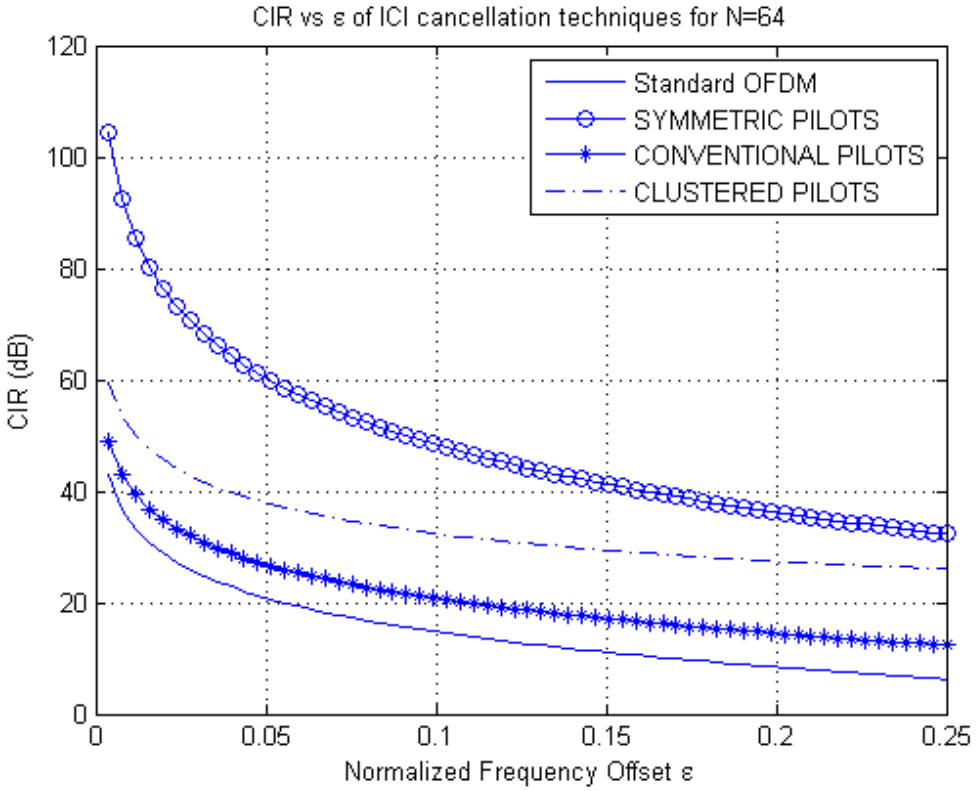

Figure 43 - CIR of CFO Estimation techniques when Ep=2 is used

Figure 42 and 43 shows the CIR comparison of CFO Estimation methods. Note that in Figure 42, when PRBS pilot signals are used, CIR decreases according to the CIR formulas. Conventional Pilots' CIR is same with standard OFDM as mentioned in 4.2.1. However, when pilot signal power is chosen to be 2, CIR increases as shown in figure 43.

5.3 Performance Comparison of Windowing Methods

It is shown in figures 44 and 45 that, windowing techniques are effective in ICI cancellation especially in low SNR's. Franks pulse Nyquist windowing performs a little better than SCOW technique. Here $\alpha = 1$ for both Franks pulse and SCOW method, $a_1 = -0.3$ for SCOW method.

Also when comparing these techniques in terms of CIR, Franks pulse performs better, that is shown in figure 46.

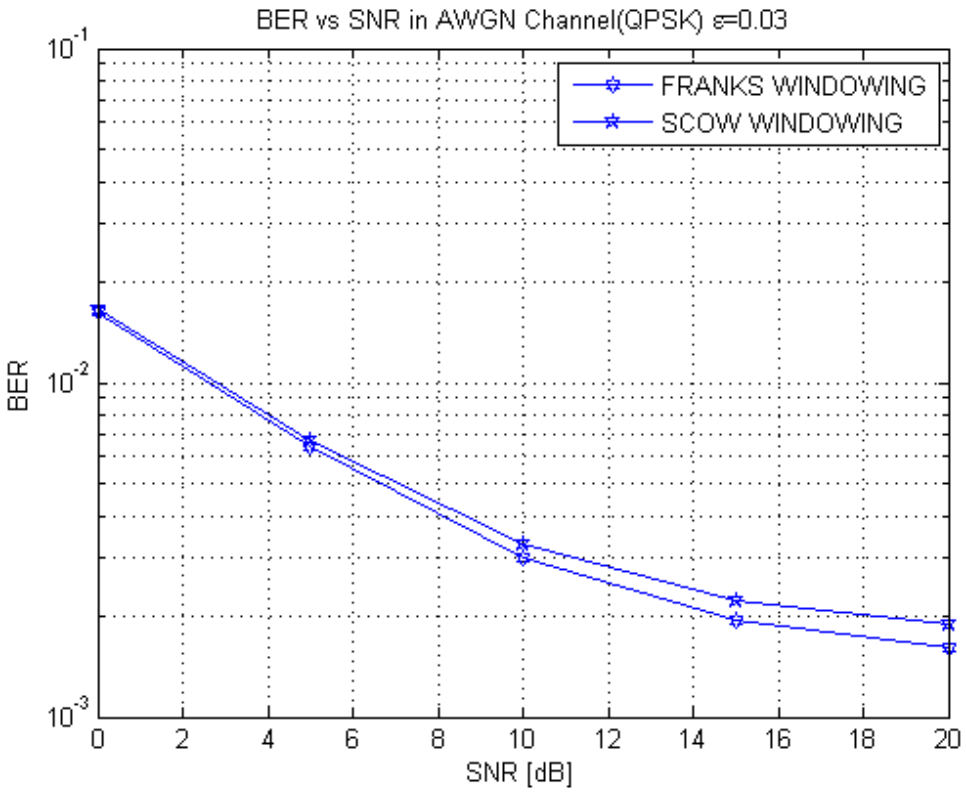

Figure 44 - BER performance in AWGN with QPSK(ε=0.03)

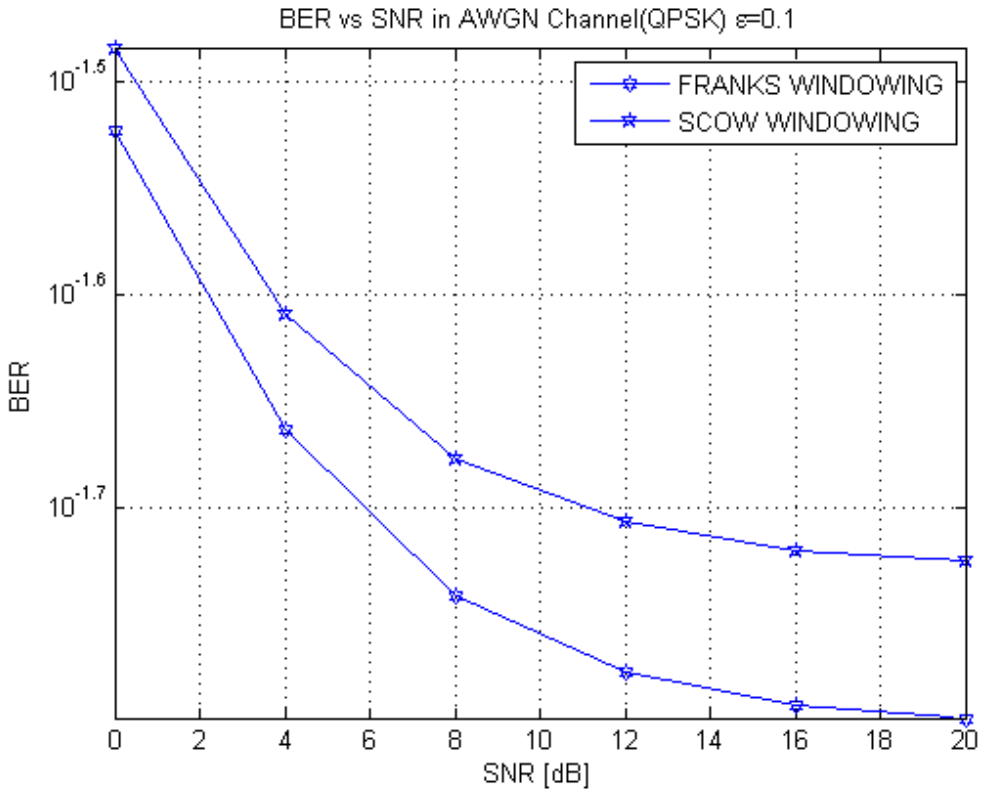

Figure 45 - BER performance in AWGN with QPSK(ε=0.1)

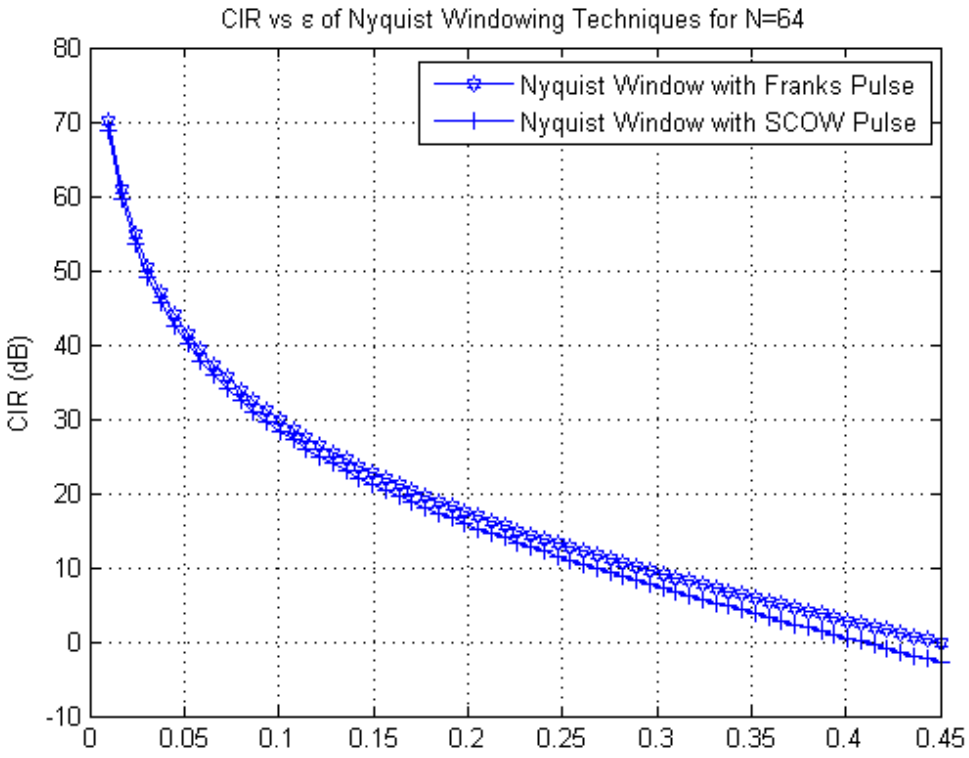

Figure 46 - CIR comparison of windowing techniques

5.4 Performance Comparison of All Methods

In this part, all repeated data methods, pilot-aided CFO estimation and windowing techniques are compared in AWGN channel and multipath fading. Also a comparison is made in terms of carrier to interference ratio (CIR). Note that windowing techniques BER performances are not compared here since their BER is calculated by a formula (76) , however repeated data methods' and pilot aided methods' BER performances are analysed by data transmission in an OFDM environment.

In figure 47 and 48, it can clearly be seen that, repeated data methods show better performance than CFO estimation methods and they have approximately 3 dB gain in high SNR's.

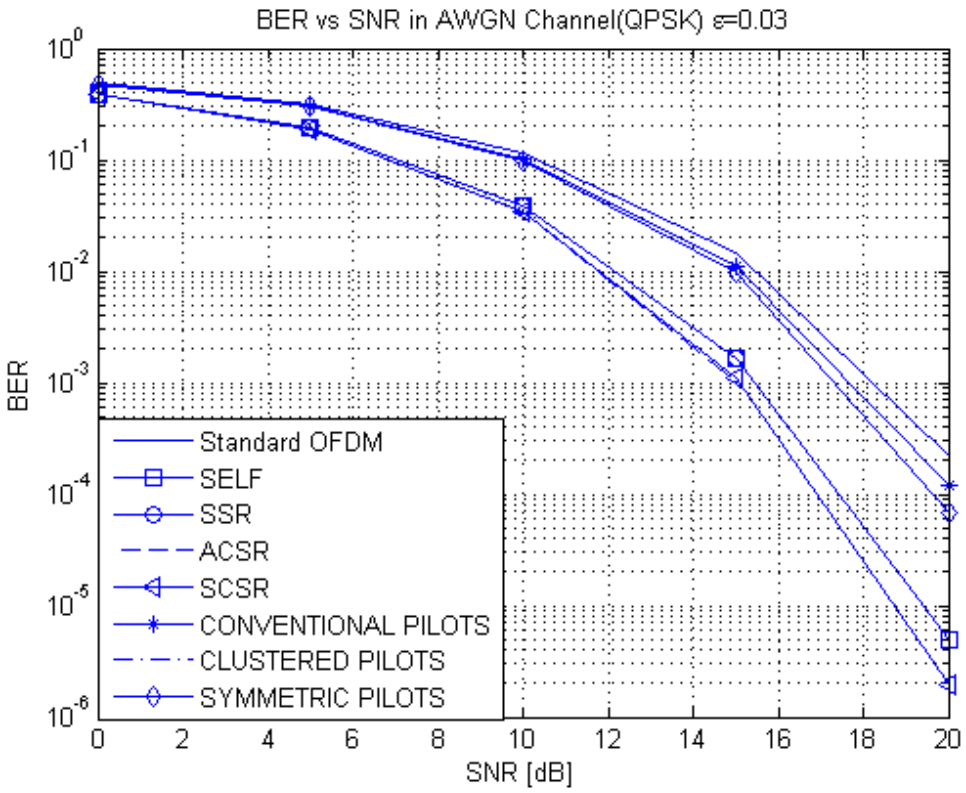

Figure 47 - BER vs SNR in AWGN Channel with QPSK (ε=0.03)

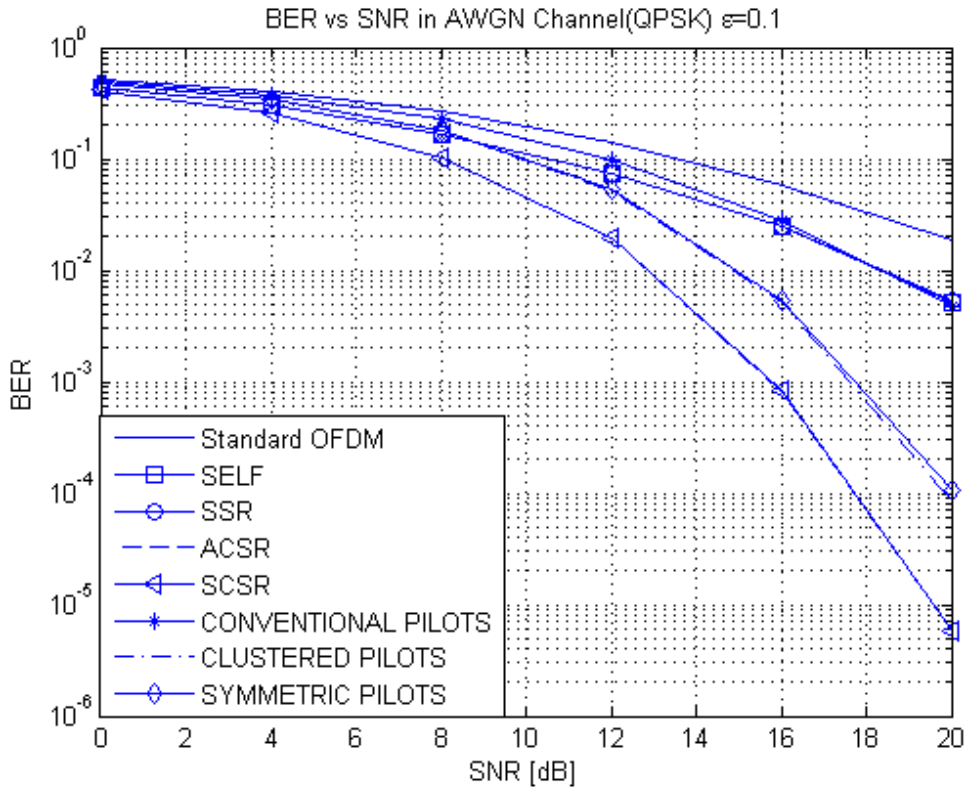

Figure 48 - BER vs SNR in AWGN Channel with QPSK (ε=0.1)

Comparing figure 47 and 48, when ε increases, the performance gain of repeated data methods over CFO estimation methods increase faster. Also when ε=0.1, the gap between SCSR and ACSR, and SELF and SSR methods increases in QPSK modulation scheme.

When modulation scheme is changed to 16 QAM but ε is same, it can be seen from figure 49 that ; SCSR and ACSR methods are more resistant to phase rotation effects ,since in 16 QAM phase rotation has an important effect on the received symbols.

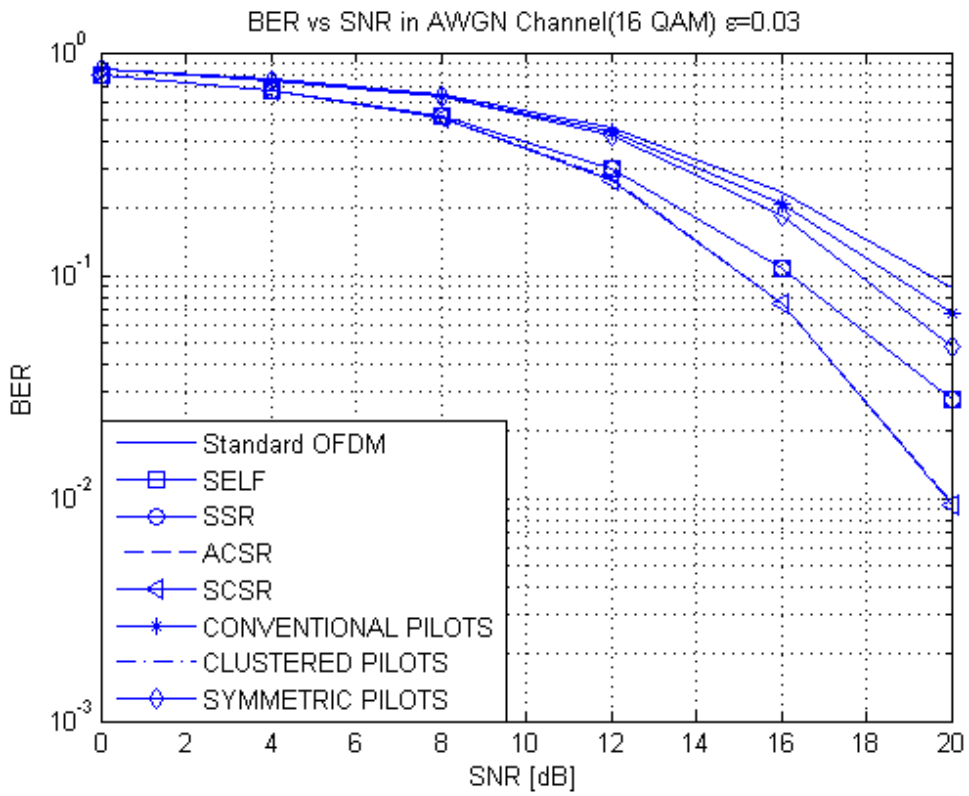

Figure 49 - BER vs SNR in AWGN Channel with 16 QAM (ε=0.03)

In figure 50, bit error performances of ICI cancellation methods are shown versus ε increase. Clustered pilots and Symmetic pilots show approximately a constant performance while ε is increasing, so do SCSR and ACSR methods. But note that SELF and SSR cancellation methods show an increasing trend of BER. At higher CFO's, SCSR and ACSR methods show the best performances, however at very small ε's, SELF and SSR methods reach their performance.

Figure 51, 52 show the performance comparison of ICI cancellation methods in multipath Rayleigh fading channel (Rural Area). Note that when f_D increases, repeated data methods are not affected very much, however pilot-aided methods are affected in a negative way. In figure 52, when QPSK is used , all bit error performances are negatively affected with respect to BPSK. ACSR method shows the best performance in QPSK, ε=0.03.

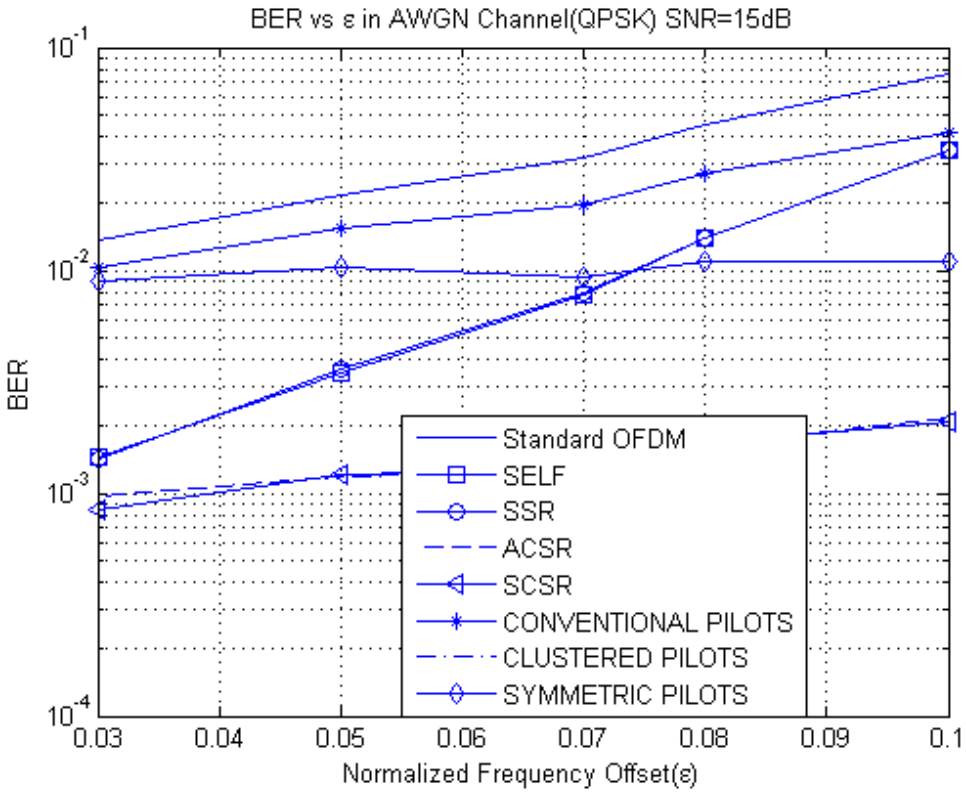

Figure 50 - BER vs ε in AWGN with QPSK (SNR=15dB)

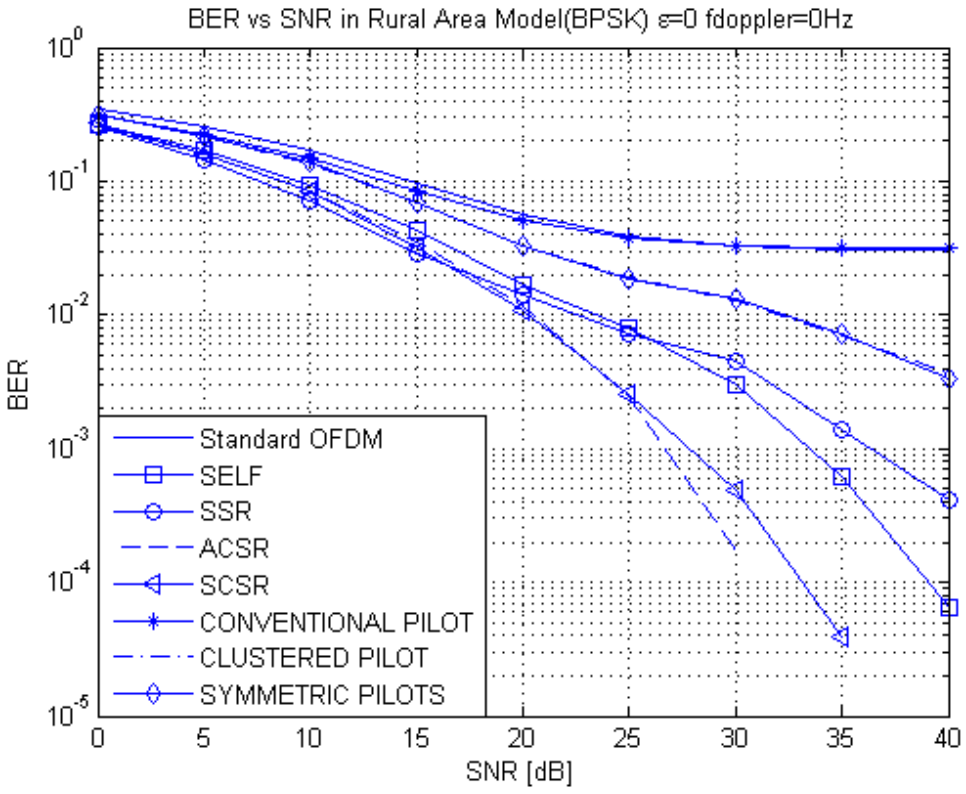

Figure 51 - BER vs SNR in Rural Area with BPSK f_D=0Hz (ε=0)

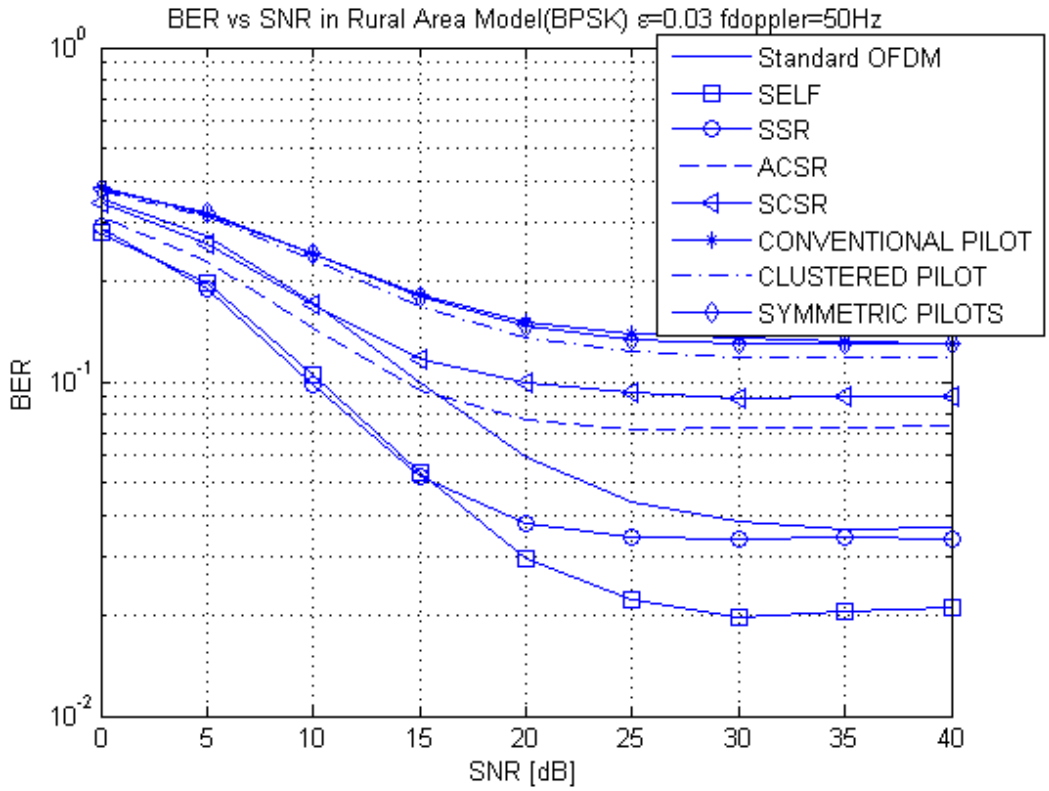

Figure 52 - BER vs SNR in Rural Area with BPSK f_D=50Hz (ε=0.03)

Figure 53 shows the CIR performance of ICI cancellation techniques when pilot power is chosen to be 2. It can be seen that Symmetric Pilots shows the best performance among the others.

But note that, if pilot signals are chosen to be PRBS, then the performances of; SSR and Symmetric Pilots, Self cancellation and Clustered Pilots, Standard OFDM and Conventional Pilots will be same.

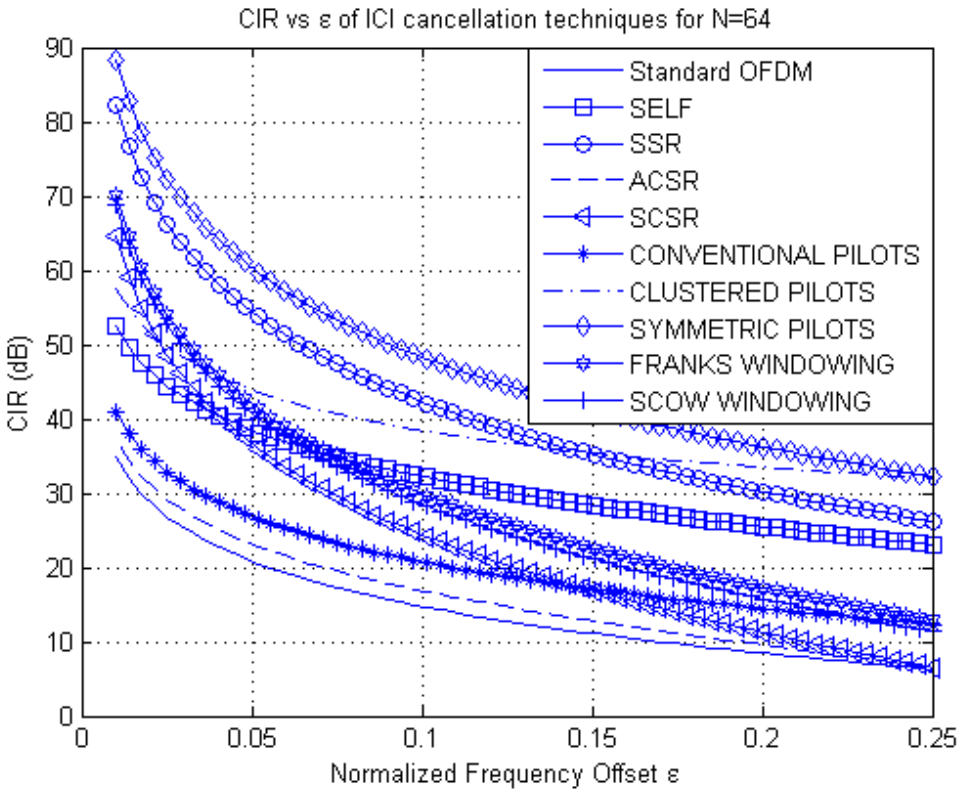

Figure 53 - CIR vs e of ICI cancellation techniques for N=64 with Ep=2 used

CHAPTER 6

CONCLUSION

The objective of this thesis was to investigate intercarrier interference (ICI) cancellation methods in OFDM systems and compare their performances in AWGN and Multipath Fading Channels. Rural Area (RA) model according to COST 207 is used for multipath fading channel.

In this thesis, we have first considered the basics of OFDM and introduced OFDM model. OFDM is a multi-carrier modulation scheme used for bandwidth efficiency. The key idea of OFDM is that a single user would make use of all orthogonal subcarriers in divided frequency bands. Therefore, the data rate can be increased significantly. IFFT modules generate these orthogonal subcarriers, and orthogonality together with the cyclic prefix structure eliminates intercarrier interference (ICI) and inter symbol interference (ISI).

However, OFDM systems have certain disadvantages; the first one is the high peak to average power ratio, which requires the use of expensive, highly linear power amplifiers and the second one is the increased sensitivity to carrier frequency offsets.

Carrier frequency offsets may exist due to Doppler shifts and differences in the oscillator frequencies at the transmitter and the receiver. The resulting offset causes a shift of the signal spectrum, which may compromise the subcarrier orthogonality. The result is an increase in the noise level due to ICI, which degrades system performance.

In this thesis, we considered this carrier frequency offset and its effects on OFDM systems. We investigated the factors that induce carrier frequency offset; those are Doppler shift and synchronization errors. Then we have analyzed the

intercarrier interference (ICI), which is a result of the carrier frequency offset and formulated the received data in terms of desired signal and ICI coefficients.

We have also analysed the carrier to interference ratio (CIR) in OFDM systems. The carrier-to-interference ratio (CIR) is the ratio of the signal power to the power in the interference components. It serves as a good indication of signal quality.

After analysing ICI in OFDM system, we discussed the solutions of the ICI. In the literature, mainly there are 3 groups of ICI cancellation techniques; windowing techniques, CFO estimation and correction methods and repeated data methods. Windowing techniques are outside of scope of this study.

CFO estimation and correction methods generally use pilot sequences. In these methods, the CFO is estimated first and then CFO correction is done. We can separate these methods into 2 groups; data-aided methods and blind methods. Data-aided methods use pilot sequences or virtual carriers to estimate CFO, however blind methods generally use some part of the transmitted data or guard interval. We implemented the “Conventional Pilots” and “Clustered Pilots” pilot-aided CFO estimation techniques for ICI cancellation. In addition, we implemented a new scheme “Symmetric Pilots”, by using the odd symmetry between pilot symbols.

Repeated data methods use only half of the bandwidth for information transmission and the redundant information in these methods can be applied to eliminate the ICI at the receiver. This elimination brings an advantage to them since these methods show really better performance than other schemes. However, these methods are not bandwidth efficient, because they use only half the bandwidth for information transmission. We implemented the “Self Cancellation scheme” and “Symmetric Symbol Repetition (SSR)” schemes to mitigate ICI effects. But these two schemes are not resistant to phase rotation effects, so two schemes named as “Adjacent Conjugate Symbol Repetition (ACSR)” and “Symmetric Conjugate Symbol Repetition(SCSR)” are implemented to mitigate both ICI and phase rotation effect.

Nyquist windowing techniques, apply windowing in front of FFT at the receiver side. These windows reduce the side lobe and this provides the carrier orthogonality. We have implemented two different types of receiver windowing functions; second order polynomial class of Nyquist windows and Nyquist window with Franks pulse used.

Pilot-aided CFO estimation techniques are compared in AWGN and multipath fading in terms of bit error rate while signal to noise ratio is changing. Also performance comparisons are done in terms of BER versus CFO and RMSE of CFO estimates versus CFO. Then carrier to interference ratio between these methods is investigated. In these simulations clustered pilots method and symmetric pilots method show nearly same performances and have a performance gain over conventional pilots method. Furthermore, BER versus pilot number plots are analysed while assuming a total budget of power to be used by pilots and data. In these simulations, we found that when pilot number increases, estimates that are more accurate are obtained and BER decreases.

Similarly, repeated data methods are compared in AWGN and multipath fading in terms of bit error rate while SNR or CFO is changing. Then a CIR comparison between repeated data methods is examined. In these simulations, SCSR and ACSR methods shows performance gain among other methods especially in higher modulation schemes such as 16 QAM.

Windowing techniques are compared in AWGN in terms of bit error rate while SNR is changing. Also a CIR comparison is made between these windowing techniques. In these simulations Franks pulse Nyquist window shows better performance than SCOW windowing technique.

Finally, all of these nine ICI cancellation methods are compared in terms of BER and CIR in both channel types. We found that repeated data methods show better performance than pilot-aided CFO estimation methods with a cost of increased bandwidth usage especially in high SNR’s.

Note that CIR is an important performance issue when comparing ICI cancellation techniques since it shows the signal power to ICI power ratio. However, phase rotation is not considered when calculating average CIR that leads ACSR and SCSR methods show bad performance in terms of CIR. This fact is conflicting with the performances of these techniques when considering BER versus SNR, since they show the best performance in terms of BER.

Consequently, we can say that CIR is an important measurement issue when comparing ICI cancellation techniques, but BER consideration is more important than CIR since decreasing bit errors in a transmission environment is vital.

REFERENCES

[1] R.W. Chang, “Synthesis of band- limited orthogonal signals for multichannel data transmission,” Bell Sys. Tech. Journal, vol. 45, Dec. 1966

[2] Zou, W.Y. and Yiyan Wu, “COFDM: an overview” IEEE Trans. On Broadcasting, vol. 41 Issue: 1, pp. 1-8, Mar. 1995

[3] Weinstein, S. and Ebert, P.; “Data Transmission by Frequency-Division Multiplexing Using the Discrete Fourier Transform” IEEE Trans. on Commun. vol. 19 Issue: 5, pp. 628 –634, Oct.1971

[4] Peled, A. and Ruiz, A.; “Frequency domain data transmission using reduced computational complexity algorithms”, Acoustics, Speech, and Signal Processing IEEE International Conference on ICASSP '80, vol. 5, pp.964 –967, Apr. 1980

[5] B. Hirosaki, “An analysis of automatic equalizers for orthogonally multiplexed QAM systems,” IEEE Trans. Commun. , vol. COM-28, pp.73-83, Jan.1980.

[6] L.J. Cimini, “Analysis and simulation of a digital mobile channel using orthogonal frequency division multiplexing”, IEEE Trans. Commun. , vol. COM-33, pp. 665-675. July 1985

[7] I. Kalet, “The multitone channel,” IEEE Trans. Commun. vol. 37, pp.119-124. Feb.1989

[8] Poularikas, Alexander D. “The handbook of formulas and tables for signal processing”, Springer, 1999

[9] Chi-Tsong Chen “System and Signal Analysis” Thomson, 1988

[10] T. S. Rappaport, “Wireless Communications: Principles & Practice”, Prentice Hall, 1995

[11] Commission of the European Communities, “COST 207: Digital Land Mobile Radio Communications, Luxembourg: Final Report,” Office for Official Publications of the European Communities, 1989.

[12] Y. R. Zheng and C. Xiao, “Simulation models with correct statistical properties for Rayleigh fading channels," IEEE Trans. Commun., vol. 51, pp. 920-928, June 2003.

[13] W.C. Jakes, “Microwave Mobile Communication”, Wiley, 1974

[14] Russell, M.; Stuber, G.L.; “Interchannel interference analysis of OFDM in a mobile environment”, Vehicular Technology Conference, 1995 IEEE 45th, vol. 2, pp. 820 –824, Jul. 1995.

[15] Anandpara M, Erwa E, Golab J, Samanta R, Wang H, „Inter-carrier interference cancellation for OFDM systems“, May 2003.

[16] J. Armstrong, “Analysis of new and existing methods of reducing intercarrier interference due to carrier frequency offset in OFDM,” IEEE Trans. Commun., vol. 47, pp. 365-369, Mar. 1999

[17] Y. Zhao and S. G. Haggman, “Sensitivity to Doppler shift and carrier frequency errors in OFDM systems - the consequences and solutions,” in IEEE GLOBECOM’96, vol. 3, pp. 1564-1568, 1996.

[18] Y. Zhao and S.-G. Haggman, “Intercarrier interference self-cancellation scheme for OFDM mobile communication systems,” IEEE Trans. Commun., vol. 49, pp. 1185–1191, July 2001.

[19] P. H. Moose, “A technique for orthogonal frequency division multiplexing frequency offset correction,” IEEE Trans. Commun., vol. 42, pp. 2908–2914, Oct. 1994.

[20] P.Tan and N.C. Beaulieu, “Reduced ICI in OFDM systems using the “better than” raised cosine pulse”, IEEE Commun. Lett., vol.8, pp.135-137, March 2004.

[21] S.H. Muller-Weinfurtner, “Optimum Nyquist windowing in OFDM receivers”, IEEE Trans. Commun., vol.49, pp.417-420, March 2001.

[22] R.Song and S. Leung, “A novel OFDM receiver with second order polynomial Nyquist window function”, IEEE Commun. Lett , 2005.

[23] L.E. Franks, “Further results on Nyquist’s problem in pulse transmission”, IEEE Trans. Commun. Tech., vol. 16, pp. 337-340, April 1968.

[24] M. Luise and R. Reggiannini, “Carrier frequency acquisition and tracking for OFDM systems,” IEEE Trans. Commun., vol. 44, pp. 1590-1598, Nov. 1996.

[25] T. M. Schmidl and D. C. Cox, “Robust frequency and timing synchronization for OFDM,” IEEE Trans. Commun., vol. 45, pp. 1613-1621, Dec. 1997.

[26] S. Kapoor, D. J. Marchok, and Y.-F. Huang, “Pilot assisted synchronization for wireless OFDM systems over fast time varying fading channels,” in Proc. IEEE VTC 1998, pp. 2077–2080.

[27] F. Classen and H. Meyr, “Frequency synchronization algorithm for OFDM systems suitable for communication over frequency selective fading channels,” in Proc. IEEE VTC 1994, pp. 1655-1659.

[28] M. Speth, S. Fechtel, G. Fock, and H. Meyr, “Optimum receiver design for OFDM-based broadband transmission–part II: a case study,” IEEE Trans. Commun., vol. 49, pp. 571-578, Apr. 2001.

[29] M. Li and W. Zhang, “A novel method of carrier frequency offset estimation for OFDM systems,” IEEE Trans. Consumer Electron., vol. 49, pp. 965-972, Nov. 2003.

[30] J. van de Beek, M. Sandell, and P. O. Borjesson, “ML estimation of time and frequency offset in OFDM systems,” IEEE Trans. Signal Processing, vol. 45, pp. 1800–1805, July 1997.

[31] H. Bölcskei, “Blind estimation of symbol timing and carrier frequency offset in wirelss OFDM systems,” IEEE Trans. Commun., vol. 49, pp. 988–999, June 2001.

[32] H. Liu and U. Tureli, “A high efficiency carrier estimator for OFDM communications,” IEEE Commun. Lett., vol. 2, pp. 104-106, Apr. 1998.

[33] U. Tureli, H. Liu, and M. Zoltowski, “OFDM blind carrier offset estimation: ESPRIT,” IEEE Trans. Commun., vol. 48, pp. 1459-1461, Sept. 2000.

[34] U. Tureli, P. J. Honan, and H. Liu, “Low-complexity nonlinear least squar carrier offset estimation for OFDM: identifiabily, diversity and performance,” IEEE Trans. Signal Processing, vol. 52, pp. 2441-2452, Sept. 2004.

[35] Sathananthan K, Athaudage C.R.N and Qiu B, “A Novel ICI Cancellation Scheme to Reduce both Frequency Offset and IQ Imbalance Effects in OFDM” Computers and Communications, 2004. Proceedings. ISCC 2004. Ninth International Symposium, vol 2, pp. 708-713, July 2004

[36] K. Sathananthan, R. M. A. P. Rajatheva, and S. B. Slimane, “Cancellation technique to reduce intercarrier interference in OFDM,” IEEE Elect. Lett., vol. 36, pp. 2078 -2079, Dec. 2000.

[37] Zhang W, Xia X.G, Ching P.C “Clustered pilot tones for carrier frequency offset estimation in OFDM systems” , IEEE TRANSACTIONS ON WIRELESS COMMUNICATIONS, vol 6, no 1, January 2007.

[38] N.C. Bealieu, C.C. Tan, and M. O. Damen, “A “better than” Nyquist pulse”, IEEE Commun. Letter, vol.5, pp.367-368, Sept. 2001.

APPENDIX A

DERIVATION OF ICI COEFFICIENTS

Start with equation (5) and substitute $Y_i(k)$ that is the Fast Fourier Transform of $y_i(n)$. Then we get [21] :

$$Y_i(k) = \sum_{n=0}^{N-1} x_i(n) \exp(\frac{j2\pi n\varepsilon}{N}) \exp(\frac{-j2\pi nk}{N})$$

$$= \sum_{n=0}^{N-1} \frac{1}{N} (\sum_{l=0}^{N-1} X_i(l) \exp(\frac{j2\pi nl}{N})) \exp(\frac{j2\pi n(\varepsilon - k)}{N})$$

$$= \frac{1}{N} \sum_{l=0}^{N-1} X_i(l) \sum_{n=0}^{N-1} \exp(\frac{j2\pi n(l+\varepsilon-k)}{N}) \qquad \text{(A.1)}$$

We can expand $\frac{1}{N} \sum_{n=0}^{N-1} \exp(\frac{j2\pi n(l+\varepsilon-k)}{N})$ using the geometric series as [21]:

$$\frac{1}{N} \sum_{n=0}^{N-1} \exp(\frac{j2\pi n(l+\varepsilon-k)}{N}) = \frac{1}{N} \frac{1-\exp(j2\pi(l+\varepsilon-k))}{1-\exp(j2\pi(l+\varepsilon-k)/N)}$$

$$= \frac{1}{N} \frac{\exp(j2\pi(l+\varepsilon-k)/2)\left[\exp(-j2\pi(l+\varepsilon-k)/2) - \exp(j2\pi(l+\varepsilon-k)/2)\right]}{\exp(j2\pi(l+\varepsilon-k)/2N)\left[\exp(-j2\pi(l+\varepsilon-k)/2N) - \exp(j2\pi(l+\varepsilon-k)/2N)\right]}$$

$$= \frac{1}{N} \exp(j\pi(l+\varepsilon-k)(1-\frac{1}{N})) \frac{\sin(\pi(l+\varepsilon-k))}{\sin(\pi(l+\varepsilon-k)/N)} \qquad \text{(A.2)}$$

Substituting (A.2) in (A.1), we get [21]:

$$Y_i(k) = \sum_{l=0}^{N-1} X_i(l) S(l-k)$$

where,

$$S(l-k) = \exp(j\pi(l+\varepsilon-k)(1-\frac{1}{N}))\frac{\sin(\pi(l+\varepsilon-k))}{N\sin(\pi(l+\varepsilon-k)/N)}$$

which are the required ICI coefficients that are given in (15).

APPENDIX B

MATLAB EXPERIMENTS IN THE STUDY

Here, the strategy used in the MATLAB experiments will be explained. We have considered two types of channel in the experiments; AWGN Channel and Multipath Fading Rayleigh Channel (Rural Area model).

In AWGN Channel, firstly the subcarrier number in an OFDM block (N=256), block number (B=4), Guard Interval length (GI=N/4), pilot spacing (L=16) and normalized frequency offset (ε is taken as 0.03 or 0.1) is identified. Then, while SNR is increasing , Monte Carlo simulation is done with 10000 trials.

In one trial; firstly N*B binary data is generated (with "randsrc" command in MATLAB) and then modulated according to BPSK, QPSK or 16 QAM with "qammod" command in MATLAB. After modulation, data is converted to parallel and IFFT is taken with "ifft" command in MATLAB. After IFFT, cyclic prefix is added to each OFDM symbol. After inserting Guard Interval, parallel data is converted to serial again and carrier frequency offset effect is added to the data block with multiplying $e^{\frac{j2\pi m\varepsilon}{N}}$.

At the receiver, data is converted to parallel again and guard interval is removed. Then FFT is taken with "fft" command in MATLAB. After FFT, data is converted to serial and demodulated with "qamdemod" command in MATLAB. Then, the demodulated data is compared with the generated binary data and BER is calculated.

In Rural Area model, in one trial, firstly N*B binary data is generated (with "randsrc" command in MATLAB) and then modulated according to BPSK, QPSK or 16 QAM with "qammod" command in MATLAB. After modulation, L pilots are inserted to each OFDM symbol, then data is converted to parallel and IFFT is taken

with “ifft” command in MATLAB. After IFFT, cyclic prefix is added to each OFDM symbol.

After inserting Guard Interval, parallel data is converted to serial again and pass into the multipath Rayleigh fading channel with “rayleighchan(T_s, f_D, delay, gain)” command in MATLAB where f_D is the maximum Doppler shift in the Jakes model, T_s is subcarrier symbol period, “delay” is the time delay of each path in microseconds and “gain” is the power gain of each path in dB. After channel effect, carrier frequency offset effect is added to the data block with multiplying $e^{\frac{j2\pi m\varepsilon}{N}}$.

At the receiver, data is converted to parallel again and guard interval is removed. Then FFT is taken with “fft” command in MATLAB. Following FFT block, the pilot signals are extracted and the estimated channel frequency response $\hat{H}(k)$ for the data sub-channels is obtained in channel estimation block with the Least Squares (LS) channel estimation technique. After that, IFFT of $\hat{H}(k)$ is taken to find out the channel impulse response. After channel estimation, estimated transmitted symbols are found by dividing the received symbols to the FFT of channel impulse response. After this equalization, data is converted to serial and demodulated with “qamdemod” command in MATLAB. Then, the demodulated data is compared with the generated binary data and BER is calculated.

Average CIR comparison plots are obtained by implementing the CIR formulas , not by transmitting data into a channel.